AUTOPHAGY: AN ESSENTIAL PROCESS FOR MAINTAINING MUSCLE FUNCTION AFTER INJURY AND THROUGHOUT LIFE

by

ANNA NICHENKO

(Under the Direction of Jarrod Call)

ABSTRACT

The ability of muscle to maintain healthy function after injury and with increasing age largely depends on the health of the mitochondrial network within the muscle fibers. Autophagy is a cellular recycling mechanism that degrades damaged organelles and proteins and plays an important role in maintaining mitochondrial network integrity in muscle. Ulk1 is an autophagy-initiating kinase, however, its contribution to mitochondrial maintenance and its necessity for proper muscle function is unknown in response to muscle injury and with aging. I designed and executed three studies to investigate the role of Ulk1-mediated autophagy in skeletal muscle. Study 1 tested the extent to which muscle injury activates an autophagy response. Injured muscles had a greater expression of autophagy-related proteins LC3II, p62, and Ulk1 which confirmed that muscle injury activates autophagy. Study 2 specifically determined if Ulk1-mediated autophagy is required for the recovery of muscle metabolic and contractile function after injury. Skeletal muscle from muscle-specific Ulk1 knockouts had reduced contractile recovery and satellite cell function compared to *Cre* negative littermates. This data suggest that Ulk1-mediated autophagy plays an important role in functional muscle recovery following injury and established that Ulk1-mediated autophagy may produce signaling cues that regulate satellite

cell activity as Ulk1 was present in the satellite cells which exhibited impaired function. Additionally, I used a fluorescently tagged plasmid to compare autophagy flux in injured and uninjured muscle and discovered that autophagosome degradation is not upregulated sufficiently to match autophagosome assembly after muscle injury which leads to an autophagy bottleneck. Study 3 tested the extent to which basal Ulk1-mediated autophagy is required for the healthy aging of skeletal muscle. Muscles from aged Ulk1 knockout mice had an accumulation of damaged mitochondria which affected type II muscle fibers resulting in weaker EDL muscles. I concluded from this data that Ulk1-mediated autophagy is required for healthy aging of muscle in terms of both metabolic and contractile function. Based on the studies described herein, it is evident that Ulk1-mediated autophagy plays an essential role in maintaining muscle function after injury and throughout life. Furthermore, Ulk1 may provide a powerful therapeutic target to improve muscle function.

INDEX WORDS: Autophagy, Mitochondria, Ulk1, Muscle injury, Aging, Autophagy flux

AUTOPHAGY: AN ESSENTIAL PROCESS FOR MAINTAINING MUSCLE FUNCTION AFTER INJURY AND THROUGHOUT LIFE.

by

ANNA NICHENKO

B.S., Valdosta State University, 2014

A Dissertation Submitted to the Graduate Faculty of The University of Georgia in Partial Fulfillment of the Requirements for the Degree

DOCTOR OF PHILOSOPHY

ATHENS, GEORGIA

2020

AUTOPHAGY: AN ESSENTIAL PROCESS FOR MAINTAINING MUSCLE FUNCTION AFTER INJURY AND THROUGHOUT LIFE.

by

ANNA NICHENKO

Major Professor:	Jarrod Call
Committee:	Hang Yin
	Luke Mortensen
	Sarah Greising

Electronic Version Approved:

Ron Walcott
Interim Dean of the Graduate School
The University of Georgia
August 2020

DEDICATION

This dissertation is dedicated to my mama, Scarlett Nichenko, who has always supported me and listened to me gripe and complain for five years while going through her own shit. I love you.

ACKNOWLEDGEMENTS

I would like to thank the following individuals, as this dissertation would not have been possible without their help and support:

Dr. Jarrod Call for taking a chance on a transfer graduate student and being an outstanding mentor and role model.

Dr. Michael Southern, Albi Schifino, and Jennifer Mcfaline-Figueroa for being great lab mates and even better friends.

Anita Qualls, Bethany Graulich, and Grant Mercer for assisting with experiments and keeping the lab entertaining.

Ginny Frederick and Megan Ware for offering endless advice, support, and volleyball breaks.

And Myrtle for making me laugh every day and keeping me sane.

TABLE OF CONTENTS

LIST OF TABLES

Page

LIST OF FIGURES

Page

CHAPTER 1

INTRODUCTION AND LITERATURE REVIEW

There are 11 different organ systems in the body and of these the skeletal muscle system accounts for the largest percentage of body mass (~40%) (Heymsfield, Thomas, Bosy-Westphal, & Müller, 2019). Skeletal muscle plays an integral role in locomotion and metabolism by controlling whole-body movement, breathing, maintaining posture, and consuming a large proportion of glucose for energy. Muscle mass and function can be negatively affected by disease, numerous types of muscle injury (volumetric muscle loss, eccentric-contraction induced, contusion, burn, ischemic reperfusion, and freeze injury) as well as with increasing age (Call, Warren, Verma, & Lowe, 2013b; Marzetti et al., 2017; Warren et al., 2007). Reductions in muscle mass or function may lead to many negative health consequences including; obesity, type II diabetes, frailty, and increased incidence of falls (Marzetti et al., 2017). These comorbidities related to declines in muscle mass and function create a large public health burden (Janssen, Shepard, Katzmarzyk, & Roubenoff, 2004), therefore research focused on mechanisms and therapeutics aimed at maintaining skeletal muscle health is of the utmost importance.

The ability of skeletal muscle to maintain healthy function and homeostasis largely depends on its ability to regenerate, repair, and remodel muscle fibers when necessary. All of these processes require energy in the form of ATP which is produced by an extensive mitochondrial network within muscle fibers. Consequently, mitochondria function plays an essential role in maintaining healthy muscle and damaged mitochondria produce reactive oxygen species (ROS) which can cause additional damage to the muscle fiber. Therefore, the

mitochondria network is tightly regulated by mitochondrial dynamic pathways including mitochondrial biogenesis, fusion, fission, and autophagy in order to maintain optimum function (Hood, Memme, Oliveira, & Triolo, 2019). Mitochondrial biogenesis denotes the synthesis of new mitochondria, which are then added to the mitochondrial network through mitochondrial fusion. When portions of the mitochondrial network become damaged or dysfunctional, they are cleaved from the network via mitochondrial fission and undergo mitochondrial-specific autophagy (mitophagy) to degrade and recycle the damaged mitochondria components. All of these are essential for maintaining mitochondrial function but mitophagy may be particularly important by removing damaged mitochondria which accumulate in muscle in the presence of disease, injury, or with age.

Essential steps of autophagy

Macro-autophagy (hereafter referred to as autophagy) is an evolutionarily conserved cellular process that occurs in the following five steps: 1) induction, 2) nucleation and expansion, 3) maturation, 4) autophagosome-lysosome fusion, and 5) degradation and efflux. The induction phase is initiated through direct phosphorylation of Unc-51 like autophagy activating kinase (Ulk1) at serine555 by AMPK (Egan et al., 2011). Ulk1, autophagy-related protein 13 (Atg13), and focal adhesion kinase family interacting protein of 200kDa (FIP200) form an induction complex that phosphorylates Beclin1, a part of the PI3K III nucleation complex (Vainshtein & Hood, 2016). The PI3K III nucleation complex signals for autophagosome membrane formation and expansion through an Atg9-mediated mechanism as well as signals for the conjugation of microtubule-associated protein 1A/B-light chain 3 (LC3 I) to the LC3 II form by Atg4 which is then attached to the autophagosome membrane (Vainshtein & Hood, 2016). During maturation, damaged organelles or proteins that were tagged by Ubiquitin or other organelle-specific damage

markers are recognized by and bind p62. p62 interacts with LC3 II inside the autophagosome to "round up" the damaged contents allowing the autophagosome membrane to form around and completely enclose the tagged damaged contents (Vainshtein & Hood, 2016). After the autophagosome is completely formed, it must then fuse with a lysosome which has a low pH and contains hydrolases to degrade the autophagosome's damaged contents. Both lysosomes and autophagosomes contain SNARE complexes to facilitate membrane tethering and fusion however the exact signaling mechanisms involved in this are still being elucidated (C. Wang et al., 2018). Once an autophagolysosome is formed, the lysosomal contents break down the autophagosome contents into their essential components of amino acids, fatty acids, and nucleotides. These essential components are then repurposed within the muscle fiber; therefore, autophagy is essentially a cellular recycling mechanism.

Activators of autophagy

Autophagy occurs in every tissue of the body and is always basally active in skeletal muscle. Because autophagy is a recycling mechanism that provides nutrients to the muscle fiber it is often upregulated in energy-deficient states such as with endurance exercise and caloric restriction (Vainshtein & Hood, 2016; Yang et al., 2016). Both endurance exercise and caloric restriction result in an abundance of AMP which activates AMPK (Vainshtein & Hood, 2016; Yang et al., 2016). When AMPK is active, it phosphorylates Ulk1 ultimately stimulating autophagosome formation and autophagy (Egan et al., 2011). Caloric restriction and endurance exercise both also inhibit mTOR which is a known inhibitor of Ulk1. In summary, the energy-deficient state associated with exercise and caloric restriction activates autophagy in two ways, by stimulating via AMPK, and by removing the inhibition of mTOR. Other cellular stimuli

create energy imbalances such as after muscle injury, however, the extent to which these activate autophagy is currently unclear.

Outcomes of autophagy

The process of autophagy has two goals; to remove damaged components within the muscle fiber and to supply fatty acids, amino acids, and nucleotides to the muscle fiber. After degradation is complete, these fatty acids and amino acids can be used as a nutrient supply to address the low nutrient state that accompanies many of the stimuli which activate autophagy. These materials can also be used as building blocks in the synthesis of new proteins and organelles or as materials in the replication of DNA which can help remodel the cell during energy-deficient states. Another interesting function is that these can be used as signaling molecules to activate downstream signaling cascades in order to help the muscle adapt and repair. In summary, the fatty acids, amino acids, and nucleotides that arise from complete autophagosome degradation provide essential materials and signaling cues for the muscle fiber.

Autophagy flux

The majority of early research on autophagy has been spent investigating autophagy protein signaling and autophagosome formation which leaves autophagosome degradation often overlooked. Autophagy is a dynamic process; therefore, the overall efficiency of autophagy depends on both the number of autophagosomes and the rate of degradation (autophagy flux). Current measures of autophagy generally involve quantifying autophagosome-related protein content and phosphorylation such as Ulk1, Beclin1, LC3I/II and other ATG proteins or by quantifying lysosome-related proteins such as LAMP2. These measurements are a poor indicator of autophagy flux as they fail to capture actual autophagosome degradation. Autophagy flux can be assessed in multiple ways including; comparing autophagosome content markers after

inhibiting lysosomal fusion or autophagolysosomal degradation through treatment with colchicine, chloroquine, or bafilomycin, or through microscopy images of fluorescently tagged DNA plasmids of autophagosome membrane components like LC3 (Moulis & Vindis, 2017). It is currently unknown if the rate of autophagosome degradation is regulated to match the rate of increased autophagosome assembly after activation, or if this regulation depends on the autophagy activating stimulus.

Mitophagy

As described above, mitochondria are extremely plastic organelles always undergoing mitochondrial dynamic processes which ensure that the best functioning mitochondria remain active within the muscle fibers (Hood et al., 2019). A large component of maintaining mitochondrial function is through the degradation of damaged mitochondria by mitophagy. Mitophagy can occur through two different signaling cascades both of which begin when there is a loss of mitochondrial membrane potential. The first is the Pink1/Parkin pathway which is initiated when the Pink1 kinase accumulates on the outer mitochondrial membrane in response to a loss of membrane potential. Parkin is then recruited and activated by Pink1 and tags the outer membrane proteins to attract p62. p62 will bind to the inside of the autophagosome (LC3II) which then forms around and engulfs the damaged portion of the mitochondria before fusing with a lysosome for degradation. The second pathway involves receptor-mediated BCL2/adenovirus E1B 19 kDa interacting protein 3 (Bnip3) recruitment to the damaged mitochondria which in turn binds LC3II within the autophagosome (Hanna et al.). Mitophagy responses to exercise and caloric restriction have been explored, however, it is still unclear if other stimuli such as muscle injury activate mitophagy or if mitophagy is necessary for the recovery of mitochondria and muscle function after such stimuli.

Ulk1's role in autophagy

Ulk1 is a unique autophagy signaling kinase that may play a dual role in autophagy regulation despite being traditionally researched as an autophagy initiation protein. Ulk1 is sensitive to changes in nutrient states meaning it is activated in low nutrient states by AMPK phosphorylation (S555, activation) and inhibited at high nutrient states by mammalian target of rapamycin (mTOR) phosphorylation (S757, inhibition) (Egan et al., 2011). Following AMPK activation of Ulk1, Ulk1 colocalizes to the mitochondria and plays an important role in directly recruiting autophagosome machinery for mitophagy in response to exercise (Laker et al., 2017). Recent research supports Ulk1 having a dual role in autophagy by suggesting that Ulk1 may also play a role in autophagosome-lysosome fusion (C. Wang et al., 2018). Ulk1 directly binds STX17 (an autophagosome SNARE protein) and increases STX17's affinity to bind lysosomal SNARE proteins which ultimately leads to fusion and autophagolysosome degradation (C. Wang et al., 2018). Because Ulk1 has dual functions in autophagy, the necessity of Ulk1 in the recovery and maintenance of muscle and mitochondrial function needs to be elucidated. Despite what is known about Ukl1 being required for autophagy initiation and its potential role in autophagy flux, there have not previously been any definitive studies on the extent to which Ulk1 is necessary for autophagy in skeletal muscle, particularly in response to natural aging and muscle injury.

To address several of the important questions raised above, my dissertation had the following specific aims and hypotheses:

Specific Aim 1: Determine the extent to which muscle injury activates an autophagy response.

Hypothesis 1: Muscle injury causes significant damage to the muscle fiber and the mitochondria therefore autophagy will be activated to degrade the damaged proteins and organelles.

Specific Aim 2: Determine if Ulk1-mediated autophagy is required for the recovery of muscle metabolic and contractile function after injury and the extent to which increased autophagosome assembly after an injury is matched by autophagosome degradation.

Hypothesis 2: Ulk1-mediated autophagy will be necessary for the recovery of mitochondrial and contractile function following traumatic muscle injury and that an appropriate autophagy flux response will match the autophagosome formation rate after injury.

Specific Aim 3: Determine the extent to which basal Ulk1-mediated autophagy is required for the healthy aging of skeletal muscle in terms of contractile and metabolic function.

Hypothesis 3: Basal Ulk1-mediated autophagy is necessary for the lifelong maintenance of mitochondria and overall healthy muscle aging.

CHAPTER 2

MITOCHONDRIAL MAINTENANCE VIA AUTOPHAGY CONTRIBUTES TO FUNCTIONAL SKELETAL MUSCLE REGENERATION AND REMODELING[1]

---

[1] Nichenko, A.S. Southern, WM. Atuan, M. Luan, J. Peissig, KB. Foltz, SJ. Beedle, AM. Warren, GL. Call, JA. 2016. *Am J Physiol Cell Physiol*. 311(2):C190-C200. Reprinted here with permission of the publisher.

Abstract

The primary objective of this study was to determine whether alterations in mitochondria affect recovery of skeletal muscle strength and mitochondrial enzyme activities following myotoxic injury. 3-methyladenine (3-MA) was administered daily to blunt autophagy (15mg/kg) and the creatine analog guanidionpropionic acid (β-GPA) (1% in chow) was administered daily to enhance oxidative capacity. Male C57BL/6 mice were randomly assigned to non-treatment (Con; n=6), 3-MA (n=6), or β-GPA (n=8) groups for 10 wk of treatment. Mice were sacrificed two weeks after myotoxic injury to assess mitochondrial remodeling during regeneration and its association with the recovery of muscle strength. Injured muscles had a greater expression of several autophagy-related proteins (e.g., pUlk1 ~2-4 fold, $p<0.049$) compared to uninjured muscles indicating a relationship between muscle regeneration/remodeling and autophagy. By 2 weeks post-injury, 3-MA-treated mice had significantly less recovery of strength (18% less, $p=0.03$) and lower mitochondrial enzyme activity (e.g., citrate synthase (CS): 22% less, $p=0.049$) compared to Con, suggesting that the autophagy process plays an important role during muscle regeneration. In contrast, muscle regeneration was nearly complete in β-GPA-treated mice, i.e., strength recovered to 93% of baseline vs.78% for Con mice. Remarkably, 14 d was sufficient for a near complete recovery of mitochondrial function in β-GPA-treated mice (e.g., no difference between injured and uninjured in CS activity, $p=0.49$), indicating a robust mitochondrial remodeling process during muscle regeneration. In conclusion, autophagy is likely activated following muscle injury and appears to play an important role in functional muscle regeneration.

Introduction

Muscle repair occurs in four main phases, i.e., degeneration, inflammation, regeneration, and remodeling (Huard, Li, & Fu, 2002). Satellite cells activated during the early muscle repair phases largely contribute to muscle regeneration primarily by providing nuclei. The latter remodeling phase plays an important role in final restoration of contractile, structural, and metabolic organelles critical to complete recovery of muscle function. There is emerging evidence indicating a transition in metabolic demand during muscle regeneration and remodeling that may signify an important role of the mitochondria in muscle repair (Ryall, 2013). Importantly, myoblast differentiation is terminated if mtDNA replication is impaired *in vitro (Hamai, Nakamura, & Asano, 1997)*. Additionally, genes associated with mitochondrial biogenesis are upregulated 3-10 d after injury *in vivo (Wagatsuma, Kotake, & Yamada, 2011)*. Therefore, the energy demands of muscle regeneration may rely in part on contribution of oxidative phosphorylation from the mitochondria. There is evidence of mitochondrial damage after muscle injury (Duguez, Feasson, Denis, & Freyssenet, 2002; Wagatsuma et al., 2011) and the cellular mechanisms responsible for removing and replacing those damaged mitochondria are not completely known.

The potential impact of impaired mitochondrial maintenance on skeletal muscle recovery is worth considering, particularly if an accumulation of dysfunctional mitochondria after several bouts of muscle injury could negatively affect muscle function. In support of this, muscle function was improved following genetically-induced mitochondrial biogenesis in a mouse model of Duchenne muscular dystrophy that is characterized by perpetual muscle injury and regeneration (*mdx* mouse) (Selsby, Morine, Pendrak, Barton, & Sweeney, 2012). Additionally, stimulating autophagy (a cellular process essential for degradation of dysfunctional and/or

damaged organelles) in the *mdx* mouse decreased the presence of dysfunctional mitochondria and was associated with an improvement in muscle function (Pauly et al., 2012). These studies suggest that manipulation of muscle mitochondria can impact muscle function and support a model in which mitochondrial remodeling after injury may utilize autophagy to remove damaged mitochondria. Accordingly, impaired or insufficient autophagy could lead to an accumulation of dysfunctional mitochondria that could adversely affect a muscle's function if the muscle were to undergo repeated bouts of injury. The role of autophagy during muscle regeneration is unclear, but autophagy is critical for maintaining skeletal muscle mass in young and aged mice (Masiero & Sandri, 2010; Sandri, 2010); therefore, autophagy may contribute to a muscle's health in many ways. Elucidating the relationship between autophagy and muscle repair could provide therapeutic targets to enhance muscle regeneration.

The primary objective of this study was to determine the extent to which alterations in mitochondria affect functional muscle regeneration and the remodeling of mitochondria after injury. A broad-range autophagy inhibitor (3-methyladenine, 3-MA) and a creatine analog (guanidinopropionic acid, β-GPA) were used to impair and enhance, respectively, the mitochondria in skeletal muscle. We hypothesized that muscle regeneration would be associated with an autophagy response and that manipulating the mitochondria would affect functional muscle and mitochondrial regeneration.

Materials and Methods

Experimental Design

Male C57Bl/6J mice aged 8 wk were purchased from Jackson Laboratories and housed at 20-23°C on a 12:12 hour light:dark cycle with food and water provided ad libitum. At 9 wk of age, mice were randomized to one of three conditions: control (Con, n=6), 3-MA-treated (n=6),

or β-GPA-treated (n=8) groups. To detect a 15% difference in strength recovery at 14 d post-injury assuming a power of 0.7 and an α-level of 0.05, sample sizes of at least 5 mice per group were determined necessary based on our previous physiological muscle contractility measurements for control C57Bl/6J mice. At least one additional mouse per group was included to account for experimental losses.

To determine if 3-MA or β-GPA affected muscle function in the absence of injury, contractile functions (i.e., peak isometric strength and fatigue) were analyzed for the ankle dorsiflexor muscles (tibialis anterior, extensor digitorum longus, extensor hallucis longus) after 8 wk of treatment. Immediately following contractile assessment of the dorsiflexor muscles, the tibialis anterior and gastrocnemius muscles were injected with cardiotoxin to induce injury. The rationale for injuring the gastrocnemius muscles was to have sufficient tissue for biochemical assessment at 14 d post-injury. Muscle strength was assessed one minute after cardiotoxin injection and used as the immediate post-injury time point. Peak isometric strength was assessed again at 14 d post-injury. This time point was selected because it gives sufficient time to allow for satellite cell activation and differentiation and because previous reports have identified this as a time when mitochondrial remodeling post-injury is ongoing (Duguez et al., 2002; Wagatsuma et al., 2011). The tibialis anterior and gastrocnemius muscles were harvested immediately after the 14 d post-injury contractile assessment. The gastrocnemius was finely minced and separated for mitochondrial enzyme activity assessment and immunoblotting analysis. Each tibialis anterior muscle was preserved for histology. All procedures were approved by the Institutional Animal Care and Use Committee at the University of Georgia.

Treatments and myotoxic injury

3-MA inhibits phosphatidylinositol and phagosome formation and is classified as a broad-range autophagy inhibitor. 3-MA-treated mice received daily subcutaneous injections of 3-MA at 15 mg kg^{-1}. β-GPA is a creatine analog that reduces phosphocreatine availability within skeletal muscle and leads to greater signaling for mitochondrial biogenesis (Oudman, Clark, & Brewster, 2013). The delivery of β-GPA was administered via rodent chow (Teklad) in a 1% proportion. All mice received chow ad libitum for the duration of the study. Muscle injury was performed as previously described (Hochreiter-Hufford et al., 2013) on unconscious mice using isoflurane (1.5%). Briefly, 40μL of cardiotoxin (*naja kaouthia*) (0.071 mg/mL; Sigma-Aldrich C9759) was injected into the left tibialis anterior muscles. The medial and lateral gastrocnemius muscles also received 40 μL injections, and a third 40 μL injection was delivered between the two portions of the gastrocnemius muscle.

In vivo assessment of muscle contractility

In vivo peak isometric torque of the dorsiflexor muscles was assessed as previously described (Call, Warren, Verma, & Lowe, 2013a). Briefly, anesthesia was induced using an induction chamber and 5% isoflurane in oxygen. Anesthesia was maintained using 1-2% isoflurane. The left hindlimb was depilated and aseptically prepared and the foot was placed in a foot-plate attached to a servomotor (Model 300C-LR; Aurora Scientific, Aurora, Ontario, Canada). Pt-Ir needle electrodes (Model E2-12; Grass Technologies, West Warwick, RI, USA) were inserted percutaneously on either side of the common peroneal nerve. The ankle joint was adjusted to a 90_o angle. Peak isometric torque was achieved by varying the position of the electrodes and the current delivered to the peroneal nerve using a 0.1-ms square wave pulse at a frequency of 200 Hz. During functional testing, the testing platform was heated to 37°C to

maintain mouse body temperature. Torque as a function of stimulation frequency was then measured during nine isometric contractions at varying stimulation frequencies (5, 10, 20, 40, 60, 80, 100, 150, and 200 Hz). Finally, muscle fatigability was assessed by 120 isometric contractions, one elicited every second using a 300-ms, 60-Hz stimulation. To account for differences in body size among mice, torque (mN•m) was normalized by body mass (kg).

Mitochondrial enzyme activity assays

Gastrocnemius muscles were homogenized in 33 mM phosphate buffer (pH 7.4) at a muscle:buffer ratio of 1:20 using a glass tissue grinder on ice. Protein concentration of each homogenate was measured using the BCA protein assay (Thermo Fisher Scientific). Citrate synthase (CS), β-hydroxy acyl-CoA dehydrogenase (β-HAD), and cytochrome c oxidase (complex IV) activities were determined as previously described (Call et al., 2008; Landisch, Kosir, Nelson, Baltgalvis, & Lowe, 2008). Isocitrate dehydrogenase (IDH) activity was measured by the reduction of NAD+ at an absorbance of 340nm (37°C). This was achieved by adding 5µL of muscle homogenate to 170µL assay buffer (pH 8.5, 0.2M Tris, 1mM $MgCl_2$), 10µL NAD+ (3.2mM, Sigma N0632), and 10µL DL-isocitrate (4.6mM, Sigma I1252). Complex I activity was measured by the reduction of cytochrome c at an absorbance of 550nm (30°C). This was achieved by adding 2.5µL muscle homogenate to 90µL of oxidized cytochrome c (0.1mM, Sigma C2506) and 90µL NADH (1mM, Sigma N8129). In separate wells with identical conditions, the same sample was analyzed with the addition of rotenone (0.1mM) to block complex I electron transport. The difference between the activities represents Complex I activity (Gianni, Jan, Douglas, Stuart, & Tarnopolsky, 2004). Complex II activity was measured by the reduction of cytochrome c at an absorbance of 550nm (30°C). This was accomplished by adding 15µL of muscle homogenate to 100µL of 0.5M sodium succinate in a 3mL cuvette for 1 minute,

followed by the addition of 100μL of sodium cyanide (0.01M) and 2.8mL of cytochrome c buffer (22.7mM). Enzyme activities were run in triplicate and are normalized to total protein content.

Immunoblot analyses

For protein analysis, the gastrocnemius was immediately homogenized with glass homogenizers in protein loading buffer and loaded on a gel for SDS-PAGE and immunoblotting as previously described (Call et al., 2015). The following antibodies (Cell Signaling, Danvers, MA) were used to probe proteins transferred to polyvinylidene fluoride membranes: cytochrome c oxidase IV (COX IV, 1:1000), cytochrome c (1:1000), LC3B (1:1000), p62/SQSTM1 (1:1000), Ulk1 (1:1000), phospho-Ulk1 (Ser555) (1:1000), Bnip3 (1:1000), Drp1 (1:1000), AMPKα (1:1000), phospho-AMPKα (Thr172) (1:1000), β-actin (1:5000). Membranes were analyzed and quantified using Bio-Rad Laboratories Image Lab software (Hercules, CA).

Real-time PCR

The ratio of mtDNA to nDNA was determined by quantitative real-time PCR. Primer sequences for mitochondrial *12S* rDNA included: *12S* forward: 5'-ACCGCGGTCATACGATTAAC-3'; *12S* reverse: 5'-CCCAGTTTGGGTCTTAGCTG-3'. Mitochondrial *12S* rDNA was analyzed relative to three reference genes: 1) nuclear *18S*: *18S* forward: 5'-TTGATTAAGTCCCTGCCCTTTGT-3'; *18S* reverse: 5'-CGATCCGAGGGCCTAACTA-3', 2) *Hsp90ab1* (Mm00833431_g1, Fisher Scientific), and 3) *Hprt* (Mm03024075_m1, Fisher Scientific).

Histological and immunofluorescence assessments

The tibialis anterior and extensor digitorum longus muscles were dissected together and frozen in 2-methylbutane cooled to -160°C in a liquid nitrogen bath. Seven-micron thick sections were cut by cryostat (Thermo Scientific HM550) and mounted on microscope

slides. Tissues were stained for immunofluorescence according to standard protocols (Beedle et al., 2012; Fortunato et al., 2014). Briefly, slides were wet with phosphate-buffered saline (PBS) and blocked with 5% donkey serum (Jackson ImmunoResearch) in PBS. Primary antibody was diluted in blocking solution and incubated overnight at 4°C. Slides were washed three times with PBS, incubated with appropriate secondary antibodies and DAPI (1:10,000; Sigma) for 30 min at room temperature, washed three times, and mounted with PermaFluor mounting medium (Thermo Scientific). Muscle sections were imaged using an X71 inverted epifluorescence microscope and CellSens software (Olympus). Entire muscle cross-sections were captured by a series of overlapping 20X images. Individual fluorescent images were merged and compiled to generate the complete muscle map in Photoshop (Adobe). Total fibers, number of antibody-positive fibers, and fiber areas were analyzed using manual tag or area measurements in Image-Pro Express (MediaCybernetics). For indirect immunofluorescence, primary antibodies were used to detect myosin heavy chains type 1, type 2a, and embryonic (BA-D5, SC-71, and F1.652, 1:30 – 1:40, Developmental Studies Hybridoma Bank); blood vessels (CD31, BD Pharmingen, 1:50); and sarcolemmal or extracellular matrix markers α-dystroglycan (aDGct 5-2 or 45-4, 1:25, Fortunato et al., 2014), β-dystroglycan (MANDAG2 7D11, 1:40, DSHB), or Collagen VI (70R-CR009x Fitzgerald, 1:1000), to identify individual fibers. For p62 analysis by immunofluorescence, slides were fixed in precooled methanol for 15 min at -20°C. After washing 5 times with PBS, slides were blocked for 30 min at room temperature in 5% donkey serum (Jackson ImmunoResearch), 2% BSA (Sigma) and 0.1% Triton-X 100 (Sigma) in PBS. Slides were incubated overnight at 4°C in anti-p62 (Sigma) and anti-perlecan (heparin sulfate proteoglycan, Millipore), both at 1:100 dilution. All slides were washed 3 times with PBS, incubated with anti-rabbit A546 1:500, anti-rat A488 1:500, and DAPI 1:10,000 for 30 min at

room temperature, washed another 3 times, and mounted with permafluor (ThermoFisher). Images were collected with the 40X objective using the IX71 microscope.

Cell culture

Mouse muscle myoblast C2C12 cells (ATCC line #CRL-1772) were expanded, according to standard protocols, in myoblast media: Dulbecco's modified Eagle's media 4.5g/L glucose (DMEM, Corning), supplemented with 15% fetal bovine serum (Atlanta Biologicals), 1:100 glutaMAX (Gibco), and 1:100 antibiotic antimycotic solution (Corning). C2C12 cells were plated in myoblast media at 120,000 cells/well in 6-well tissue-culture treated plates. Approximately 24 hours after plating, myoblast media was removed and replaced with saline vehicle (2 wells), 1 mM 3-MA (2 wells), or 1 mM β-GPA (2 wells) in differentiation media (DMEM, 2% FBS, 1:100 glutaMAX, 1:100 antibiotic antimycotic). Media with saline, 3-MA or β-GPA was refreshed every 48 hours. After 6 days of differentiation, 1 drop of nuclear stain NucBlue (ThermoFisher) was added to each well and incubated for 30 min at room temperature. Phase contrast (grayscale) and blue fluorescent (NucBlue) images were collected from three different locations from each well using an IX71 Olympus epifluorescent microscope with Cell Sens software. Images were analyzed for the number of cells with myotube-like morphology (elongated, with or without multiple nuclei) for each 10X field and averaged across all images per well.

Statistical Analysis

Data are presented in the results as mean ± SD. Two-way repeated measures analysis of variance (RM-ANOVA) was used to analyze the data. The between-subject factor was treatment group (Con vs. 3-MA vs. β-GPA) and the repeated measure factor varied between time point (Pre- vs. Post-injury) and limb (uninjured vs. injured). Data were required to pass normality

(Shapiro-Wilk) and equal variance tests (Brown-Forsythe *F* test) before proceeding with the RM-ANOVA. Differences among groups are only reported where significant interactions were observed and subsequently tested with Tukey's *post hoc* test using JMP statistical software (SAS, Cary, NC). Group main effects are reported where significant interactions were not observed. An α level of 0.05 was used for all analyses.

Results

Effect of treatments on body mass and uninjured muscle contractility

To determine the impact of treatment on uninjured muscle, dorsiflexor contractility was assessed immediately prior to muscle injury, i.e., 8 weeks after initiation of 3-MA, β-GPA, or Con treatment. Autophagy inhibition with 3-MA had no effect on body mass, muscle strength, or muscle fatigue after 8 wk of treatment (Fig. 2.1A-C). β-GPA-treated mice, however, did not gain body mass during the treatment period and generated torques ~20% less compared to Con and 3-MA-treated mice (Fig. 2.1A-B). β-GPA-treated mice subjected to a metabolically challenging contractile test had greater fatigue resistance than Con mice (contraction number 100 to 150; $P \leq 0.045$) and 3-MA-treated mice (contraction number 90 to 150; $P \leq 0.041$; Figure 2.1C). By the end of the fatigue protocol, β-GPA-treated mice were generating 40% of the peak isometric torque measured before the fatigue protocol while Con and 3-MA-treated mice were only generating 29% (Figure 2.1C). These data suggest that the 3-MA regimen did not impact skeletal muscle contractility while β-GPA resulted in a weaker muscle but was effective in increasing dorsiflexor muscle fatigue resistance.

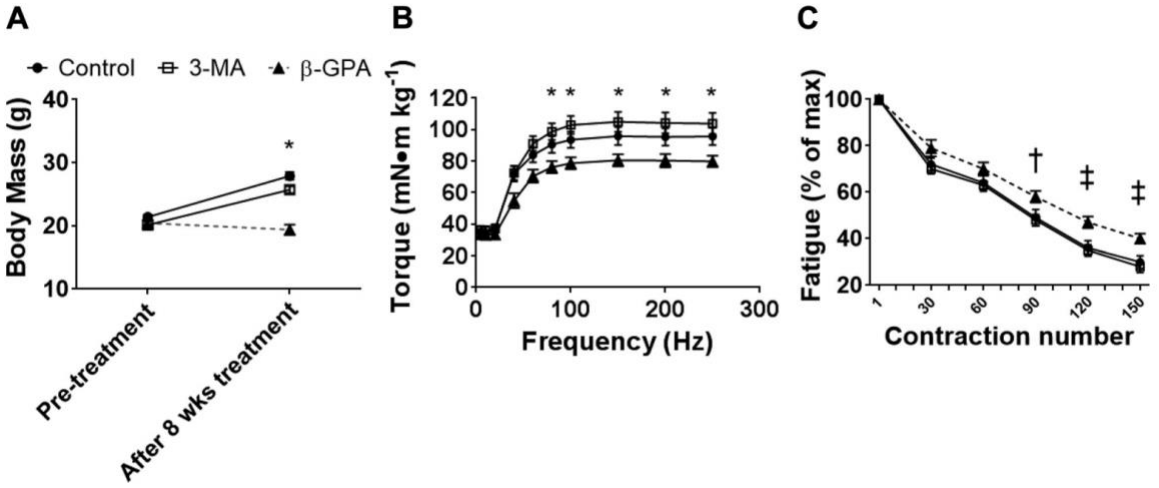

Figure 2.1: Effect of the 3-MA and β-GPA treatments on body masses and uninjured muscle contractility.
A) Body mass at 9 wk of age (Pre-treatment) and after 8 weeks of treatment. B) Isometric torque as a function of stimulation frequency. C) Torque loss from a fatiguing bout of contractions. Fatigue was calculated as a percentage of the greatest torque generated during the 120-contraction protocol. * β-GPA is significantly less than Con and 3-MA ($P < 0.05$). † β-GPA is significantly greater than 3-MA ($P < 0.05$). ‡ β-GPA is significantly greater than Con and 3-MA ($P < 0.05$).

Effect of treatments on recovery of contractile function following injury

After 8 wk of 3-MA or β-GPA treatment, a myotoxic injury model was used to damage skeletal muscle and initiate muscle regeneration in the tibialis anterior and gastrocnemius muscle. There was no difference among groups in peak isometric torque of the dorsiflexors immediately following cardiotoxin injection ($P = 0.95$) indicating muscle damage was equivalent across groups. Peak isometric torque of the dorsiflexors was again tested 14 d post-injury to assess the effectiveness of muscle regeneration in the three different groups. 3-MA-treated mice were significantly weaker compared to Con and β- GPA-treated mice at 14 d post-injury (Fig. 2.2A). In fact, 3-MA-treated mice had only recovered to 58% of pre-injury strength by 14 d post-injury, which is in stark contrast to the recovery of Con (78%) and β-GPA-treated mice (93%; Fig. 2.2B). This suggests that a broad-acting autophagy inhibitor can negatively impact functional muscle regeneration.

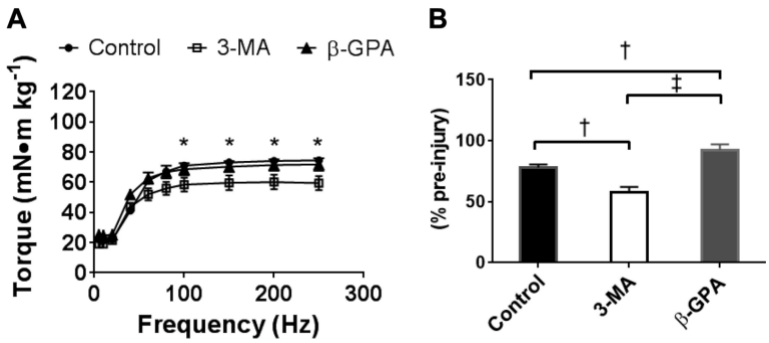

Figure 2.2: Effect of the 3-MA and β-GPA treatments on recovery of muscle contractility at 14 days post-injury.
A) Isometric torque as a function of stimulation frequency. B) Percent recovery of peak isometric torque at 14 days post-injury. * 3-MA is significantly less than Con and β-GPA ($P < 0.05$). † Significantly different than Control ($P<0.05$). ‡ Significantly different than β-GPA ($P < 0.01$).

Effect of treatments on uninjured and injured muscle mitochondrial enzyme activities following injury

To assess functional regeneration of mitochondria after injury, mitochondrial enzyme activities from injured and uninjured gastrocnemius muscles were assessed for critical enzymes in Krebs cycle, β-oxidation, and the electron transport chain. Significant interactions between treatment and limbs (injured vs. uninjured) were observed for citrate synthase ($P = 0.008$) and complex IV ($P = 0.045$) activities (Fig. 2.3A-F). Citrate synthase and complex IV activities were greater in uninjured muscle from β-GPA-treated mice compared to uninjured muscle from Con and 3-MA-treated mice, supporting the ability of β-GPA to enhance oxidative capacity in uninjured skeletal muscle. Similarly, these enzyme activities were greater in the injured muscle from β-GPA-treated mice compared to injured muscle from Con and 3-MA-treated mice, suggesting β-GPA may also enhance recovery of mitochondrial enzyme activities after injury. Only main effects were observed for β-HAD, IDH, complex I, and complex II activities, indicating that activities were lower in injured compared to uninjured muscles independent of

treatment ($P \leq 0.034$). Activities were greater in β-GPA-treated and Con mice compared to 3-MA-treated mice independent of injury ($P \leq 0.035$) for β-HAD and complex II activities, and greater in β-GPA-treated mice compared to 3-MA-treated mice independent of injury ($P \leq 0.048$) for IDH and complex I activities (Fig. 2.3A-F). To assess mitochondrial enzyme activity recovery, the difference between injured and contralateral uninjured muscles in muscle enzyme activities for each mouse was calculated (shown as % deficit). For citrate synthase (CS), IDH, β-HAD, and complex IV activities, there were no significant differences between uninjured and injured muscles after 14 d of recovery from Con ($P \geq 0.087$) and β-GPA-treated mice ($P \geq 0.074$) whereas the enzyme activity difference between injured and uninjured muscles for 3-MA-treated mice was 25-35% for all enzymes measured ($P \leq 0.042$). This analysis supports that use of a broad-acting autophagy inhibitor during muscle regeneration significantly impairs the recovery of muscle mitochondrial enzyme activities.

Effect of treatments on uninjured and injured muscle mitochondrial protein content following injury

COX IV and cytochrome C protein content were assessed using immunoblotting for comparison with the enzyme activity results (Fig. 2.4A-C). Independent of injury, COX IV protein expression was slightly but significantly greater in β-GPA muscle compared to Con and 3-MA muscle (38%, $P < 0.001$; Fig. 2.4B). Independent of treatment, cytochrome c protein expression was ~52% greater in uninjured muscle compared to injured muscle ($P = 0.031$; Fig. 2.4C). There was a trend ($P = 0.09$) for greater cytochrome c protein content in β-GPA-treated muscle compared to Con and 3-MA-treated muscle. Importantly, there was no statistical difference in mitochondrial protein contents between Con and 3-MA-treated mice.

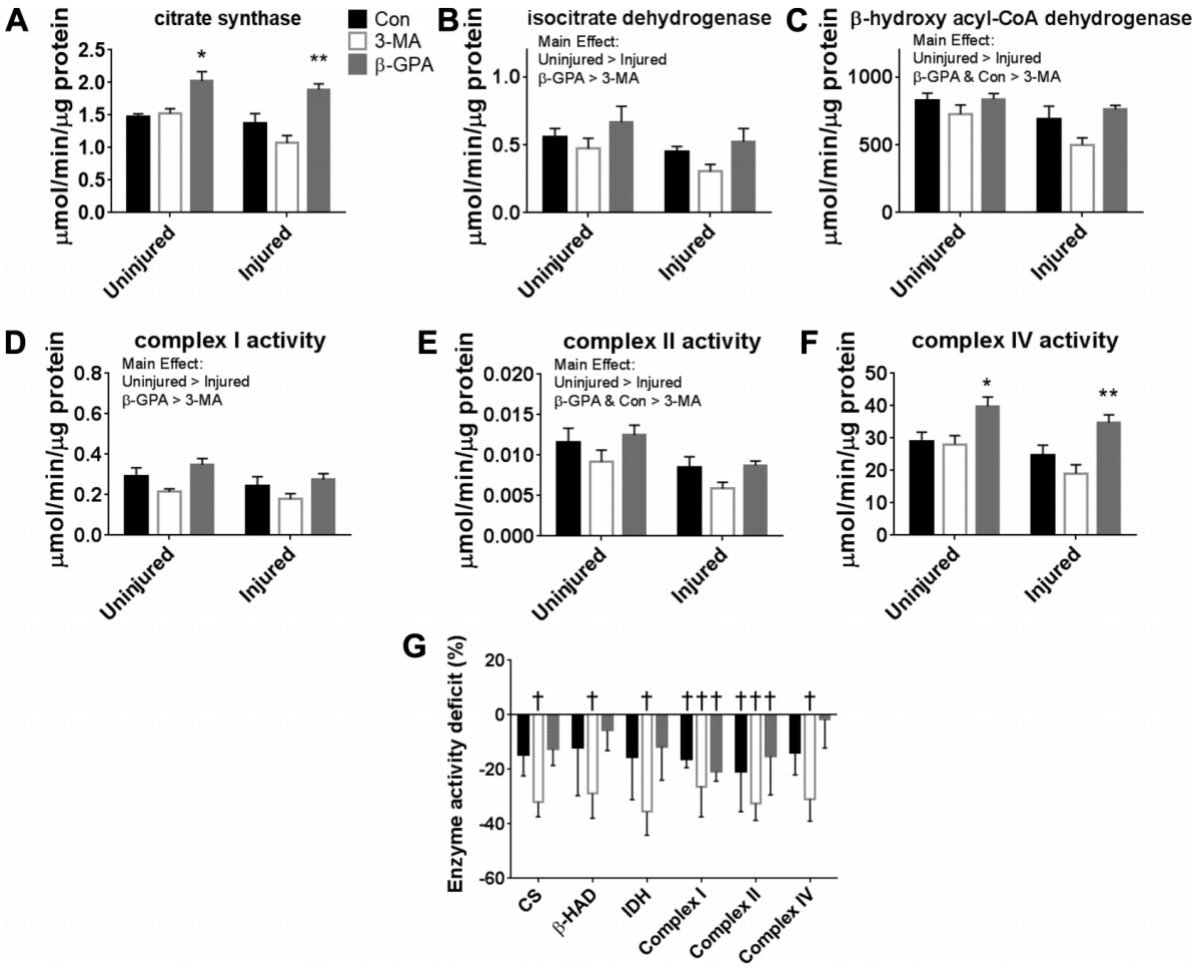

Figure 2.3: Effect of treatments and muscle injury on mitochondrial enzyme activity.
A-F) Uninjured and injured muscle mitochondrial enzyme activities from Con, 3-MA, and β-GPA mice. G) Percent deficit of specific enzyme activities in injured gastrocnemius muscles 14 days post-injury compared to contralateral uninjured muscle. * Significantly different than Con and 3-MA in uninjured muscle ($P < 0.05$). ** Significantly different than Con and 3-MA in injured muscle. † Significantly different than contralateral uninjured ($P < 0.05$).

Effect of treatments on uninjured and injured muscle mtDNA:nDNA ratio following injury

mtDNA content was assessed by quantitative PCR analysis of the mtDNA:nDNA ratio, which has been shown to correlate well with mitochondrial enzyme activities and reflect mitochondrial biogenesis (H. Wang, Hiatt, Barstow, & Brass, 1999; Wu et al., 1999). There was a significant interaction between treatment and injury for the mtDNA:nDNA ratio (P=0.042), and the mtDNA:nDNA ratio was greater in uninjured muscles from β-GPA-treated mice compared to

uninjured muscles from 3-MA-treated mice and compared to injured muscles from β-GPA-treated, 3-MA-treated, and control mice (Fig. 2.4D).

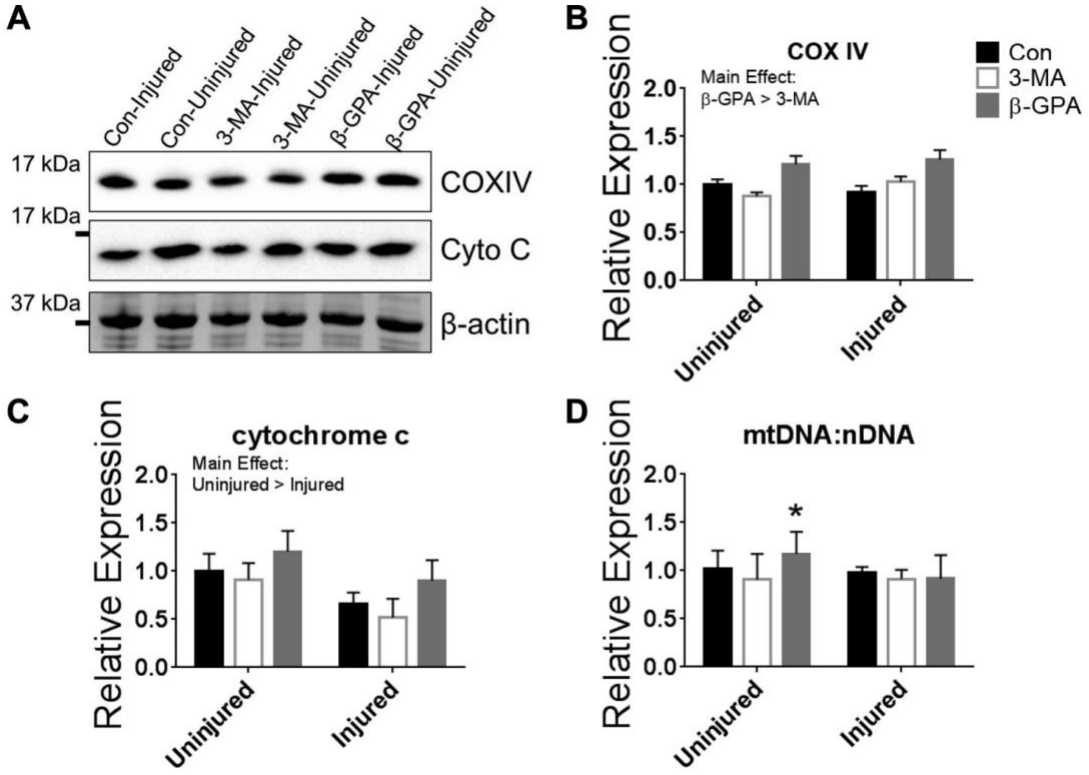

Figure 2.4: Effect of treatments and muscle injury on markers of mitochondrial content. A-C) Immunoblot images of cytochrome c oxidase IV (COX IV) and cytochrome c in gastrocnemius muscle (30 μg total protein). β-actin was probed as loading control. Quantitative and statistical analyses are presented in panels B-C (n=6-8/group). D) Quantitative PCR for *12S* of mtDNA was assessed relative to nDNA reference genes *18S*, *Hprt*, and *Hsp90ab1* to determine the mtDNA:nDNA ratio. Quantitative and statistical analysis is presented in panel D (n=6-8/group). * Statistically different than uninjured 3-MA, injured Con, injured 3-MA, and injured β-GPA.

Effect of treatments on markers of muscle regeneration after injury

To determine if impaired muscle regeneration contributed to muscle strength and mitochondrial function recovery deficits in 3-MA-treated mice, histological assessment of regenerating tissue was quantified by the percentage of fibers that were centrally nucleated and

the presence of fibers with embryonic myosin heavy chain (eMHC). There was no difference in the number of centrally nucleated fibers among treatments (Fig. 2.5A). However, injured muscles from β-GPA-treated mice did have a lesser percentage of fibers that were eMHC-positively stained compared to Con mice (Fig. 2.5B). At this time point, residual eMHC is very low; therefore, a physiological significance of this difference is unlikely. Lastly, the proportion of centrally nucleated muscle fibers with more than one central nuclei was analyzed. Notably, there were fewer fibers with multiple central nuclei in injured muscle from β-GPA-treated mice compared to Con mice (Fig. 2.5C).

To further investigate the impact of treatment on muscle regeneration, specifically to test if 3-MA negatively impacts myogenic differentiation and if β-GPA positively impacts myogenic differentiation, myotube formation was assessed by treating C2C12 cells with vehicle (Con), 3-MA or β-GPA during a 6 day differentiation protocol. Successful myotube differentiation, as measured by elongated tube-like morphology, was observed with all treatment conditions (Fig. 2.5D) suggesting a 1mM 3-MA treatment does not impair myogenic differentiation. β-GPA-treated C2C12 cells (1mM) had ~60% more myotube-like cells compared to control and 3-MA-treated C2C12 cells after differentiation (Fig. 2.5D). The finding that there were fewer regenerated fibers with multiple central nuclei in β-GPA mice following injury (Fig. 2.5C) and the enhanced differentiation in C2C12 cells *in vivo* suggest that β-GPA may enhance differentiation over proliferation after injury.

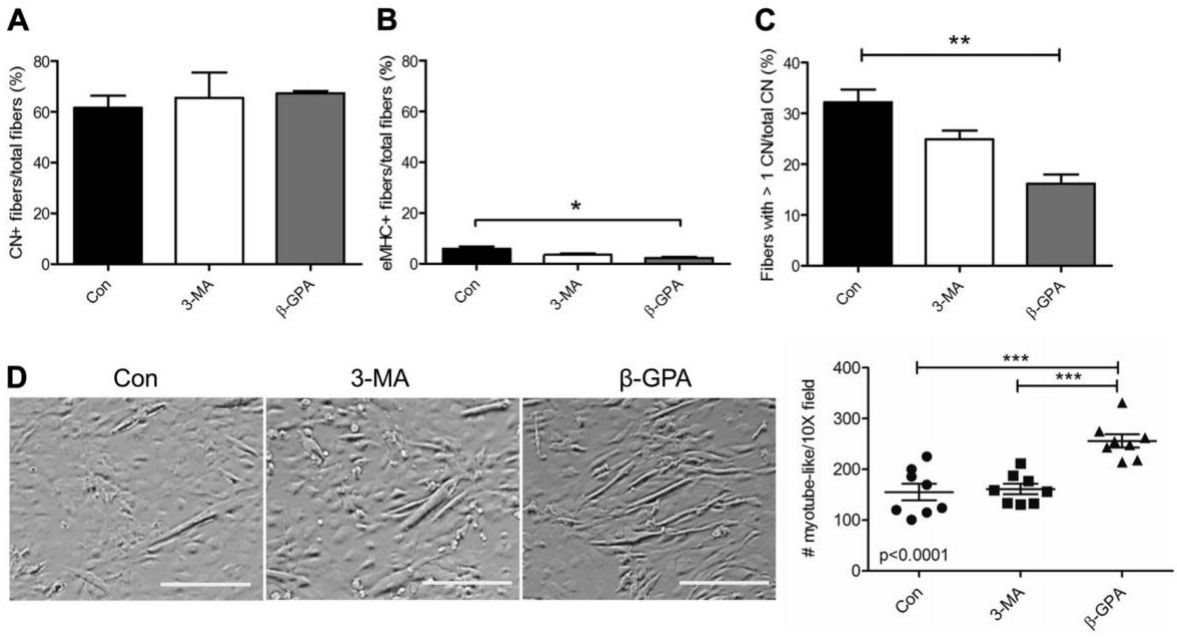

Figure 2.5: Effect of the 3-MA and β-GPA treatments on markers of muscle regeneration and myogenic differentiation *in vivo* and *in vitro*.
A-B) Quantification of regeneration in injured muscle demonstrates similar long-term regeneration by central nucleation (A) and slightly reduced active regeneration [embryonic myosin heavy chain (eMHC)] in β-GPA-treated mice 14 days post-injury. C) The number of fibers with greater than one central nucleus as a proportion of the total number of regenerated fibers denoted a significant reduction in multi-central nucleated fibers with β-GPA and a nonsignificant trend to reduction with 3-MA. D) C2C12 mouse myoblasts differentiated in low serum for 6 days with vehicle saline (Con), 1 mM 3-MA or 1 mM β-GPA treatment. Phase contrast images with NucBlue nuclear staining (10X objective) were analyzed for cells with myotube-like morphology. Each data point is the average of three 10X images from a single well. The experiment was repeated four times, with two wells per condition for each experiment. Scale bar: 50μm. * Statistically different than Con ($P < 0.05$). ** Statistically different than Con ($P < 0.01$). *** Statistically different than β-GPA ($P < 0.001$).

Effect of treatments on uninjured and injured muscle autophagy-related protein content following injury

To explore how autophagy may be contributing to the remodeling phase, we assessed the content of several autophagy-related proteins in injured and uninjured gastrocnemius muscle (Fig. 2.6A). A greater rate in the initiation and resolution of autophagy (i.e., autophagy flux) was investigated by detecting LC3-II, the phosphatidylethanolamine (PE)-conjugated form of LC3-I that attaches to the autophagosome membrane, and p62, a cargo receptor for ubiquitinated

substrates degraded by the autophagosome membranes (He et al., 2012; Mizushima, Levine, Cuervo, & Klionsky, 2008). Independent of treatment, total LC3, LC3-II, and p62 protein content was greater in injured muscle compared to uninjured muscle ($P \leq 0.003$), suggesting enhanced autophagosome assembly during muscle regeneration. Additionally, muscle injury caused an accumulation of autophagic marker p62, as there was intra-cellular p62 puncta visible in injured muscle tissue sections from control, 3-MA, and β-GPA-treated mice compared to uninjured muscle sections (Fig. 2.6B). The extent to which these data signify autophagy flux during muscle regeneration is limited by the single time point study design (i.e., 14 d post-injury), but supports the premise that autophagy is induced even 14-d post-injury.

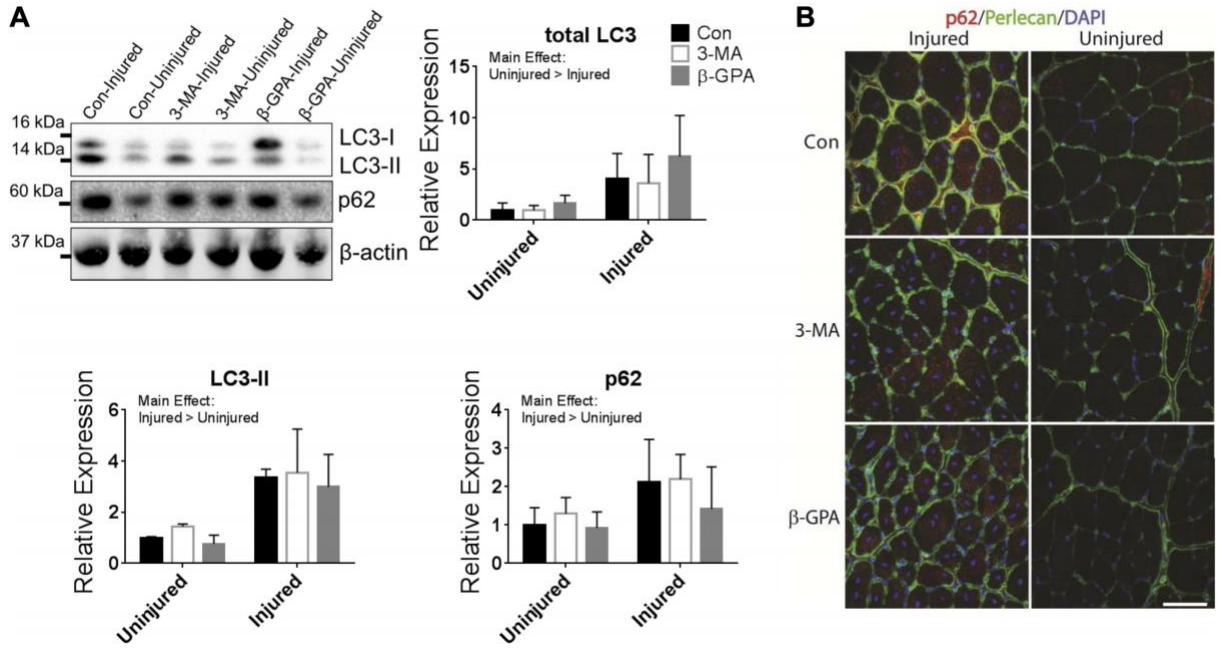

Figure 2.6: Effect of treatments and injury on markers of autophagosome assembly and autophagy flux.
A) Immunoblot images of LC3-I, LC3-II, and p62. β-actin was probed as loading control. Quantitative and statistical analysis are presented below and on the right (n=6-8/group). B) TA muscle sections from control (Con), 3-MA, and β-GPA-treated mice were immunostained with anti-p62 and anti-perlecan to detect the presence of p62 puncta. DAPI-stained nuclei are blue. Scale bar: 200μm

Total Ulk1 content (autophagy-related protein associated with degradation of mitochondria) was not different across treatment groups or injury at 14 d post-injury ($P = 0.455$) (data not shown). However, there was a significant interaction of injury and treatment group for phosphorylated (activated) Ulk1 (pUlk1, Fig. 2.7; $P = 0.049$). In all treatment groups, injured muscles had greater activation of Ulk1 compared to uninjured muscle (~2-fold). Also, there was a greater basal activation of Ulk1 in uninjured β-GPA muscle compared to uninjured 3-MA muscle. Because Ulk1 activation is associated with mitophagy and the degradation of dysfunctional mitochondria, we further investigated the mitophagy protein Bnip3 which interacts with LC3 and plays a critical role in mitophagy (Band, Joel, Hernandez, & Avivi, 2009; Zhang & Ney, 2009). Bnip3 protein content was significantly elevated in all injured muscle relative to uninjured contralateral muscles independent of treatment (Fig. 2.7; $P < 0.001$). Protein content for Drp1, a specialized protein that facilitates the removal of damaged or dysfunctional mitochondria from the mitochondrial network prior to mitophagy, was significantly greater in β-GPA and Con mice compared to 3-MA-treated mice independent of injury ($P = 0.049$), and greater in injured muscle compared to uninjured muscle independent of treatment (Fig. 2.7; $P = 0.023$). We observed no significant difference across groups in AMPK protein content (data not shown, $P = 0.877$), although phosphorylated AMPK (pAMPK) was significantly greater in injured muscle compared to uninjured muscle independent of treatment ($P = 0.012$).

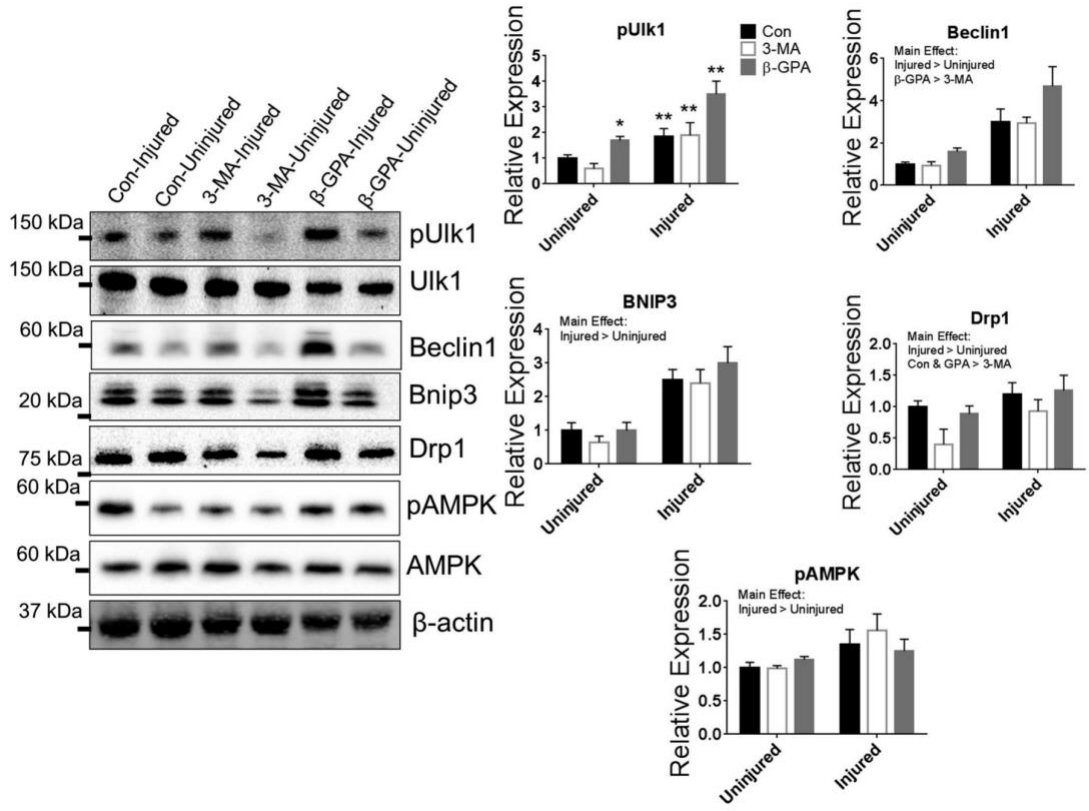

Figure 2.7: Effect of treatments and injury on autophagy-related protein content. Immunoblot images of 28hosphor-Ulk1 (pUlk1, serine555), total Ulk1, Beclin1, Bnip3, Drp1, phosphor-AMPK (pAMPK), and total AMPK. B-actin was probed as loading control. Quantitative and statistical analysis are presented on the right (n=6-8/group). * Significantly different than 3-MA ($P < 0.05$). ** Significantly greater than contralateral uninjured muscle within each group respectively ($P < 0.05$).

Discussion

The mitochondrial network is a dynamic system essential for energy balance, redox homeostasis, and may have an emerging role in regenerating skeletal muscle and satellite cells. Because the mitochondrial network can be damaged with muscle injury (Duguez et al., 2002; Wagatsuma et al., 2011) there is sufficient need to investigate the mechanisms of mitochondrial regeneration. However, mitochondrial regeneration remains a relatively under-investigated area of muscle repair. Herein, we sought to investigate the contribution of autophagy to mitochondrial regeneration during muscle repair. Our data indicates a robust induction of autophagy during

muscle regeneration (Fig. 2.6 & 2.7), and we show that a broad-acting autophagy inhibitor negatively affects functional regeneration of skeletal muscle both in terms of muscle strength and mitochondrial enzyme activities (Fig. 2.2 & 2.3). We show that muscle with enhanced mitochondrial content (i.e., β-GPA mice) demonstrates a near full recovery of muscle and mitochondrial enzyme activities by 14 d post-injury (Fig. 2.3), which demonstrates that β-GPA may positively influence muscle repair. We posit that the regeneration process is facilitated in part by autophagy, and we discuss below the broader impacts and limitations of our findings.

The recovery of muscle strength is the most functionally relevant marker of successful muscle regeneration (Warren, Lowe, & Armstrong, 1999). We decided to assess the relative success of muscle regeneration at 14 days post-injury based on the following rationale: 1) satellite cell contribution to muscle regeneration, specifically differentiation and fusion, is largely complete by 14 d post-injury and 2) others have reported that markers of mitochondrial biogenesis have returned to baseline by 14 d post-injury. Therefore, 14 d post-injury represents in our minds a critical transition period between muscle regeneration and muscle remodeling, when newly synthesized proteins are being utilized to repair or rebuild damaged organelles (i.e., mitochondria). Importantly, 3-MA-treated mice showed a substantial lack of strength recovery in stark contrast to β-GPA-treated mice (Fig. 2.2), and this finding is not completely explained by differences in myogenic differentiation (Fig. 2.5). The functional deficit in injured muscle from 3-MA-treated mice may instead reflect an important role for the mitochondria during muscle repair, i.e., to meet the energy demands of muscle regeneration. The muscle contractions used to assess strength at 14 days post-injury were not aerobically demanding (i.e., 200ms duration with 45 s in between) therefore the mitochondrial dysfunction in injured 3-MA muscle (Fig. 2.3) is unlikely to directly contribute to the observed muscle weakness (Fig. 2.2). Instead, the

dysfunctional mitochondria may limit aspects of late-stage satellite cell-mediated regeneration and/or remodeling. For instance, C2C12 myoblasts have been reported to experience significant shifts during differentiation to a predominately oxidative metabolism *in vitro* (Leary, Battersby, Hansford, & Moyes, 1998), and inhibition of mitochondrial biogenesis during muscle regeneration negatively affected the recovery of fiber cross-sectional area at 10-d post-injury (Wagatsuma et al., 2011). It stands to reason then that mitochondrial function and dysfunction in injured muscle may play an important role in the success of muscle regeneration, which is supported by our use of β-GPA to enhance oxidative capacity and our finding that this treatment improved the functional recovery of muscle strength and mitochondrial enzyme activities (Fig. 2.2 & 2.3).

Analysis of the mitochondrial network during the early phases of muscle regeneration following myotoxic injury, i.e., within the first 10 d, shows several mitochondrial functional deficits and not surprisingly structural abnormalities as well (Duguez et al., 2002; Wagatsuma et al., 2011). However, the removal and rebuilding of the mitochondrial network following many muscle injuries has been a relatively overlooked aspect of muscle recovery in general, and it is worth speculating that the accumulation of dysfunctional mitochondrial after several rounds of injury with impaired remodeling could lead to satellite cell dysfunction. Several studies have suggested that there is an accumulation of damaged mitochondria in skeletal muscle with age (Calvani et al., 2013), and that altered autophagy signaling can contribute to the age-related mitochondrial dysfunction (Wohlgemuth et al., 2011; Wohlgemuth, Seo, Marzetti, Lees, & Leeuwenburgh, 2010). Our current study implemented the chronic use of a broad-acting autophagy inhibitor to recapitulate disease models with defective autophagy but without the co-morbidities. While 3-MA and other autophagy inhibitors are used in standard practice to

compare rates of protein degradation with and without sufficient autophagy, these inhibitors are not without their limitations. 3-MA and other phosphatidylinositol inhibitors are broad-acting and therefore can have non-specific effects, and indeed have been shown to negatively impact other protein degradation processes. Notwithstanding, 3-MA-treated muscles did show signs of impaired mitochondrial function (i.e., reduced SDH and β-HAD activities) (Fig. 2.3). It is reasonable that an accumulation of dysfunctional mitochondria during chronic 3-MA treatment contributed to impaired muscle regeneration seen herein. For example, three weeks of high-fat diet, which induces mitochondrial dysfunction (Bonnard et al., 2008), impaired muscle regeneration in otherwise healthy mice (Woo et al., 2011). A direct link between mitochondrial dysfunction and satellite function has yet to be made but moving forward it is worth considering therapeutic modalities that could potentially enhance mitochondrial function to improve aforementioned diseased conditions (e.g., aging and obesity). Our work suggests that β-GPA treatment may have important clinical applications as a dietary intervention to improve the maintenance of the mitochondria and remodeling during muscle regeneration.

β-GPA is a creatine analog which hinders the ATP-phosphocreatine system thereby promoting mitochondrial biogenesis potentially through an AMPK-mediated signaling pathway (Chaturvedi et al., 2009; Pandke, Mullen, Snook, Bonen, & Dyck, 2008). While β-GPA is marked as safe for human consumption, its effective dose and acute/chronic effects have not been widely investigated, potentially for several reasons. First, β-GPA-treated mice are reported to have greater mitochondrial enzyme activities (Oudman et al., 2013), but the effective dose (1-2% of food intake by weight) and cost may in part contribute to a lack of scalability to human studies. Second, decrements in body mass and muscle strength have been reported as side effects of β-GPA treatment (as seen herein, Fig. 2.1) (Oudman et al., 2013), and this is potentially

disadvantageous for populations in which the mitochondrial benefit of β-GPA is needed (e.g., aging). However, β-GPA may be a potential dietary supplement to bolster mitochondrial capacity in individuals who cannot participate in aerobic exercise, or as a means to augment beneficial exercise training adaptations. Our work with β-GPA was used to manipulate the mitochondrial network in a way that contrasted autophagy inhibition with 3-MA. In line with reported effects of β-GPA, β-GPA-treated mice had greater fatigue resistance and mitochondrial enzyme activities in uninjured muscle. Interestingly, beyond the previously discussed finding of greater recovery of strength and mitochondrial enzyme activity, β-GPA-treated mice also demonstrated a greater basal level of pUlk1, the autophagy-related protein associated with induction of mitochondrial autophagy. This finding may simply reflect that the level of basal autophagy may be related to oxidative capacity in skeletal muscle (Lira et al., 2013). We believe these observations warrant more investigation into the role of β-GPA on mitochondrial maintenance.

The maintenance of the mitochondrial network involves the fusion of newly synthesized mitochondria following mitochondrial biogenesis balanced against the fission of damaged mitochondria to be degraded by autophagy (Calvani et al., 2013). We observed a fairly robust autophagy response to muscle injury even 14 days after injury (Fig. 2.6 & 2.7). Most interesting was the data supporting the specific degradation of mitochondria also known as mitophagy, which included greater activation of Ulk1 and greater BNIP3 and Drp1 protein content in injured muscle. While necrotic processes associated with inflammatory cell accumulation after muscle damage may be sufficient to degrade damaged mitochondria, this work supports at least a role for autophagy during the regeneration process and autophagy may represent a target for enhancing the regenerative process in situations when inflammatory processes are compromised (e.g., such as in aging). Our data suggest a disconnect between mitochondrial protein content

(Fig. 2.4; no statistical difference between Con & 3-MA-treated mice) and enzyme activities (Fig. 2.3; statistical differences between Con & 3-MA-treated mice) suggesting that damaged/dysfunctional mitochondrial proteins in 3-MA treated mice were not being properly degraded during the regeneration and remodeling processes following muscle injury.

In conclusion, there is an autophagy response to severe muscle damage that is detectable two weeks post-injury. A chronic and continuous treatment with a broad-acting autophagy inhibitor impaired functional muscle regeneration and mitochondrial remodeling after injury suggesting that successful autophagy after muscle injury plays is important for muscle repair. In particular, mitochondrial enzyme activities, but not mitochondrial protein content, were negatively affected by autophagy inhibition in 3-MA-treated mice during muscle regeneration. This coincided with less recovery of pre-injury strength in 3-MA-treated mice that is in stark contrast to the recovery of strength in β-GPA-treated mice, which also demonstrated a near full recovery of mitochondrial enzyme activities. We posit that mitochondrial function plays a minor albeit significant role in muscle regeneration, and that a link between mitochondrial maintenance and autophagy during muscle repair should be further explored.

References

Band, M., Joel, A., Hernandez, A., & Avivi, A. (2009). Hypoxia-induced BNIP3 expression and mitophagy: in vivo comparison of the rat and the hypoxia-tolerant mole rat, Spalax ehrenbergi. *FASEB J, 23*(7), 2327-2335. doi:10.1096/fj.08-122978

Beedle, A. M., Turner, A. J., Saito, Y., Lueck, J. D., Foltz, S. J., Fortunato, M. J., . . . Campbell, K. P. (2012). Mouse fukutin deletion impairs dystroglycan processing and recapitulates muscular dystrophy. *J Clin Invest, 122*(9), 3330-3342. doi:10.1172/JCI63004

Bonnard, C., Durand, A., Peyrol, S., Chanseaume, E., Chauvin, M. A., Morio, B., . . . Rieusset, J. (2008). Mitochondrial dysfunction results from oxidative stress in the skeletal muscle of diet-induced insulin-resistant mice. *J Clin Invest, 118*(2), 789-800. doi:10.1172/JCI32601

Call, J. A., Chain, K. H., Martin, K. S., Lira, V. A., Okutsu, M., Zhang, M., & Yan, Z. (2015). Enhanced skeletal muscle expression of extracellular superoxide dismutase mitigates streptozotocin-induced diabetic cardiomyopathy by reducing oxidative stress and aberrant cell signaling. *Circ Heart Fail, 8*(1), 188-197. doi:10.1161/CIRCHEARTFAILURE.114.001540

Call, J. A., Voelker, K. A., Wolff, A. V., McMillan, R. P., Evans, N. P., Hulver, M. W., . . . Grange, R. W. (2008). Endurance capacity in maturing mdx mice is markedly enhanced by combined voluntary wheel running and green tea extract. *J Appl Physiol (1985), 105*(3), 923-932. doi:10.1152/japplphysiol.00028.2008

Call, J. A., Warren, G. L., Verma, M., & Lowe, D. A. (2013). Acute failure of action potential conduction in mdx muscle reveals new mechanism of contraction-induced force loss. *J Physiol, 591*(Pt 15), 3765-3776. doi:10.1113/jphysiol.2013.254656

Calvani, R., Joseph, A. M., Adhihetty, P. J., Miccheli, A., Bossola, M., Leeuwenburgh, C., . . . Marzetti, E. (2013). Mitochondrial pathways in sarcopenia of aging and disuse muscle atrophy. *Biol Chem, 394*(3), 393-414. doi:10.1515/hsz-2012-0247

Chaturvedi, R. K., Adhihetty, P., Shukla, S., Hennessy, T., Calingasan, N., Yang, L., . . . Beal, M. F. (2009). Impaired PGC-1alpha function in muscle in Huntington's disease. *Hum Mol Genet, 18*(16), 3048-3065. doi:10.1093/hmg/ddp243

Duguez, S., Feasson, L., Denis, C., & Freyssenet, D. (2002). Mitochondrial biogenesis during skeletal muscle regeneration. *Am J Physiol Endocrinol Metab, 282*(4), E802-809. doi:10.1152/ajpendo.00343.2001

Fortunato, M. J., Ball, C. E., Hollinger, K., Patel, N. B., Modi, J. N., Rajasekaran, V., . . . Beedle, A. M. (2014). Development of rabbit monoclonal antibodies for detection of alpha-dystroglycan in normal and dystrophic tissue. *PLoS One, 9*(5), e97567. doi:10.1371/journal.pone.0097567

Gianni, P., Jan, K. J., Douglas, M. J., Stuart, P. M., & Tarnopolsky, M. A. (2004). Oxidative stress and the mitochondrial theory of aging in human skeletal muscle. *Exp Gerontol, 39*(9), 1391-1400. doi:10.1016/j.exger.2004.06.002

Hamai, N., Nakamura, M., & Asano, A. (1997). Inhibition of mitochondrial protein synthesis impaired C2C12 myoblast differentiation. *Cell Struct Funct, 22*(4), 421-431.

He, C., Bassik, M. C., Moresi, V., Sun, K., Wei, Y., Zou, Z., . . . Levine, B. (2012). Exercise-induced BCL2-regulated autophagy is required for muscle glucose homeostasis. *Nature, 481*(7382), 511-515. doi:10.1038/nature10758

Hochreiter-Hufford, A. E., Lee, C. S., Kinchen, J. M., Sokolowski, J. D., Arandjelovic, S., Call, J. A., . . . Ravichandran, K. S. (2013). Phosphatidylserine receptor BAI1 and apoptotic cells as new promoters of myoblast fusion. *Nature, 497*(7448), 263-267. doi:10.1038/nature12135

Huard, J., Li, Y., & Fu, F. H. (2002). Muscle injuries and repair: current trends in research. *J Bone Joint Surg Am, 84-A*(5), 822-832.

Landisch, R. M., Kosir, A. M., Nelson, S. A., Baltgalvis, K. A., & Lowe, D. A. (2008). Adaptive and nonadaptive responses to voluntary wheel running by mdx mice. *Muscle Nerve, 38*(4), 1290-1303. doi:10.1002/mus.21141

Leary, S. C., Battersby, B. J., Hansford, R. G., & Moyes, C. D. (1998). Interactions between bioenergetics and mitochondrial biogenesis. *Biochim Biophys Acta, 1365*(3), 522-530.

Lira, V. A., Okutsu, M., Zhang, M., Greene, N. P., Laker, R. C., Breen, D. S., . . . Yan, Z. (2013). Autophagy is required for exercise training-induced skeletal muscle adaptation and improvement of physical performance. *FASEB J, 27*(10), 4184-4193. doi:10.1096/fj.13-228486

Masiero, E., & Sandri, M. (2010). Autophagy inhibition induces atrophy and myopathy in adult skeletal muscles. *Autophagy, 6*(2), 307-309.

Mizushima, N., Levine, B., Cuervo, A. M., & Klionsky, D. J. (2008). Autophagy fights disease through cellular self-digestion. *Nature, 451*(7182), 1069-1075. doi:10.1038/nature06639

Oudman, I., Clark, J. F., & Brewster, L. M. (2013). The effect of the creatine analogue beta-guanidinopropionic acid on energy metabolism: a systematic review. *PLoS One, 8*(1), e52879. doi:10.1371/journal.pone.0052879

Pandke, K. E., Mullen, K. L., Snook, L. A., Bonen, A., & Dyck, D. J. (2008). Decreasing intramuscular phosphagen content simultaneously increases plasma membrane FAT/CD36 and GLUT4 transporter abundance. *Am J Physiol Regul Integr Comp Physiol, 295*(3), R806-813. doi:10.1152/ajpregu.90540.2008

Pauly, M., Daussin, F., Burelle, Y., Li, T., Godin, R., Fauconnier, J., . . . Petrof, B. J. (2012). AMPK activation stimulates autophagy and ameliorates muscular dystrophy in the mdx mouse diaphragm. *Am J Pathol, 181*(2), 583-592. doi:10.1016/j.ajpath.2012.04.004

Ryall, J. G. (2013). Metabolic reprogramming as a novel regulator of skeletal muscle development and regeneration. *FEBS J, 280*(17), 4004-4013. doi:10.1111/febs.12189

Sandri, M. (2010). Autophagy in health and disease. 3. Involvement of autophagy in muscle atrophy. *Am J Physiol Cell Physiol, 298*(6), C1291-1297. doi:10.1152/ajpcell.00531.2009

Selsby, J. T., Morine, K. J., Pendrak, K., Barton, E. R., & Sweeney, H. L. (2012). Rescue of dystrophic skeletal muscle by PGC-1alpha involves a fast to slow fiber type shift in the mdx mouse. *PLoS One, 7*(1), e30063. doi:10.1371/journal.pone.0030063

Wagatsuma, A., Kotake, N., & Yamada, S. (2011). Muscle regeneration occurs to coincide with mitochondrial biogenesis. *Mol Cell Biochem, 349*(1-2), 139-147. doi:10.1007/s11010-010-0668-2

Wang, H., Hiatt, W. R., Barstow, T. J., & Brass, E. P. (1999). Relationships between muscle mitochondrial DNA content, mitochondrial enzyme activity and oxidative capacity in

man: alterations with disease. *Eur J Appl Physiol Occup Physiol, 80*(1), 22-27. doi:10.1007/s004210050553

Warren, G. L., Lowe, D. A., & Armstrong, R. B. (1999). Measurement tools used in the study of eccentric contraction-induced injury. *Sports Med, 27*(1), 43-59.

Wohlgemuth, S. E., Lees, H. A., Marzetti, E., Manini, T. M., Aranda, J. M., Daniels, M. J., . . . Anton, S. D. (2011). An exploratory analysis of the effects of a weight loss plus exercise program on cellular quality control mechanisms in older overweight women. *Rejuvenation Res, 14*(3), 315-324. doi:10.1089/rej.2010.1132

Wohlgemuth, S. E., Seo, A. Y., Marzetti, E., Lees, H. A., & Leeuwenburgh, C. (2010). Skeletal muscle autophagy and apoptosis during aging: effects of calorie restriction and life-long exercise. *Exp Gerontol, 45*(2), 138-148. doi:10.1016/j.exger.2009.11.002

Woo, M., Isganaitis, E., Cerletti, M., Fitzpatrick, C., Wagers, A. J., Jimenez-Chillaron, J., & Patti, M. E. (2011). Early life nutrition modulates muscle stem cell number: implications for muscle mass and repair. *Stem Cells Dev, 20*(10), 1763-1769. doi:10.1089/scd.2010.0349

Wu, Z., Puigserver, P., Andersson, U., Zhang, C., Adelmant, G., Mootha, V., . . . Spiegelman, B. M. (1999). Mechanisms controlling mitochondrial biogenesis and respiration through the thermogenic coactivator PGC-1. *Cell, 98*(1), 115-124. doi:10.1016/S0092-8674(00)80611-X

Zhang, J., & Ney, P. A. (2009). Role of BNIP3 and NIX in cell death, autophagy, and mitophagy. *Cell Death Differ, 16*(7), 939-946. doi:10.1038/cdd.2009.16

CHAPTER 3

MITOCHONDRIAL-SPECIFIC AUTOPHAGY LINKED TO MITOCHONDRIAL DYSFUNCTION FOLLOWING TRAUMATIC FREEZE INJURY IN MICE[1]

[1] Nichenko, A.S. Southern, WM. Tehrani, KF. Qualls, AE. Flemington, AB. Mercer, GH. Yin, A. Mortensen, LJ. Yin, H. Call, JA. 2020. *Am J Physiol Cell Physiol*. 318(2):C242-C252. Reprinted here with permission of the publisher.

Abstract

The objective of this study was to interrogate the link between mitochondrial dysfunction and mitochondrial-specific autophagy in skeletal muscle. C57BL/6J mice were used to establish a timecourse of mitochondrial function and autophagy induction after fatigue (n=12), eccentric contraction-induced injury (n=20), or traumatic freeze injury (FI, n=28); and only FI resulted in a combination of mitochondrial dysfunction, i.e., decreased mitochondrial respiration, and autophagy induction. Moving forward, we tested the hypothesis that mitochondrial-specific autophagy is important for the timely recovery of mitochondrial function after FI. Following FI, there is a significant increase in several mitochondrial-specific autophagy-related protein contents including Drp1, BNIP3, Pink1, and Parkin (~2-fold, $p<0.02$). Also, mitochondrial-enriched fractions from FI muscles showed LC3II co-localization suggesting autophagosome assembly around the damaged mitochondrial. Unc-51 like autophagy activating kinase (Ulk1) is considered necessary for mitochondrial-specific autophagy and herein we utilized a mouse model with Ulk1 deficiency in adult skeletal muscle (*myogenin-cre*). While Ulk1 knockouts had contractile weakness compared to littermate controls (-27%, $p<0.02$) the recovery of mitochondrial function was not different, and this may be due in part to a partial rescue of Ulk1 protein content within the regenerating muscle tissue of knockouts from differentiated satellite cells in which Ulk1 was not genetically altered via *myogenin-cre*. Lastly, autophagy flux was significantly less in injured vs. uninjured muscles (-26%, $p<0.02$) despite the increase in autophagy-related protein content. This suggests autophagy flux is not upregulated to match increases in autophagy machinery after injury and represents a potential bottleneck in the clearance of damaged mitochondria by autophagy.

Introduction

Mitochondria play an important role during muscle regeneration because they provide crucial energy for the repair of initial membrane disruption, the remodeling of damaged muscle fibers, and satellite cell proliferation and differentiation (Garcia-Prat et al., 2016; X. Wang et al., 2013). Mitochondria can be affected by muscle injury, as we and others have reported a decrease in mitochondrial content and a subsequent rise in mitochondrial biogenesis during muscle regeneration (Call et al., 2017; Duguez et al., 2002; Nichenko et al., 2016; Wagatsuma et al., 2011). Our first motivation for this study was to define the extent to which fatigue, eccentric contraction-induced injury, and traumatic freeze injury cause mitochondrial dysfunction. Each of these muscle stressors has been implicated in mitochondrial stress without thorough assessment of mitochondrial oxygen consumption, i.e., respiration. Additionally, fatigue, eccentric contraction-induced injury and freeze injury are reported to increase autophagy, a cellular response indicative of mitochondrial damage, which we have previously linked to the success of the regenerative process (Call et al., 2017; Nichenko et al., 2016).

We have previously highlighted that when portions of the mitochondria network are stressed or damaged there is an increase in proteins related to autophagy (Call et al., 2017; Nichenko et al., 2016). Autophagy is a cellular process which degrades dysfunctional organelles and proteins into their original amino acid and fatty acid components to be recycled in the cell. Autophagy is always basally active in skeletal muscle but can increase in response to stress stimuli such as exercise or caloric restriction (Lira et al., 2013; Yang et al., 2016). Autophagy is initiated under such stressful conditions by phosphorylation of the autophagy-related protein Unc-51 like autophagy activating kinase (Ulk1) at serine 555 by AMPK (Egan et al., 2011)). Ulk1-mediated autophagy has been reported by us and others to play an important role in

exercise-induced metabolic adaptations and recovery of muscle strength following traumatic injury, and is considered to be necessary for mitochondrial-specific autophagy referred to as mitophagy (Call et al., 2017; Egan et al., 2011; Laker et al., 2017; Tian et al., 2015). The secondary objective of this study was to further define the link between mitochondrial stress and Ulk1-mediated autophagy, and to determine if Ulk1 was necessary for the functional recovery of mitochondria following muscle injury. Understanding the specific role of Ulk1-mediated autophagy after muscle fiber damage may be leveraged to develop targeted therapeutic modalities to address muscle regeneration in conditions such as aging and muscular dystrophy where deficits in muscle repair and autophagy have been reported (Marzetti et al., 2013; Pauly et al., 2012; Sandri, Coletto, Grumati, & Bonaldo, 2013).

We initially hypothesized that fatigue, eccentric contraction-induced injury, and traumatic freeze injury would cause a temporary loss in mitochondrial function. We also hypothesized that these muscle stressors would subsequently cause an increase in mitochondrial-specific autophagy (to degrade the dysfunctional mitochondria), and that Ulk1-mediated autophagy would therefore be necessary for the timely recovery of mitochondrial function following muscle fiber damage. Herein, we quickly determined that only traumatic freeze injury corresponds to a loss of mitochondrial function and we subsequently interrogated the link between this traumatic injury and the autophagy response.

Methods

Ethical Approval

All animal protocols were approved by the University of Georgia Animal Care and Use Committee under the national guidelines set by the Association for Assessment and Accreditation of Laboratory Animal Care.

Animal Models

Male and female C57BL/6J mice aged 3-4 months were bred in-house and housed 5 per cage in a temperature-controlled facility with a 12:12 hour light:dark cycle. Muscle-specific Unc-51 like autophagy knockout mice (Ulk1 MKO) with *myogenin-Cre* and LoxP flanked *Ulk1*and their *myogenin-Cre* negative littermates (LM) were used to test the necessity of Ulk1 for mitochondrial function and strength recovery after traumatic freeze injury. All mice had *ab libitum* access to food and water throughout the experiments.

Experimental Design

This study was originally designed to investigate the time course of mitochondrial dysfunction and subsequent autophagic response to fatigue, eccentric contraction-induced injury, and traumatic freeze injury as these muscle stressors have all been linked to mitochondrial damage. Early results strongly indicating a lack of mitochondrial dysfunction following fatigue and eccentric contraction-induced injury; therefore, only traumatic freeze injury was utilized on mouse cohorts two and three that further investigated the link between mitochondrial damage and autophagy.

The first cohort of wildtype C57BL/6J mice were used to assess the time course of mitochondrial function and autophagy induction after various muscle stressors (Fig. 3.1). Briefly, mice were randomized into 3 groups; (i) a non-damaging metabolically fatiguing challenge

(n=12), (ii) eccentric contraction-induced injury (n=20)(Call, Eckhoff, Baltgalvis, Warren, & Lowe, 2011), and (iii) traumatic freeze injury (n=28). Tissues were analyzed for mitochondrial function, mitochondrial content, and autophagy induction immediately, 6 hours, and one day post for all groups. No additional time points were assessed for the fatigue group because initial data indicated there were no significant changes (Fig. 3.2 & 3.3). Additional time points, 3 and 7 days post, were assessed for the eccentric-contraction induced and freeze injury groups to characterize changes in mitochondrial function during the first week of recovery.

A second cohort of wildtype C57BL/6J mice were used to analyze mitochondrial-specific autophagy following traumatic freeze injury based on results from the first cohort (Fig. 3.1). Unilateral freeze injuries were performed on all mice before randomization into two groups. The first group (n=7) were used to probe mitochondrial-specific autophagy-related proteins at 7 days after injury via immunoblot. The second group (n=10) were used to determine the accumulation of autophagy-related proteins to the mitochondria relying on differential centrifugation and immunoblot.

A third cohort of mice included Ulk1 MKO and LM mice to test the necessity of Ulk1 for autophagy flux (i.e., ongoing autophagy) and for recovery of mitochondrial function after injury (Fig. 3.1) (Egan et al., 2011; Kim, Kundu, Viollet, & Guan, 2011; Kundu et al., 2008). A first group of Ulk1 MKO and LM mice were electroporated with the GFP-LC3-RFP-LC3Δ plasmid obtained from Addgene (RRID: Addgene_84572) that allows fluorescent assessment of autophagy flux as a GFP portion is quenched during autophagy flux while the RFP portion serves as an external reference control. Mice were bilaterally transfected 3 weeks prior to unilateral freeze injury (n=6), and 7 days after injury, autophagy flux was assessed via GFP:RFP ratio captured through two-photon microscopy imaging. A second group of Ulk1 MKO and LM

mice (n=20) underwent unilateral freeze injuries and the recovery of peak-isometric dorsiflexion torque and mitochondrial function were determined at 14 days post injury. The selection of 14 days after injury was based on the results from cohort 1 showing mitochondrial function was less than one-third of uninjured at 7 days after injury (Fig. 3.2), and results from our previous studies indicating 14 days is sufficient to observe differences in mitochondrial content with insufficient autophagy (Call et al., 2017; Nichenko et al., 2016)

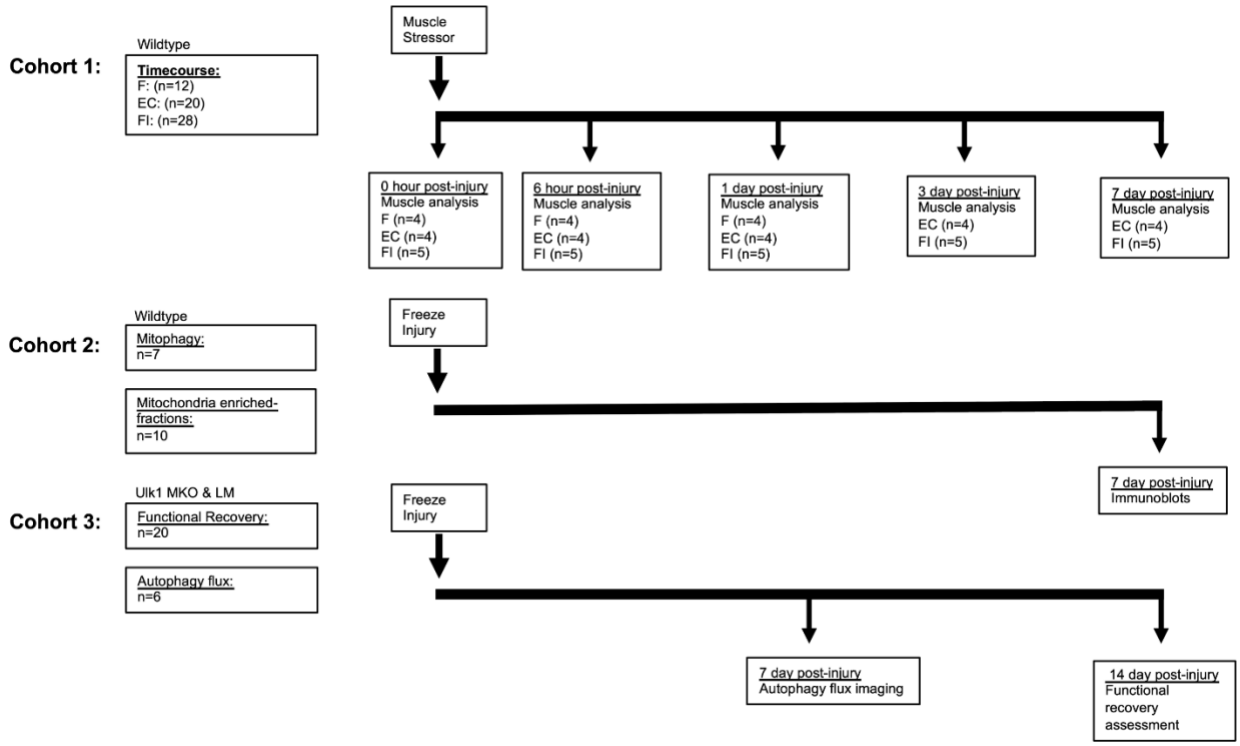

Figure 3.1: Study Design
Diagram representing the 3 different cohorts of mice used in the study. Cohort 1 was used to determine the time course of mitochondrial dysfunction and autophagy induction after different muscle stressors. Cohort 2 was used to determine the amount of mitochondrial-specific autophagy after traumatic freeze injury. Cohort 3 was used to determine the necessity of Ulk1-mediated autophagy in the recovery of mitochondrial function and in regulating autophagy flux.

Metabolic Fatiguing Protocol

Mice were anesthetized using 1-2% isoflurane in oxygen, and left hind limb was shaved and aseptically prepared. The foot was positioned into a foot-plate attached to the servomotor

(Model 129 300C-LR; Aurora Scientific, Aurora, Ontario, Canada) where the ankle joint was adjusted to a 90° angle and secured at the knee joint. Platinum-Iridium (Pt-Ir) needle electrodes were inserted percutaneously on both sides of the peroneal nerve and the testing platform was maintained at 37°C throughout the optimization and muscle stressor protocols. Optimal muscle stimulation was achieved by finding peak-isometric torque of the ankle dorsiflexors (tibialis anterior (TA), extensor digitorum longus (EDL), extensor hallucis longus muscles) through increasing the current stimulating the peroneal nerve at a 200 Hz pulse frequency prior to executing the muscle stressor protocol. The fatiguing protocol consisted of 30 minutes of continuous 10Hz stimulation which was modeled after muscle activation during a 30 minute treadmill run (Baltgalvis et al., 2012).

Eccentric Contraction-Induced Injury

Mice were prepared, optimal muscle stimulation was verified following the methods listed above, and eccentric contraction-induced injury protocol was executed as previously described (Call et al., 2011; Call et al., 2013b). Briefly, for the eccentric contraction-induced injury, the foot was passively moved from the 0° position (perpendicular to the tibia) to 20° of dorsiflexion. The ankle dorsiflexor muscles were stimulated at 200 Hz for a 100-ms isometric contraction followed by an additional 50-ms stimulation while moving from 20° dorsiflexion to 20° plantarflexion at an angular velocity of 2000°/s. Eccentric contractions were repeated every 10 seconds until a total of 100 electronically stimulated eccentric contractions were complete.

Freeze Injury

Freeze injury was performed as previously described (Warren et al., 2007). Before surgery, mice were anesthetized using isoflurane and given a local anesthetic injection of bupivacaine (5mg/kg) (Klionsky et al.). Afterwards, the left limb was aseptically prepared, a

1.5cm incision was made over the TA muscle, and a steel probe cooled with dry ice was applied to the belly of the TA for 10 seconds. Upon completion of the freeze injury, the incision was closed with nylon suture and mice were administered meloxicam (2mg/kg) for pain management immediately and again 12 hours after surgery (Warren et al., 2007).

Oxygen Consumption Rates

Mitochondrial function was assessed via oxygen consumption rates in dissected permeabilized muscle fiber bundles from both the stressed and contralateral control limb using methods adapted from Kuznetsov et al. and as we have previously described (Kuznetsov et al., 2008; Southern et al., 2017). To ensure we were testing homogenously stressed muscle fibers, entire EDL muscles were permeabilized for the eccentric contraction-induced injury and fatiguing protocol and TA muscle fibers were dissected from the affected area for the freeze injury group. Oxygen consumption rates were made through the use of a Clark-type electrode (Hansetech) kept at a constant 25°C with constant stirring. State III respiration was accomplished by addition of glutamate (10mM), malate (5mM), succinate (10mM), and ADP (5mM). Oxygen consumption rates during State III respiration were normalized to tissue mass loaded into chamber.

Enzyme Assays

Both citrate synthase (Klionsky et al.) and succinate dehydrogenase (SDH) enzyme assays were performed to quantify mitochondrial content in the stressed and contralateral control limbs after muscle fatigue, eccentric contraction-induced injury, and freeze injury. The portion of muscle remaining after fiber dissection for oxygen consumption rates was weighed and homogenized in 33mM phosphate buffer (pH 7.4) at a muscle to buffer ratio of 1:40 using a glass tissue grinder. Citrate Synthase activity was measured from the reduction of DTNB overtime as

previously described (Nichenko et al., 2016). Succinate Dehydrogenase activity was measured from the reduction of cytochrome c as previously described (Foltz et al., 2016).

Immunoblot

The following autophagy-related proteins were analyzed using immunoblot (1:1000 dilution) to determine protein contents within whole muscle homogenates or enriched fractions, i.e., cytosolic and mitochondrial: Beclin1 (RRID:AB_1903911); LC3 B (RRID:AB_915950); DRP1 (D6C7) (RRID:AB_10950498); Pink1 (RRID:AB_11179069); Parkin (RRID:AB_10693040); BNIP3 (RRID:AB_2259284); CoxIV (RRID:AB_2085424); Ulk1 (RRID:AB_11178668). Protein was extracted from stressed and contralateral control muscles. 25 μg of total protein was separated by SDS-PAGE, transferred onto a PVDF membrane, and immunoblotted as previously described (Nichenko et al., 2016). Immunoblots were normalized to total protein in lane and quantified using Bio-Rad Laboratories Image Lab software (Hercules, CA) (Collins, An, Peller, & Bowser, 2015; Vigelso et al., 2015; Zeitler, Gerrer, Haas, & Jimenez-Soto, 2016).

Differential Centrifugation

Differential centrifugation was used to gain insight into mitochondrial-specific autophagy following muscle fiber damage utilizing an approach reported by Laker and colleagues analyzing the amount of autophagy-related protein LC3 present in mitochondrial-enriched fractions (Laker et al., 2017). To obtain mitochondrial-enriched fractions and cytosolic fractions, differential centrifugation was performed on injured and contralateral uninjured TA muscles 14 days after injury as described (Laker et al., 2017). Briefly, muscles were homogenized in fractionation buffer [20 mM HEPES, 250 mM Sucrose, 0.1 mM EDTA, plus protease and phosphatase] in a glass tissue homogenizer at a 1:20 tissue to buffer ratio. Homogenates were then spun at

800×*g* for 10 min at 4°C, supernatant was removed and then spun at 9000×*g* for 10 min at 4°C. The supernatant was again removed and resuspended in an equal volume of 2x lamelli buffer resulting in the cytosolic fraction. The remaining mitochondrial pellets were resuspended in fractionation buffer then spun at 11,000×*g* for 10 min at 4°C. Resulting mitochondrial-enriched pellets were resuspended in 20 µl of 2x lamelli buffer resulting in the mitochondrial-enriched fraction. Both fractions were boiled for 5 min at 97°C, then frozen at −80°C until immunoblot analysis.

Autophagy Flux Plasmid Transfection

Autophagy flux was assessed utilizing the *in vivo* expression of a GFP-LC3-RFP-LC3Δ plasmid imaged via 2-photon microscopy. GFP-LC3-RFP-LC3Δ plasmid (Addgene, #84572) was prepared by CsCl gradient centrifugation method from 1 L inoculated LB media (Sambrook & Russell, 2006). In vivo electroporation of the TA muscle was performed as previously described (Aihara & Miyazaki, 1998). Briefly, 30ug/ul of plasmid was injected into the TA. A BTX ECM 830 system equipped with 5mm 2-needle arrays was used for electroporation. 3 electrical pulses set at a voltage of 100V and pulse length of 50msec were used for transfection. After 3 pulses were completed the needles were reversed and three additional pulses were done with the same settings.

2-photon Scanning Microscopy and image analysis

We used our home-built microscope (Tehrani et al., 2019) for multi-photon microscopy of TA muscles. We used 940 nm excitation laser for excitation and GFP and 775 nm light for excitation of RFP (both 120 fs, linearly polarized). For GFP and RFP we used 509/22 nm and 585/40 nm (Semrock) filters respectively. Bundles of muscle fibers were extracted, stabilized on a dissection gel, and placed under the microscope's objective lens. Imaging was performed using

a 60x water immersion objective lens (Olympus LUMFLN 60x) directly on the tissue immersed in Krebs Ringer buffer. To process the images, we first denoised the images by 3D Gaussian blur filtering (standard deviation = 380nm) and produced a binary mask from the RFP channel data using Otsu's method. We then applied the same mask to both channels, and calculated the average fluorescence reading of the masked area in each channel, and the ratios of GFP to RFP for each stack.

Immunofluorescent staining for satellite cells

Satellite cell dynamics were evaluated as previously described (Xie et al., 2018). Briefly, injured muscles from MKO mice (n=6) and LM mice (n=6) were isolated at 10 days post-injury and subjected to cryo-sectioning. Muscle sections were stained with primary antibody, Pax7 (1:5; DSHB at the University of Iowa) and Ki67 (1:1000; RRID:AB_302459) overnight at 4 degrees, followed with a secondary antibody stain at room temperature for 1 hour. To evaluate satellite cell dynamics, muscle cross-sections (at 3 representative levels) were used to enumerate the total number of satellite cells (Pax7+), proliferating satellite cells (Pax7+/Ki67+), and self-renewing satellite cells (Pax7+/Ki67-).

Statistics

Differences in mitochondrial function, mitochondrial content and autophagy protein expression after different muscle stressors were analyzed by two-way repeated measures (RM) analysis of variance (ANOVA) with the repeated measures being the injured vs. uninjured contralateral control limb and the other factor being time. Differential centrifugation immunoblots were analyzed by two-way RM ANOVA with the repeated measures being the injured vs. uninjured contralateral control limb and the other factor being fraction (mitochondria-enriched or cytosolic). Ulk1 KO and LM comparisons were analyzed by two-way RM ANOVA

with the repeated measures being the injured vs. uninjured contralateral control limb and the other factor being genotype. All data were required to pass normality (Shapiro-Wilk) and equal variance tests (Brown-Forsythe *F* test) before proceeding with the two-way RM ANOVA. Significant interactions were tested with Tukey's *post hoc* test using JMP statistical software (SAS, Cary, NC) to find differences between groups. Group main effects are reported where significant interactions were not observed. An α level of 0.05 was used for all analyses and all values are means ± SD.

Results

Time course of mitochondrial dysfunction and content after different muscle stressors

Across all conditions of muscle stress, there was no effect of time on mitochondrial function or content in the contralateral control limb ($p \geq 0.55$) therefore only the collective mean (dashed line) and standard deviations (grey region) are represented in each panel of Fig. 3.2. There was no difference in mitochondrial function or enzyme content between stressed and contralateral control limbs at any time point after the metabolic fatigue protocol (Main Effect: Limb, $p \geq 0.24$, Fig. 3.2A). Similarly, there was no difference in mitochondrial function or content following the eccentric contraction-induced injury protocol (Main Effect: Limb, $p \geq 0.17$, Fig. 3.2B). Mitochondrial function was significantly decreased 6 hours after traumatic freeze injury (20% of uninjured), continued to decline to its lowest functional capacity one day after injury (12% of uninjured), and by seven days after injury had recovered to ~34% of uninjured control limbs (Significant Interaction: $p=0.006$, Fig. 3.2C). Mitochondrial content was not significantly different from contralateral control limbs until day 7 post-injury (Significant Interaction, $p \leq 0.021$, Fig. 3.2C) suggesting a disproportionate loss of mitochondrial function early after freeze injury.

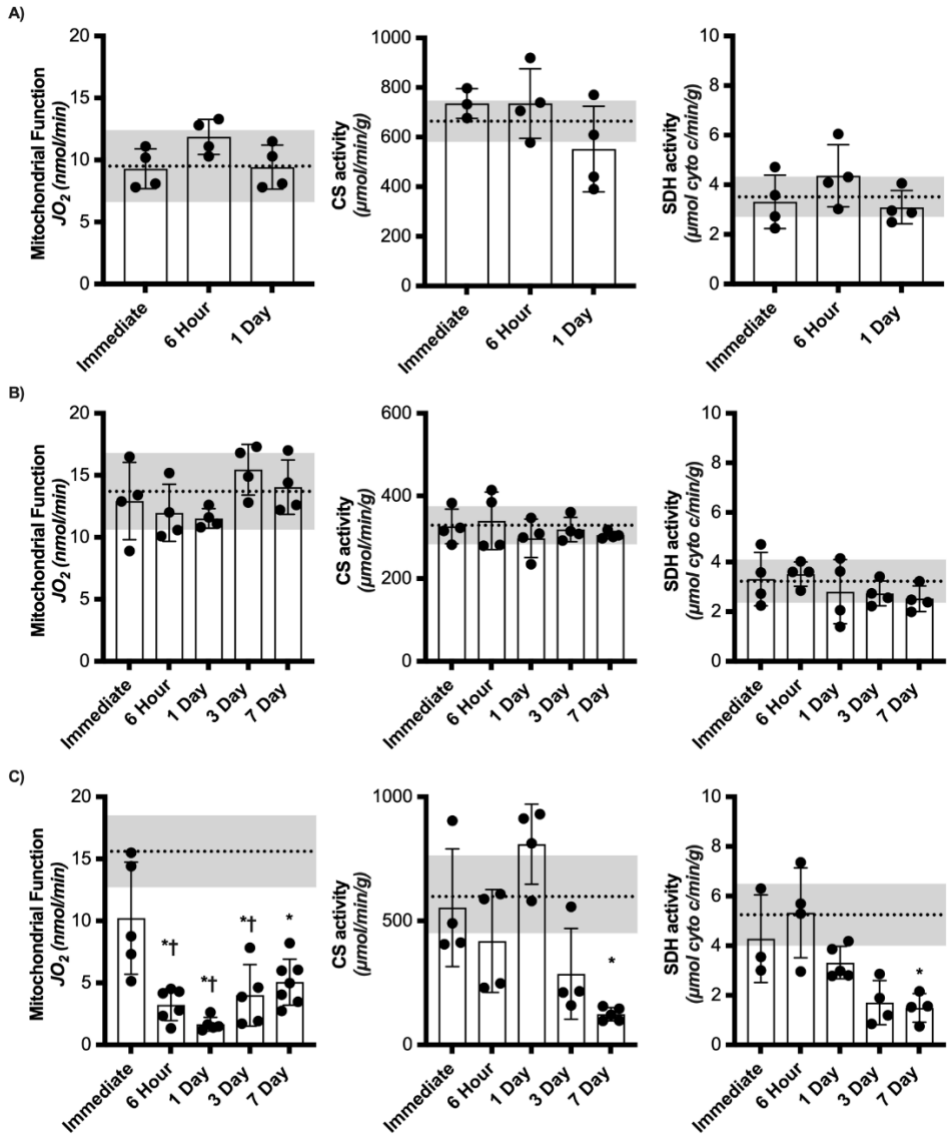

Figure 3.2: Time course of mitochondrial function and content changes after different muscle stressors.

Oxygen consumption measurements of permeabilized TA or EDL muscle fibers and mitochondrial enzyme assays (CS and SDH) immediately, 6 hours, 1, 3, and 7 days after A) fatiguing protocol (n=12), B) Eccentric contraction-induced injury (n=20), C) traumatic freeze injury (n=28). Dashed line represents average contralateral control limb and shaded grey regions are ± SD of control limb. Stressed limb data are presented as means ± SD. Differences in mitochondrial function and content at different time points after muscle stress were analyzed by RM ANOVA with the repeated measures being the injured vs. uninjured contralateral control limb and the other factor being time. * Significantly different from uninjured, † significantly different from immediate injured.

Time course of autophagy induction after different muscle stressors

Immunoblots of Beclin1 and LC3II were analyzed to determine the time course of autophagy induction after different muscle stressors. There was no change in relative expression of Beclin1 or LC3II in the stressed limb compared to the control limb after the fatiguing protocol ($p \geq 0.728$, Fig. 3.3A). Beclin1 expression increased 2-fold 3 days after the eccentric contraction-induced injury and remained elevated through 7 days post injury (Significant Interaction, $p=0.014$, Fig. 3.3B), however, no significant change was observed with LC3II ($p=0.9023$). In contrast, traumatic freeze injury resulted in a robust autophagy induction evident by a 28-fold increase in Beclin1 expression and a 5-fold increase in LC3II at 7 days after injury ($p \leq 0.008$, Fig. 3.3C).

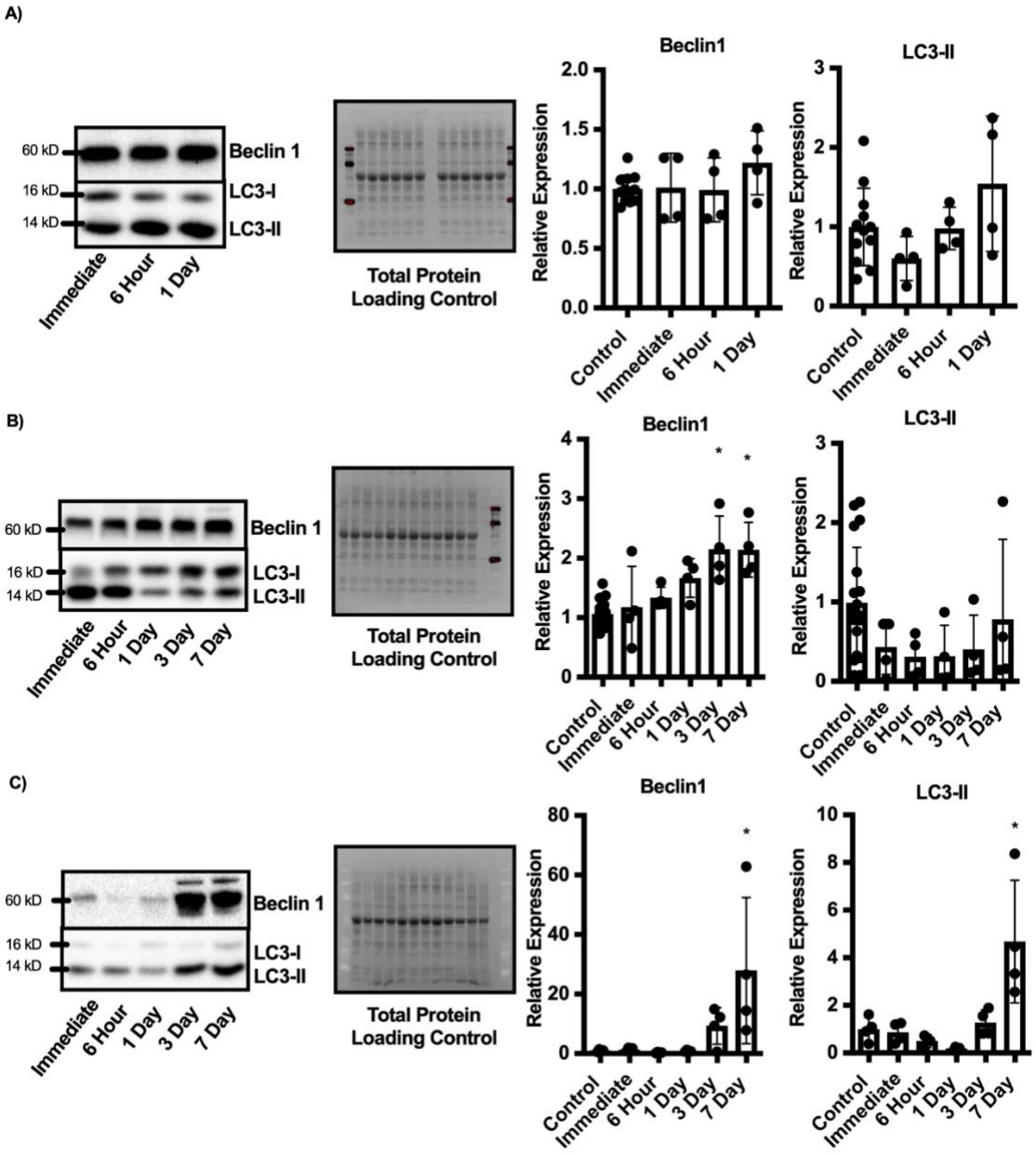

Figure 3.3: Time course of autophagy-related protein expression after different muscle stressors. Representative immunoblot and semi-quantitative analysis of Beclin1 and LC3II relative expression compared to control uninjured limb immediately, 6 hours, 1, 3, and 7 days after A) fatiguing protocol (n=12), B) Eccentric contraction-induced injury (n=20), C) traumatic freeze injury (n=28). Blots are normalized to total protein as a loading control and presented as relative expression to control uninjured limbs. Data are presented as means ± SD. Differences in protein expression at different time points after muscle stress were analyzed by RM ANOVA with the repeated measures being the injured vs. uninjured contralateral control limb and the other factor being time.* significantly different from control limb.

Mitochondrial specific autophagy after traumatic freeze injury

Because autophagy induction appeared to accompany mitochondrial dysfunction after freeze injury (Fig. 3.2 & 3.3), immunoblots of mitochondrial-specific autophagy related proteins were analyzed. The mitochondrial fission associated protein Drp1, the mitochondrial-specific autophagy machinery recruiting protein Bnip-3, and the damaged mitochondrial targeting proteins pink1 and parkin expression increased ~2-fold after injury ($p \leq 0.0138$, Fig. 3.4A). Additionally, cytosolic fractions and mitochondrial-enriched fractions were subject to immunoblot analysis of LC3II to further elucidate the extent of mitochondrial-specific autophagy. COXIV expression was increased 8-fold in the mitochondrial-enriched fractions compared to the cytosolic fractions (Fig. 3.4B) (COXIV Main Effect: Fraction, $p=0.049$). Interestingly, LC3II expression was 37 times greater in the injured mitochondrial-enriched fractions compared to the injured cytosolic fractions suggesting a large mitochondrial-specific autophagy response to traumatic freeze injury (Fig. 3.4B) (Significant Interaction, $p=0.017$), in agreement with previous reports of accumulation of autophagy-related proteins at the mitochondria after physiological muscle stress (Call et al., 2017; Laker et al., 2017).

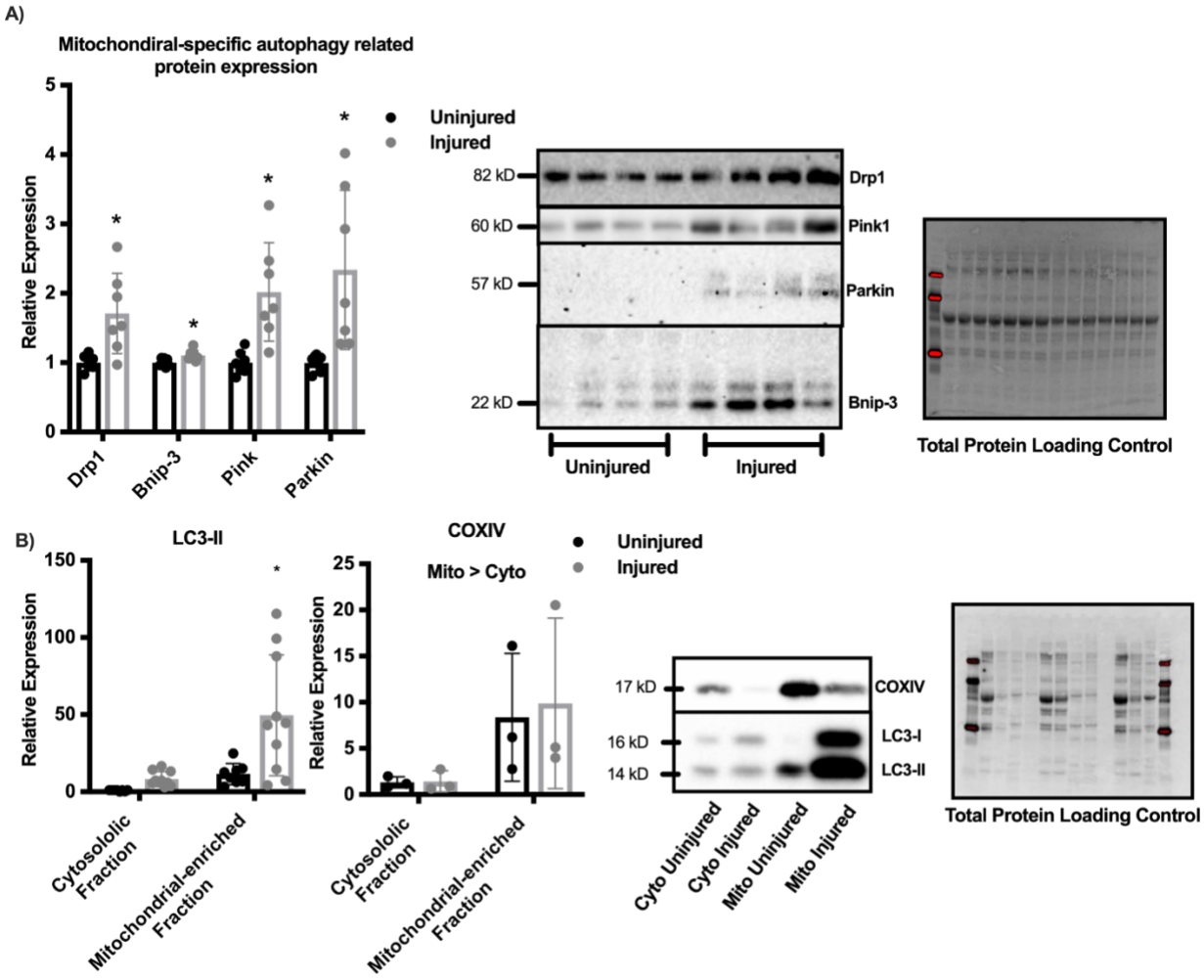

Figure 3.4: Mitochondrial-specific autophagy related protein expression and mitochondria localized autophagy response after freeze injury.
A) Semi-quantitative analysis of Drp1, Bnip-3, Pink, and Parkin protein expression 7 days after freeze injury and representative immunoblot images. (n=7) Blots are normalized to total protein as a loading control. Differences in protein expression after injury were detected by RM ANOVA between uninjured and injured limbs. *significantly different from uninjured limb. B) Semi-quantitative analysis of LC3II expression and COXIV expression in cytosolic and mitochondrial-enriched fractions from mice 7 days after freeze injury followed by representative immunoblot images (n=8). Blots are normalized to total protein as a loading control and presented as relative expression to uninjured cytosol fraction. Differences were analyzed by two-way RM ANOVA with the repeated measures being the injured vs. uninjured contralateral control limb and the other factor being fraction (mitochondria-enriched or cytosolic). * significantly different from all other groups. Data are presented as means ± SD.

Recovery of strength, mitochondrial function, and mitochondrial content in Ulk1 MKO mice after traumatic freeze injury

Mitochondrial-specific autophagy is mediated by the autophagy-related protein Ulk1 (Call et al., 2017). We and others have investigated the role of Ulk1 following muscle stress and specifically mitochondrial stress (Laker et al., 2017; Nichenko et al., 2016) however, whether Ulk1 is required for the recovery of mitochondrial function after injury has not been investigated. To ascertain the role of Ulk1-mediated autophagy in the recovery of mitochondrial function, we crossed *myogenin-Cre* mice with floxed-*Ulk1* mice to generate muscle-specific *Ulk1* knockout mice (MKO) (Call et al., 2017). Prior to injury we observed no difference in max torque measurements between MKO and littermate (LM), genetically wildtype mice, however 14 days after injury MKO mice produced 27% less torque than the LM mice (Main Effect: Injury and Genotype, $p \leq 0.012$, Fig 3.5A). Mitochondrial function was decreased 43% in the injured limbs independent of genotype (Main Effect: Injury, $p < 0.0001$, Fig 3.5B), and mitochondrial content was reduced by 34% and 58%, CS and SDH respectively, independent of genotype (Main Effect: Injury, $p \leq 0.0006$, Fig 3.5C, Fig 3.5D).

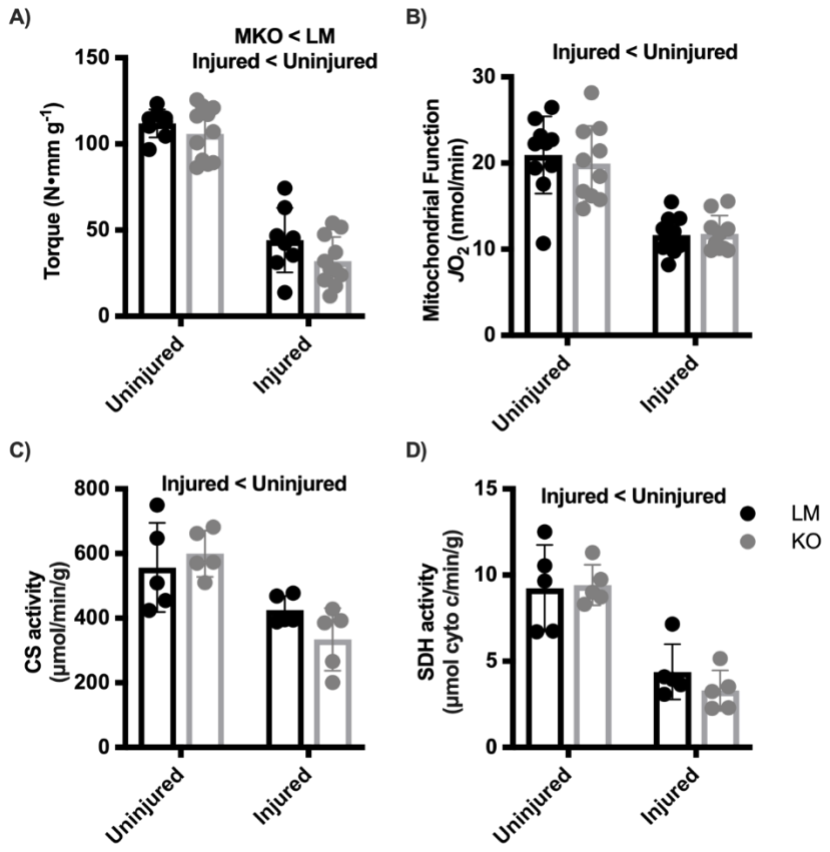

Figure 3.5: Muscle torque, mitochondrial function, and mitochondrial content before and after injury in Ulk1 MKO
A) Comparison of Ulk1 MKO (n=10) and LM (n=10) dorsiflexion muscle torque before (uninjured) and 14 days after freeze injury. B) Oxygen consumption of permeabilized TA muscle in injured and contralateral uninjured limbs 14 days after freeze injury. C) Citrate Synthase activity and D) Succinate Dehydrogenase activity in TA muscles of LM (n=5) and Ulk1 MKO (n=5) mice in both injured and contralateral control limbs. Differences were analyzed by two-way RM ANOVA with the repeated measures being the injured vs. uninjured contralateral control limb and the other factor being genotype. Main effects are reported.

Autophagy-related protein induction in Ulk1 MKO mice after freeze injury

LC3II expression increased more than 7-fold in the injured limbs compared to the uninjured limb, independent of genotype (Main Effect: Injury, $p \leq 0.0001$, Fig 3.6B). Additionally, Beclin1 expression increased more than 14-fold with injury, independent of genotype (Main Effect: Injury, $p \leq 0.0001$, Fig 3.6B). Prior to injury, MKO mice had no Ulk1

expression as expected, however after injury both the LM and MKO mice had similar levels of Ulk1 protein content (Main Effect: Injury and Genotype, $p \leq 0.042$, Fig 3.6B).

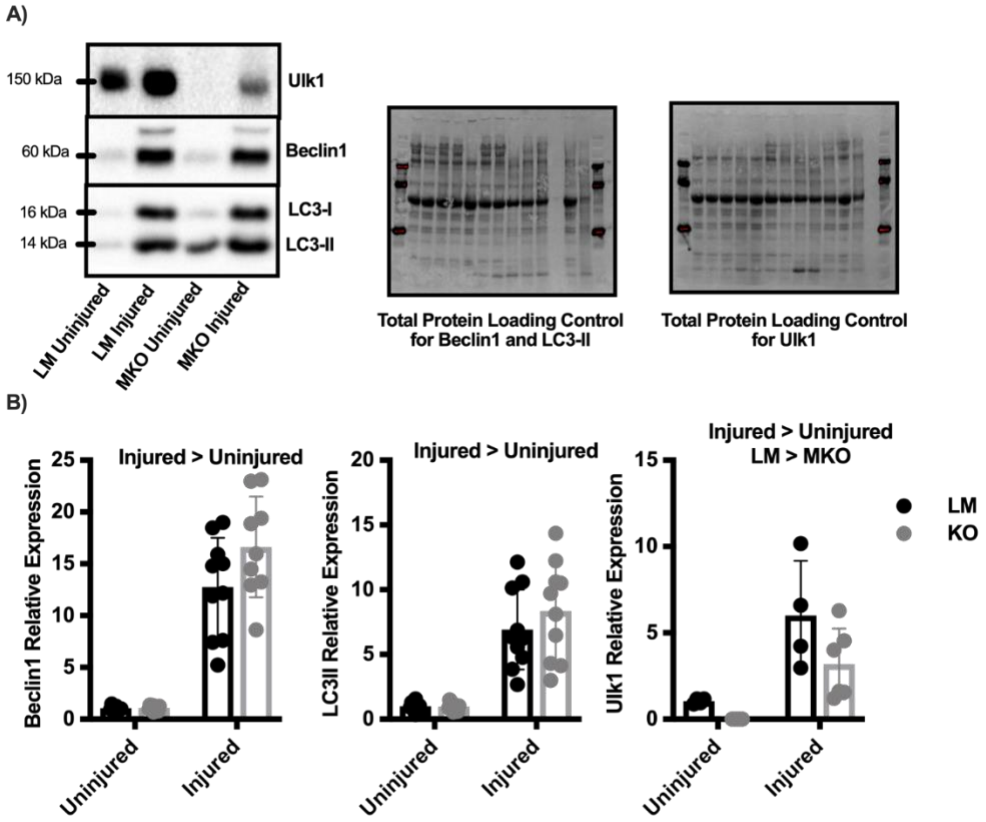

Figure 3.6: Autophagy related protein induction in Ulk1 MKO mice after traumatic freeze injury A) Representative immunoblots and B) semi-quantitative analysis of Beclin1, LC3II, and Ulk1 protein expression in both injured and contralateral uninjured limbs of Ulk1 MKO (n=10) and LM (n=10) mice 14 days after freeze injury. Blots are normalized to total protein as a loading control and presented as relative expression to LM uninjured limbs. Data are presented as individual values ± SD. Differences were analyzed by two-way RM ANOVA with the repeated measures being the injured vs. uninjured contralateral control limb and the other factor being genotype. Main effects are reported.

Reduced autophagy flux after injury in both LM and Ulk1 MKO mice

Static measurements of autophagy are a poor indicator of dynamic autophagy activity, therefore we measured autophagy flux using a GFP-LC3-RFP-LC3Δ plasmid where the GFP portion is incorporated into the autophagosome and is consequently degraded when the

autophagolysosome degrades. The RFP portion is cleaved and remains in the cytosol to serve as an internal control, therefore an increase in the GFP:RFP ratio signifies less autophagy flux. At 7 days after freeze injury, the GFP:RFP ratio increased 26% in the injured limb compared to the uninjured limb, independent of genotype (Main effect: Injury, p=0.0189, Fig. 3.7). This is a striking feature as it suggests autophagy flux does not increase to meet the demands of increased number of autophagosomes (e.g., greater autophagy-related protein content, Figs. 3.2-3.3).

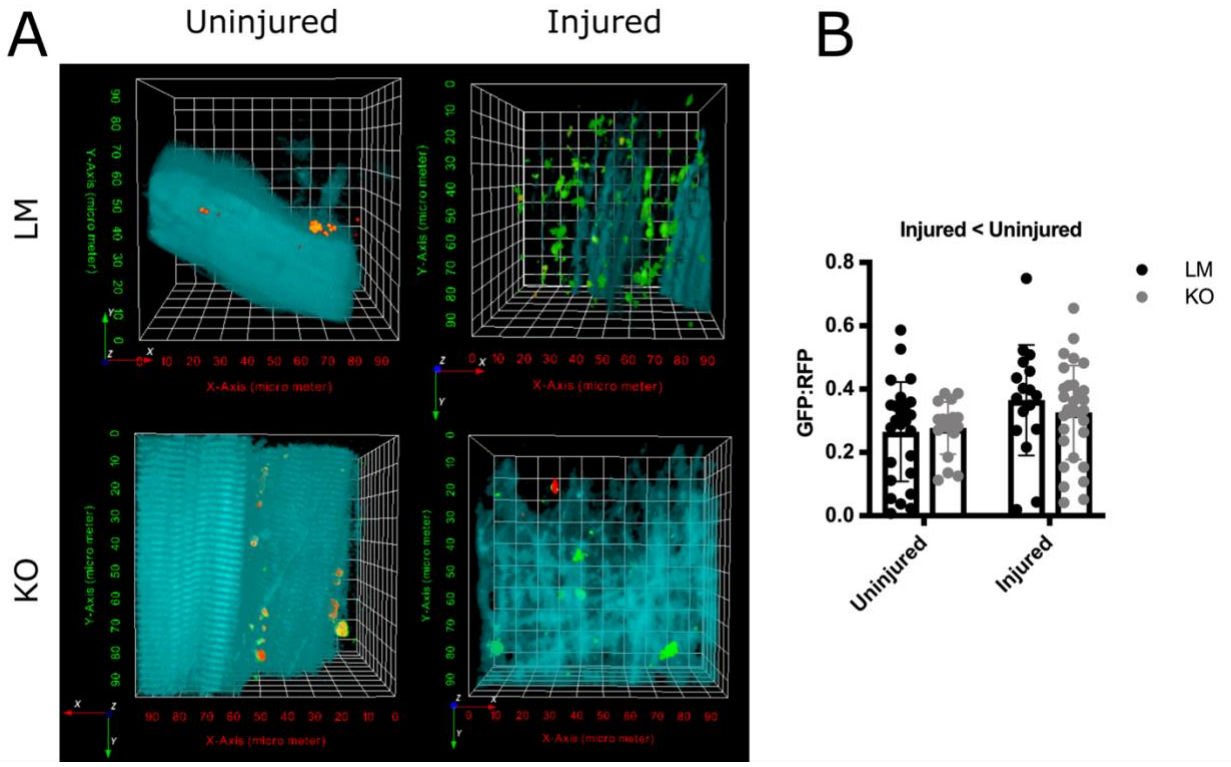

Figure 3.7: Autophagy flux is reduced in mice after traumatic freeze injury.
A) Representative two-photon microscopy images from TA muscles of LM and ULK MKO mice transfected with GFP-LC3-RFP-LC3ΔG plasmid. B) Quantitative analysis of the GFP:RFP ratio which represents autophagosome turnover. Autophagy flux was greater in uninjured muscle as opposed to injured muscle. Data are presented as individual values ± SD. Differences were analyzed by two-way RM ANOVA with the repeated measures being the injured vs. uninjured contralateral control limb and the other factor being genotype. Main effects are reported.

Impaired satellite cell proliferation in Ulk1 MKO mice

At the conclusion of our study we decided to explore satellite cell dynamics in Ulk1 KO mice because: (i) the strength deficit in the Ulk1 MKO mice, which is in agreement with our previous reports (Klionsky et al.), suggests Ulk1 knockout in myofibers impairs regenerative myogenesis and (ii) satellite cells are essential stem cells for regenerative myogenesis in skeletal muscle. 10 days post-injury there were a greater number of total and proliferating satellite cells in the freeze injured muscles of LM compared to Ulk1 MKO mice ($p \leq 0.016$, Fig. 3.8), and no difference between mice in the number of self-renewing SC ($p=0.140$). This result suggest that Ulk1 may influence satellite cell dynamics during muscle regeneration, even when Ulk1 deficiency is in the adult muscle fiber, not satellite cells.

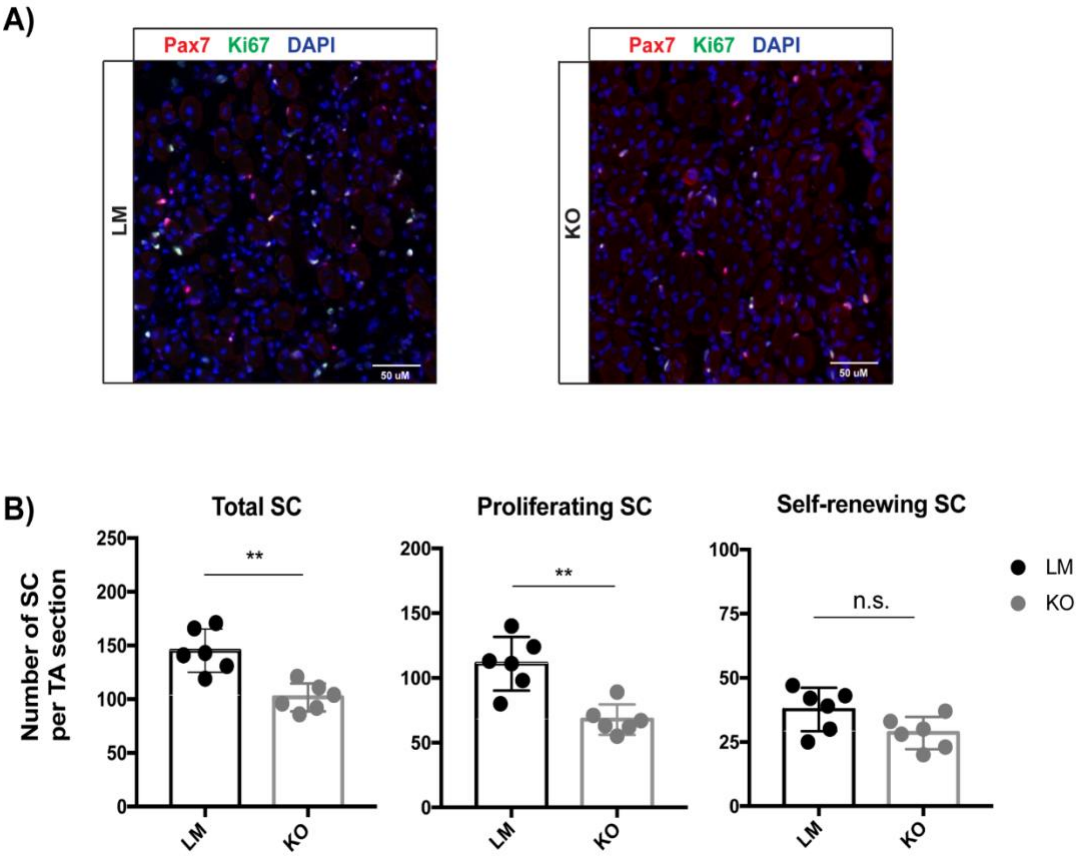

Figure 3.8: Muscle-specific Ulk1 knockout impairs satellite cell proliferation after traumatic freeze injury
A) Representative immunofluorescence imaging of muscle cross-sections from LM (n=6) and Ulk1 MKO (n=6) mice at 10 days after injury. Arrowheads: $Pax7^{+}/Ki67^{+}$ proliferative satellite cells. Asterisks: $Pax7^{+}/Ki67^{-}$ self-renewing satellite cells. B) Numbers of total, proliferating, and self-renewing satellite cells per muscle cross-section.

Discussion

A primary goal for this study was to address several knowledge gaps in the field related to mitochondrial dysfunction after skeletal muscle stress, and the role of autophagy in mediating a response between the two. Mitochondria are appreciated as contributing to the regenerative potential, plasticity, and overall quality of skeletal muscle, and, therefore, investigating the muscle fiber-mitochondrial relationship may produce important targets for rehabilitation and disease prevention. However, there appear to be inconsistencies in the literature regarding what types of muscle stressors elicit mitochondrial dysfunction (Laker et al., 2017; Rattray, Caillaud, Ruell, & Thompson, 2011; Rattray, Thompson, Ruell, & Caillaud, 2013; Silva et al., 2013), as well as the extent to which autophagy is necessary for the timely repair of mitochondrial dysfunction after muscle stress (Call et al., 2017). Herein, we relied upon oxygen consumption as the marker of mitochondrial function, enzyme activities of succinate dehydrogenase and citrate synthase as markers of mitochondrial content, and a muscle-specific Ulk1 knockout mouse to test the necessity of autophagy for the recovery of mitochondrial function and content.

The first knowledge gap we explored was the extent to which three often utilized muscle stressors (fatigue, eccentric contraction-induced injury, and traumatic injury) that produce a loss in muscle contractility (Le, Lowe, & Kyba, 2016; Warren et al., 2007) and an autophagic response (Ato et al., 2017; Call et al., 2017; Nichenko et al., 2016) will cause mitochondrial dysfunction, i.e., a decline in oxygen consumption. Reduced mitochondrial oxygen consumption

was only observed after traumatic freeze injury and was not decreased until 6 hours after injury (Fig. 3.2) in stark contrast to the immediate ~70% loss in force production (Warren et al., 2007). Fatiguing exercises and eccentric contraction-induced injury have been reported to cause mitochondrial dysfunction (Laker et al., 2017; Molnar et al., 2006) in contrast to our findings. A likely explanation for these conflicting findings may be the tools utilized to investigate mitochondrial dysfunction and/or damage. Specifically, immunohistological techniques like confocal microscopy used by Laker & Drake et al (Laker et al., 2017) are useful for mechanistic investigations into localized mitochondrial events but do not necessarily reflect changes across the entire mitochondrial network; whereas oxygen consumption measurements test the functional capacity of the entire mitochondrial reticulum but do not capture more nuanced physiology such as fission and fusion events. It is irrefutable that functional, biochemical, and immunohistological approaches can provide valuable insight into mitochondrial physiology, yet when appropriate, future studies may consider the culminative advantage of combining more than one technique to avoid further inconsistencies in the literature.

We and others have previously reported that traumatic muscle injury results in a loss of mitochondrial content (Call et al., 2017; Duguez et al., 2002; Nichenko et al., 2016; Wagatsuma et al., 2011), and herein we report that it also results in a loss of mitochondrial function (Fig. 3.2). A remaining question was the extent to which mitochondrial-specific autophagy, sometimes referred to as mitophagy, participates in the clearing of dysfunctional mitochondria after traumatic muscle injury. Laker & Drake et al. demonstrated that mitochondrial-specific autophagy was critical for clearing damaged, i.e, ROS-producing mitochondria after muscle fatigue (Laker et al., 2017); therefore, it is logical to hypothesize that mitochondrial-specific autophagy may occur after a more severe muscle stressor such as traumatic muscle injury in

order to clear away the dysfunctional mitochondria. To address this knowledge gap, we analyzed mitophagy-related proteins as well as autophagy-related proteins in mitochondrial-enriched fractions and cytosolic fractions. We found a 2-fold increase in mitophagy related proteins and a robust accumulation of autophagy-related protein localized to the mitochondria after freeze injury suggesting that autophagy does participate in the clearance of dysfunctional mitochondrial after traumatic muscle injury (Fig. 3.4). This is the first study linking autophagy to mitochondrial dysfunction in injured skeletal muscle and understanding the process of clearing dysfunctional mitochondria after muscle injury may provide targets to facilitate muscle recovery.

In order to specifically test the extent to which mitochondrial-specific autophagy is important for muscle recovery after traumatic muscle injury we utilized a Ulk1 MKO mouse model. We and others have reported that Ulk1 may play an important role in both mitochondrial function and strength recovery after injury (Call et al., 2017; Nichenko et al., 2016) . Our initial results suggested that Ulk1 is not required for the recovery of mitochondrial function after freeze injury (Fig. 3.5); however, there is a major consideration worth noting. Our Ulk1 MKO mouse model is a *myogenin-Cre* driven gene knockout, meaning Ulk1 is not expressed in adult muscle fibers, but is present in Pax7-expressing satellite cells. Quiescent satellite cells are activated upon injury, proliferate, differentiate, and ultimately provide new myonuclei for the regenerating fiber leading to Ulk1 expression in the regenerated muscle fiber. Additionally, following traumatic muscle injury there are many other cell types that migrate into the injured territory to aid in muscle regeneration. These include inflammatory cells such as neutrophils and macrophages, fibro-adipogenic precursor cells (FAPs), fibroblasts, and endothelial cells all of which potentially express Ulk1 sufficient for autophagy induction (Wosczyna & Rando, 2018). This premise is supported by our immunoblots showing Ulk1 protein content within the injured limbs of Ulk1

MKO mice (Fig. 3.6). This is a clear physiological limitation of this study and limits our ability to determine the necessity of Ulk1 for mitochondrial remodeling after traumatic injury. To circumvent this problem for future experiments, we are exploring the use of *Pax7*$_{CreER}$ mouse lines to effectively knockout Ulk1 in satellite cells and adult muscle fibers.

Previous muscle damage research, including our own, has failed to investigate the dynamic properties of autophagy after skeletal muscle injury. Specifically, our previous work (Call et al., 2017; Nichenko et al., 2016) and this current work (Fig. 3.3) shows that the autophagy-related protein response scales to the magnitude of muscle damage after injury, but it remains unclear the extent to which autophagy flux matches the increases in autophagy machinery. Autophagy flux is described as the rate at which the entire process of autophagy occurs; meaning how quickly autophagosomes form around damaged content, fuse with lysosomes and subsequently degrade (Klionsky et al., 2016). In contrast, an increase in autophagy machinery is a static measurement and is not always connected to an increase in autophagy flux. Static measurements of LC3II protein content are often used as proxies for autophagy flux but can actually indicate (i) an inhibition in lysosomal fusion to the autophagosome, (ii) inhibition of autolysosome degradation, (iii) an increase in the amount of autophagosomes (without an increase in flux), or (iv) an increase in autophagy flux (Klionsky et al., 2016). Therefore, in order to asses changes in autophagy flux after injury we used a GFP-LC3-RFP-LC3Δ plasmid to assess autophagosome turnover through a GFP:RFP ratio. We found that autophagy flux was actually decreased in the injured limb compared to the uninjured (Fig. 3.7). This reduction in flux may represent a limiting factor, or bottleneck, in the ability of autophagy to quickly clear away damaged proteins and organelles, and serve as a novel target to expedite the healing process in injured skeletal muscle. As mentioned above, we cannot make an

interpretation on the role of Ulk1 in mediating autophagy flux due to the partial protein content rescue following injury (Fig 3.6). However, it is intriguing to consider for future studies that the Ulk1 contribution from differentiating satellite cells may provide protection from changes in autophagy flux capacity when Ulk1 is deficient in the adult muscle fiber.

In this study, our finding that Ulk1 MKO impairs satellite cell proliferation (Fig. 3.8) raises an intriguing question – how does muscle fiber autophagy indirectly affect satellite cell dynamics? Satellite cells are essential stem cells for muscle regeneration and after traumatic injury (e.g., freeze injury), satellite cells exit quiescence and proliferate to form myoblasts (Yin, Price, & Rudnicki, 2013). Myofiber-derived FGF2 and FGF6 are important mitogens for satellite cells during muscle regeneration (Anderson, Mitchell, McGeachie, & Grounds, 1995; Chakkalakal, Jones, Basson, & Brack, 2012; Floss, Arnold, & Braun, 1997; Kastner, Elias, Rivera, & Yablonka-Reuveni, 2000; Olwin & Hauschka, 1986). One possibility is that Ulk1-dependent autophagy may be pivotal for FGF2/6 expression and secretion in damaged myofibers. Alternatively, Ulk1-dependent autophagy may contribute to the degeneration of damaged myofibers by autophagy induced cell death, which would be critical for setting the stage for satellite cell proliferation via timely recruitments of macrophages and FAPs. No matter what mechanism is involved, the observations in this study suggest an indirect positive influence of autophagy in myofibers on satellite cell proliferation, which may be therapeutically targeted in the future for improving muscle regeneration.

In conclusion, this work advances the field in three substantive ways. First, physiological muscle stressors that cause a decrease in muscle contractility and potentially result in mitochondrial stress do not always elicit a decline in mitochondrial function, as assessed via oxygen consumption. Second, despite an increase in autophagy machinery, autophagy flux is

actually decreased following traumatic muscle injury, and this may represent a critical bottleneck to address with targeted therapies to enhance the recovery of muscle function. Third, autophagy appears to participate in the clearance of damaged mitochondria following traumatic injury in line with what has been reported following non-injurious muscle stressors (Laker et al., 2017). Therefore, future investigations into the role of autophagy following muscle stress associated with mitochondria should strongly consider an evaluation of mitochondrial function to complement a localized analysis of mitochondria stress and the use of a lysosomal inhibitor or plasmid to determine autophagy flux. Unfortunately, we were unable to fully determine the necessity of Ulk1 for timely recovery of mitochondrial function due to the limitation of the mouse model; however, we are intrigued by the strength deficits in the mice and potential crosstalk between Ulk1 in the adult muscle fiber and satellite cells during muscle regeneration.

References

Aihara, H., & Miyazaki, J. (1998). Gene transfer into muscle by electroporation in vivo. *Nat Biotechnol, 16*(9), 867-870. doi:10.1038/nbt0998-867

Anderson, J. E., Mitchell, C. M., McGeachie, J. K., & Grounds, M. D. (1995). The time course of basic fibroblast growth factor expression in crush-injured skeletal muscles of SJL/J and BALB/c mice. *Exp Cell Res, 216*(2), 325-334. doi:10.1006/excr.1995.1041

Ato, S., Makanae, Y., Kido, K., Sase, K., Yoshii, N., & Fujita, S. (2017). The effect of different acute muscle contraction regimens on the expression of muscle proteolytic signaling proteins and genes. *Physiol Rep, 5*(15). doi:10.14814/phy2.13364

Baltgalvis, K. A., Call, J. A., Cochrane, G. D., Laker, R. C., Yan, Z., & Lowe, D. A. (2012). Exercise training improves plantar flexor muscle function in mdx mice. *Med Sci Sports Exerc, 44*(9), 1671-1679. doi:10.1249/MSS.0b013e31825703f0

Call, J. A., Eckhoff, M. D., Baltgalvis, K. A., Warren, G. L., & Lowe, D. A. (2011). Adaptive strength gains in dystrophic muscle exposed to repeated bouts of eccentric contraction. *J Appl Physiol (1985), 111*(6), 1768-1777. doi:10.1152/japplphysiol.00942.2011

Call, J. A., Warren, G. L., Verma, M., & Lowe, D. A. (2013). Acute failure of action potential conduction in mdx muscle reveals new mechanism of contraction-induced force loss. *J Physiol, 591*(15), 3765-3776. doi:10.1113/jphysiol.2013.254656

Call, J. A., Wilson, R. J., Laker, R. C., Zhang, M., Kundu, M., & Yan, Z. (2017). Ulk1-mediated autophagy plays an essential role in mitochondrial remodeling and functional

regeneration of skeletal muscle. *Am J Physiol Cell Physiol*, ajpcell.00348.02016. doi:10.1152/ajpcell.00348.2016

Chakkalakal, J. V., Jones, K. M., Basson, M. A., & Brack, A. S. (2012). The aged niche disrupts muscle stem cell quiescence. *Nature, 490*(7420), 355-360. doi:10.1038/nature11438

Collins, M. A., An, J., Peller, D., & Bowser, R. (2015). Total protein is an effective loading control for cerebrospinal fluid western blots. *J Neurosci Methods, 251*, 72-82. doi:10.1016/j.jneumeth.2015.05.011

Duguez, S., Feasson, L., Denis, C., & Freyssenet, D. (2002). Mitochondrial biogenesis during skeletal muscle regeneration. *Am J Physiol Endocrinol Metab, 282*(4), E802-809. doi:10.1152/ajpendo.00343.2001

Egan, D. F., Shackelford, D. B., Mihaylova, M. M., Gelino, S., Kohnz, R. A., Mair, W., . . . Shaw, R. J. (2011). Phosphorylation of ULK1 (hATG1) by AMP-activated protein kinase connects energy sensing to mitophagy. *Science, 331*(6016), 456-461. doi:10.1126/science.1196371

Floss, T., Arnold, H. H., & Braun, T. (1997). A role for FGF-6 in skeletal muscle regeneration. *Genes Dev, 11*(16), 2040-2051.

Foltz, S. J., Luan, J., Call, J. A., Patel, A., Peissig, K. B., Fortunato, M. J., & Beedle, A. M. (2016). Four-week rapamycin treatment improves muscular dystrophy in a fukutin-deficient mouse model of dystroglycanopathy. *Skelet Muscle, 6*, 20. doi:10.1186/s13395-016-0091-9

Garcia-Prat, L., Martinez-Vicente, M., Perdiguero, E., Ortet, L., Rodriguez-Ubreva, J., Rebollo, E., . . . Munoz-Canoves, P. (2016). Autophagy maintains stemness by preventing senescence. *Nature, 529*(7584), 37-42. doi:10.1038/nature16187

Kastner, S., Elias, M. C., Rivera, A. J., & Yablonka-Reuveni, Z. (2000). Gene expression patterns of the fibroblast growth factors and their receptors during myogenesis of rat satellite cells. *J Histochem Cytochem, 48*(8), 1079-1096. doi:10.1177/002215540004800805

Kim, J., Kundu, M., Viollet, B., & Guan, K. L. (2011). AMPK and mTOR regulate autophagy through direct phosphorylation of Ulk1. *Nat Cell Biol, 13*(2), 132-141. doi:10.1038/ncb2152

Klionsky, D. J., Abdelmohsen, K., Abe, A., Abedin, M. J., Abeliovich, H., Acevedo Arozena, A., . . . Zughaier, S. M. (2016). Guidelines for the use and interpretation of assays for monitoring autophagy (3rd edition). *Autophagy, 12*(1), 1-222. doi:10.1080/15548627.2015.1100356

Kundu, M., Lindsten, T., Yang, C. Y., Wu, J., Zhao, F., Zhang, J., . . . Thompson, C. B. (2008). Ulk1 plays a critical role in the autophagic clearance of mitochondria and ribosomes during reticulocyte maturation. *Blood, 112*(4), 1493-1502. doi:10.1182/blood-2008-02-137398

Kuznetsov, A. V., Veksler, V., Gellerich, F. N., Saks, V., Margreiter, R., & Kunz, W. S. (2008). Analysis of mitochondrial function in situ in permeabilized muscle fibers, tissues and cells. *Nat Protoc, 3*(6), 965-976. doi:10.1038/nprot.2008.61

Laker, R. C., Drake, J. C., Wilson, R. J., Lira, V. A., Lewellen, B. M., Ryall, K. A., . . . Yan, Z. (2017). Ampk phosphorylation of Ulk1 is required for targeting of mitochondria to lysosomes in exercise-induced mitophagy. *Nat Commun, 8*(1), 548. doi:10.1038/s41467-017-00520-9

Le, G., Lowe, D. A., & Kyba, M. (2016). Freeze Injury of the Tibialis Anterior Muscle. *Methods Mol Biol, 1460,* 33-41. doi:10.1007/978-1-4939-3810-0_3

Lira, V. A., Okutsu, M., Zhang, M., Greene, N. P., Laker, R. C., Breen, D. S., . . . Yan, Z. (2013). Autophagy is required for exercise training-induced skeletal muscle adaptation and improvement of physical performance. *Faseb j, 27*(10), 4184-4193. doi:10.1096/fj.13-228486

Marzetti, E., Calvani, R., Cesari, M., Buford, T. W., Lorenzi, M., Behnke, B. J., & Leeuwenburgh, C. (2013). Mitochondrial dysfunction and sarcopenia of aging: from signaling pathways to clinical trials. *Int J Biochem Cell Biol, 45*(10), 2288-2301. doi:10.1016/j.biocel.2013.06.024

Molnar, A. M., Servais, S., Guichardant, M., Lagarde, M., Macedo, D. V., Pereira-Da-Silva, L., . . . Favier, R. (2006). Mitochondrial H2O2 production is reduced with acute and chronic eccentric exercise in rat skeletal muscle. *Antioxid Redox Signal, 8*(3-4), 548-558. doi:10.1089/ars.2006.8.548

Nichenko, A. S., Southern, W. M., Atuan, M., Luan, J., Peissig, K. B., Foltz, S. J., . . . Call, J. A. (2016). Mitochondrial maintenance via autophagy contributes to functional skeletal muscle regeneration and remodeling. *Am J Physiol Cell Physiol, 311*(2), C190-200. doi:10.1152/ajpcell.00066.2016

Olwin, B. B., & Hauschka, S. D. (1986). Identification of the fibroblast growth factor receptor of Swiss 3T3 cells and mouse skeletal muscle myoblasts. *Biochemistry, 25*(12), 3487-3492.

Pauly, M., Daussin, F., Burelle, Y., Li, T., Godin, R., Fauconnier, J., . . . Petrof, B. J. (2012). AMPK activation stimulates autophagy and ameliorates muscular dystrophy in the mdx mouse diaphragm. *Am J Pathol, 181*(2), 583-592. doi:10.1016/j.ajpath.2012.04.004

Rattray, B., Caillaud, C., Ruell, P. A., & Thompson, M. W. (2011). Heat exposure does not alter eccentric exercise-induced increases in mitochondrial calcium and respiratory dysfunction. *Eur J Appl Physiol, 111*(11), 2813-2821. doi:10.1007/s00421-011-1913-4

Rattray, B., Thompson, M., Ruell, P., & Caillaud, C. (2013). Specific training improves skeletal muscle mitochondrial calcium homeostasis after eccentric exercise. *Eur J Appl Physiol, 113*(2), 427-436. doi:10.1007/s00421-012-2446-1

Sambrook, J., & Russell, D. W. (2006). The inoue method for preparation and transformation of competent e. Coli: "ultra-competent" cells. *CSH Protoc, 2006*(1). doi:10.1101/pdb.prot3944

Sandri, M., Coletto, L., Grumati, P., & Bonaldo, P. (2013). Misregulation of autophagy and protein degradation systems in myopathies and muscular dystrophies. *J Cell Sci, 126*(Pt 23), 5325-5333. doi:10.1242/jcs.114041

Silva, L. A., Bom, K. F., Tromm, C. B., Rosa, G. L., Mariano, I., Pozzi, B. G., . . . Pinho, R. A. (2013). Effect of eccentric training on mitochondrial function and oxidative stress in the skeletal muscle of rats. *Braz J Med Biol Res, 46*(1), 14-20.

Southern, W. M., Nichenko, A. S., Shill, D. D., Spencer, C. C., Jenkins, N. T., McCully, K. K., & Call, J. A. (2017). Skeletal muscle metabolic adaptations to endurance exercise training are attainable in mice with simvastatin treatment. *PLoS One, 12*(2), e0172551. doi:10.1371/journal.pone.0172551

Tehrani, K. F., Latchoumane, C. V., Southern, W. M., Pendleton, E. G., Maslesa, A., Karumbaiah, L., . . . Mortensen, L. J. (2019). Five-dimensional two-photon volumetric microscopy of in-vivo dynamic activities using liquid lens remote focusing. *Biomed Opt Express, 10*(7), 3591-3604. doi:10.1364/boe.10.003591

Tian, W., Li, W., Chen, Y., Yan, Z., Huang, X., Zhuang, H., . . . Feng, D. (2015). Phosphorylation of ULK1 by AMPK regulates translocation of ULK1 to mitochondria and mitophagy. *FEBS Lett, 589*(15), 1847-1854. doi:10.1016/j.febslet.2015.05.020

Vigelso, A., Dybboe, R., Hansen, C. N., Dela, F., Helge, J. W., & Guadalupe Grau, A. (2015). GAPDH and beta-actin protein decreases with aging, making Stain-Free technology a superior loading control in Western blotting of human skeletal muscle. *J Appl Physiol (1985), 118*(3), 386-394. doi:10.1152/japplphysiol.00840.2014

Wagatsuma, A., Kotake, N., & Yamada, S. (2011). Muscle regeneration occurs to coincide with mitochondrial biogenesis. *Mol Cell Biochem, 349*(1-2), 139-147. doi:10.1007/s11010-010-0668-2

Wang, X., Pickrell, A. M., Rossi, S. G., Pinto, M., Dillon, L. M., Hida, A., . . . Moraes, C. T. (2013). Transient systemic mtDNA damage leads to muscle wasting by reducing the satellite cell pool. *Hum Mol Genet, 22*(19), 3976-3986. doi:10.1093/hmg/ddt251

Warren, G. L., Summan, M., Gao, X., Chapman, R., Hulderman, T., & Simeonova, P. P. (2007). Mechanisms of skeletal muscle injury and repair revealed by gene expression studies in mouse models. *J Physiol, 582*(Pt 2), 825-841. doi:10.1113/jphysiol.2007.132373

Wosczyna, M. N., & Rando, T. A. (2018). A Muscle Stem Cell Support Group: Coordinated Cellular Responses in Muscle Regeneration. *Dev Cell, 46*(2), 135-143. doi:10.1016/j.devcel.2018.06.018

Xie, L., Yin, A., Nichenko, A. S., Beedle, A. M., Call, J. A., & Yin, H. (2018). Transient HIF2A inhibition promotes satellite cell proliferation and muscle regeneration. *J Clin Invest*. doi:10.1172/jci96208

Yang, L., Licastro, D., Cava, E., Veronese, N., Spelta, F., Rizza, W., . . . Fontana, L. (2016). Long-Term Calorie Restriction Enhances Cellular Quality-Control Processes in Human Skeletal Muscle. *Cell Rep, 14*(3), 422-428. doi:10.1016/j.celrep.2015.12.042

Yin, H., Price, F., & Rudnicki, M. A. (2013). Satellite cells and the muscle stem cell niche. *Physiol Rev, 93*(1), 23-67. doi:10.1152/physrev.00043.2011

Zeitler, A. F., Gerrer, K. H., Haas, R., & Jimenez-Soto, L. F. (2016). Optimized semi-quantitative blot analysis in infection assays using the Stain-Free technology. *J Microbiol Methods, 126*, 38-41. doi:10.1016/j.mimet.2016.04.016

CHAPTER 4

LIFELONG ULK1-MEDIATED AUTOPHAGY DEFICIENCY IN MUSCLE INDUCES MITOCHONDRIAL DYSFUNCTION AND CONTRACTILE WEAKNESS[1]

[1] Nichenko, AS. Sorensen, JR. Southern, WM. Qualls, AE. Schifino, AG. Mcfaline-Figueroa, J. Greising, SM. Call, JA. To be submitted to *The Journals of Gerontology: Series A.*

Abstract

The accumulation of damaged mitochondria due to insufficient autophagy has been implicated in the pathophysiology of sarcopenia resulting in reduced contractile and metabolic function. Ulk1 is an autophagy-related kinase that initiates autophagosome assembly and may also play a role in autophagosome degradation (i.e., autophagy flux), but the contribution of Ulk1 to healthy muscle aging is unclear. The purpose of this study was to investigate the role of Ulk1-mediated autophagy in skeletal muscle aging. At age 22 months (80% survival rate), muscle contractile and metabolic function were assessed using electrophysiology in muscle specific Ulk1 knockout mice (MKO) and their littermate controls (LM). Specific peak-isometric torque of the ankle dorsiflexors (normalized by tibialis anterior muscle cross-sectional area) and specific force of the fast-twitch extensor digitorum longus muscles were less in MKO mice compared to LM mice ($p<0.03$). Permeabilized muscle fibers from MKO mice had greater mitochondrial content, yet lower mitochondrial oxygen consumption and greater reactive oxygen species production compared to fibers from LM mice ($p<0.04$). Altered neuromuscular junction innervation patterns and changes in autophagosome numbers and/or flux in muscles from MKO may have contributed to decrements in contractile and metabolic function. Results from this study support an important role of Ulk1-mediated autophagy in skeletal muscle with age, reflecting Ulk1's dual role in maintaining mitochondrial integrity through autophagosome assembly and degradation. A lifetime of insufficient Ulk-1-mediated autophagy in skeletal muscle exacerbates age-related contractile and metabolic dysfunction.

Introduction

Autophagy is an evolutionarily conserved cellular process for degrading damaged and dysfunctional proteins and organelles and has been strongly associated with the pathophysiology of sarcopenia (Brunk & Terman, 2002; Marzetti et al., 2013; Rajawat, Hilioti, & Bossis, 2009). Studies investigating autophagy in older adults and rodents report less basal autophagy signaling as well as less mitochondrial-specific autophagy, i.e. mitophagy, signaling with age (Aas et al., 2019; Arribat et al., 2019; Balan et al., 2019; Carnio et al., 2014; Wohlgemuth et al., 2011). Moreover, autophagy-related protein knockout models indicate an exacerbated aging phenotype supporting an important role for autophagy in healthy skeletal muscle aging (Bujak et al., 2015; Carnio et al., 2014; Carter, Kim, Erlich, Zarrin-Khat, & Hood, 2018; Wohlgemuth, Seo, Marzetti, Lees, & Leeuwenburgh, 2010; Zhou et al., 2017). For example, Carnio et al. discovered geriatric mice with deficient ATG7, an autophagy-related protein important for autophagosome assembly, have weaker muscles that present with greater levels of muscle fiber atrophy and dysfunctional neuromuscular junctions (NMJs) compared to age-matched controls(Carnio et al., 2014). Autophagy is a dynamic process that can be altered not only by changing the number of autophagosomes assembled but also by changing the rate of autophagosome degradation, i.e., autophagy flux. In addition to changes in autophagosome assembly there is compelling research to suggest that autophagic flux is also decreased with age (Carter et al., 2018; Wohlgemuth et al., 2010; Zhou et al., 2017). Therefore, it appears that autophagy is inextricably linked with aging and reductions in both autophagosome number and flux may lead to an accumulation of damaged organelles and proteins which contribute to sarcopenia.

The accumulation of damaged and dysfunctional mitochondria with age is thought to contribute to sarcopenia due to metabolic insufficiency and a greater production of reactive oxygen

species (ROS) (Baumann, Kwak, Liu, & Thompson, 2016; Calvani et al., 2013; Green, Galluzzi, & Kroemer, 2011; Ziegler, Wiley, & Velarde, 2015). These damaged and ROS-producing mitochondria can be degraded through mitophagy, which is regulated in part through Unc-51 like autophagy activating kinase, Ulk1 (Egan et al., 2011; Kundu et al., 2008; Laker et al., 2017). Ulk1 has long been thought of as an autophagy initiating protein that controls autophagosome assembly, but recent mechanistic investigations in yeast have suggested that Ulk1 may also be involved in signaling for autophagosome-lysosome fusion which leads to autophagosome degradation (autophagy flux) (Wang et al., 2018). We have recently reported that the degradation of dysfunctional mitochondria associated with muscle injury through Ulk1-mediated autophagy is critical for the timely recovery of muscle function (Nichenko et al., 2020). Interestingly, after muscle injury we also observe an autophagy flux bottleneck during the regeneration process (Nichenko et al., 2020). Ulk1 appears to play a mechanistic role in autophagosome assembly and flux yet the extent to which it influences sarcopenia is unclear.

In light of the dual role of Ulk1, the purpose of this study was to investigate the effects of lifelong insufficient Ulk1-mediated autophagy on aging skeletal muscle phenotype in an effort to understand the contribution of reduced autophagy to sarcopenia. We hypothesized that lifelong Ulk1-defiency will exacerbate sarcopenia as indicated by a worsening of skeletal muscle contractile and metabolic function. Herein, we utilize highly sensitive electrophysiological techniques to assess muscle contractile and metabolic function in aged mice with genetic deletion of Ulk1 and their littermate controls.

Methods

Ethical Approval

Animal protocols were approved by the University of Georgia Animal Care and Use Committee under the national guidelines set by the Association for Assessment and Accreditation of Laboratory Animal Care.

Animal Models

Muscle-specific Ulk1 knock-out mice (MKO) with *myogenin-Cre* and LoxP flanked *Ulk1* and their *myogenin-Cre* negative littermates (LM) were bred in-house and housed 5 per cage in a temperature-controlled facility with a 12:12 hour light:dark cycle and aged to either 16 months (middle-aged) or 22 months (old). 4 month old mice (Klionsky et al.) were used for young adult controls in Ulk1 protein content analysis. All mice had *ab libitum* access to food and water throughout the duration of the experiment.

Experimental Design

This study was originally designed to assess aging muscle health and function in a model of lifelong autophagy deficiency. The first cohort of mice consisted of Ulk1 MKO (n=10) and LM (n=10) mice that underwent longitudinal tracking of body mass and *in vivo* muscle strength every two months beginning at 12 months of age. Mice were sacrificed at 22 months of age based on a greater than 80% survivorship rate of our colony and published estimates (Turturro et al., 1999). At sacrifice, muscles were harvested for *in vitro* muscle function analysis, mitochondrial function analysis, enzyme kinetics, immunohistochemistry, and immunoblots.

A second cohort of middle-aged mice were used to assess autophagy related protein content and autophagy flux to determine how these might contribute to long-term physiological impairments. Mice were sacrificed at 16 months of age because the 16-month timepoint was the

first longitudinal measurement where we observed an age-related decline in muscle function in the old mice.

A third cohort of young adult mice were sacrificed at 4 months old and the TA muscle was collected for immunoblots of Ulk1 and pUlk1(s555) protein content.

In vivo assessment of muscle function

Peak isometric torque of the ankle dorsiflexors was assessed as previously described (Nichenko et al., 2016). Briefly, mice were anesthetized using 1-2% isoflurane in oxygen, the left hind limb was shaved and aseptically prepared, and the foot was positioned into a foot-plate attached to the servomotor (Model 129 300C-LR; Aurora Scientific, Aurora, Ontario, Canada) where the ankle joint was adjusted to a 90° angle and secured at the knee joint. Platinum-Iridium (Pt-Ir) needle electrodes were inserted percutaneously on both sides of the peroneal nerve and the testing platform was maintained at 37°C throughout the optimization and muscle stressor protocols. Optimal muscle stimulation was achieved by finding peak-isometric torque of the ankle dorsiflexors (tibialis anterior (TA), extensor digitorum longus (EDL), and extensor hallucis longus (Klionsky et al.) muscles through increasing the current in increments of 0.2 mAmps. The force frequency relationship was assessed by measuring torque as a function of the following stimulation frequencies; 5, 10, 20, 40, 60, 80, 100, 150, and 200 Hz. Muscle torque (mN·m) was normalized to body mass (kg) to account for the large variability in body size.

Glucose Tolerance Test

Glucose tolerance test were performed 4 days prior to sacrifice. Mice were fasted overnight (12 hours) before the test. On morning of the GTT, a baseline measure of blood glucose was taken by tail snip bleed using a glucose monitor (EvenCare G3). Mice were then

injected with sterilized D-glucose (200 mg/ml, i.p.) at 2 mg/g in normal saline and blood glucose was measured in 15 min increments for the next two hours.

In vitro assessment of muscle function

Extensor digitorum longus and soleus muscles were excised and analyzed for force-generating capacities as previously described (Baltgalvis, Call, Nikas, & Lowe, 2009; Call & Lowe, 2016; Moran, Warren, & Lowe, 2005). Muscles were mounted on a dual-mode muscle lever system (300B-LR; Aurora Scientific Inc., Aurora, ON, Canada) in a 0.38-ml bath assembled filled with Krebs Ringer bicarbonate that was maintained at 25ºC. Contractile characteristics tested included the following: peak twitch force, maximal isometric tetanic force, time-to-peak twitch force and twitch half-relaxation time, and the maximal rates of tetanic contraction and relaxation.

Oxygen Consumption Rates

Mitochondrial function was assessed through oxygen consumption rates collected through a Clark-type electrode (Oroboros O2k). The medial portion of the gastrocnemius muscle was dissected into fiber bundles and permeabilized with saponin as previously described (Nichenko et al., 2020). Mitochondrial respiration was accomplished by the addition of glutamate (10mM), malate (5mM), succinate (10mM), ADP (5mM), and FCCP (1uM). Oxygen consumption rates during leak (glutamate, malate and succinate), state III (leak, ADP) and uncoupled respiration (FCCP) were normalized to citrate synthase values to account for mitochondrial content.

ROS production

Reactive oxygen species production was assessed by quantifying resoflourin (red fluorescence) produced from the reaction of H_2O_2 and Amplex UltraRed (AmR, 10uM)

catalyzed by horseradish peroxidase (HRP, 1U/ml) during the oxygen consumption measurements. ROS rates were normalized by oxygen consumption rates during leak respiration to account for differences in total oxygen flux through the system.

Enzyme Assays

Citrate synthase enzyme activity was assessed to quantify mitochondrial content. The lateral portion of the gastrocnemius muscle remaining after fiber dissection was homogenized in 33mM phosphate buffer (pH 7.4) at a muscle to buffer ratio of 1:40 using a glass tissue grinder. Citrate Synthase activity was measured from the reduction of DTNB overtime as previously described (Nichenko et al., 2016).

Mitochondrial DNA analysis

Relative mtDNA copy number analysis was performed by the Oklahoma Nathan Shock Center on Aging by using the $2^{-\Delta\Delta ct}$ method as previously described (Masser, Clark, Van Remmen, & Freeman, 2016).

Autophagy flux measurement (Chloroquine treatment)

The second cohort of mice (middle-aged) were used to assess differences in basal autophagy flux between Ulk1 MKO and LM mice. Mice were i.p. injected with 100mg/kg of Chloroquine and sacrificed two hours after injection based on previously published guidelines for measuring autophagy flux (Moulis & Vindis, 2017). TA muscles were removed after sacrifice and processed for immunoblots of LC3II.

Immunohistology

First, the TA muscle was cut cross-sectionally at 8 µm at the mid-belly of the muscle. Immunohistochemical staining of the TA muscle was conducted with a combination of $MyHC_{Slow}$ (BA-F8, mouse monoclonal IgG2b; 5 µg/ml), $MyHC_{Fast}$ (F59, mouse monoclonal

IgG1; 5 µg/ml), $MyHC_{2A}$ (SC-71, mouse monoclonal IgG1; 5 µg/ml), $MyHC_{2B}$ (BF-F3, mouse monoclonal IgM; 5 µg/ml), DAPI (Molecular Probes D21490, 1 µg/ml), and Wheat Germ Agglutinin (WGA, Molecular Probes W11262; 594-conjugated, 3 µg/ml). Second, the diaphragm muscle was cut longitudinally at 30 µm through the mid-costal region of the muscle and stained with combinations of α-bungarotoxin (Molecular Probes B13422; 488-conjugated, 1µg/ml), neurofilament (2H3, mouse monoclonal IgG1; 0.5 µg/ml), and synaptic vesicle (SV2, mouse monoclonal IgG1; 2 µg/ml). Anti-BA-F8, F59, SC-71, BF-F3, 2H3, and SV2 were all obtained from the Developmental Studies Hybridoma Bank. For non-conjugated probes, appropriately paired secondary Alexa-Fluor conjugated antibodies at a dilution of 1:200 (Invitrogen A21123 or A21242; or Jackson ImmunoResearch Laboratories 115-005-020) were used. In all cases, the expected staining patterns in normal skeletal muscle were observed and the specificity of anti-labeling was confirmed by the absence of staining outside expected structures and was consistent with manufacturer's technical information.

Fluorescent Images were acquired at the University of Minnesota Imaging Center using a Nikon C2 automated upright laser scanning confocal microscope using 10x, 20x, or 40x Plan Apo objectives (NIR 0.45, 0.75, and 1.0 NA, working distance 4.0, 1.0 and 0.2 mm, respectively) with dual GaSP detectors (Nikon corporation). Skeletal muscle fibers of the entire TA muscle were first classified singly as type I based on the expression of $MyHC_{Slow}$ and collectively as type II (type IIa, IIb, and IIx); less than 1% of all TA muscle fibers across groups were type I and were excluded from further analysis. Next, the entire TA muscle was used to quantify the number of centrally located nuclei (both single and multiple) and total fibers. Fiber type specific distributions and cross-sectional area (CSA) was determined from representative images obtained systematically from three distinct regions of the TA muscle at the bone, middle, and

superficial aspects; fibers were classified as type IIa, IIb, or IIx based on stating of $MyHC_{2A}$, $MyHC_{2B}$, or absence of staining respectively. FIJI (Bethesda, MD (Schneider, 2012 #257)) was used to calculate the CSA and the proportion of fiber types. An average of 560±124 fibers per animal were analyzed with no genotype difference for fiber type distribution at the distinct regions of the TA muscle ($p=0.5386$), so fibers were averaged across animals. Images of diaphragm muscle NMJs were obtained at a Z-step size of 1µm to identify pre- and post-synaptic terminals. An average of 93±39 *en face* NMJs per animal were classified as innervated or denervated based on complete or incomplete co-localization of the pre- and post-synaptic terminals, respectively. For display purposes only, images were down-converted, without introducing any changes in brightness or contrast and produced in Adobe Photoshop (Adobe Systems Inc). Laser intensity was consistent across imaging of the same probes. During all imaging and investigation, investigators were blinded to the experimental group.

Immunoblot

For autophagy-related protein content analysis, protein was extracted from stressed and contralateral control muscles. 30µg of total protein was separated by SDS-PAGE, transferred onto a PVDF membrane, and immunoblotted as previously described (Nichenko et al., 2016). The following primary antibodies (Cell Signaling, Danvers, MA) were used: Ulk1 (1:500), pUlk1 (1:500), DRP1 (1:1000), BNIP3(1:1000), Pink1(1:500), Parkin (1:500), and LC3B (1:1000). Immunoblots were normalized to total protein in lane and quantified using Bio-Rad Laboratories Image Lab software (Hercules, CA) (Collins, An, Peller, & Bowser, 2015; Vigelso et al., 2015; Zeitler, Gerrer, Haas, & Jimenez-Soto, 2016).

Statistics

Changes in body mass, *in vivo* torque, EC50, and glucose tolerance were analyzed by two-way repeated measures ANOVA with one factor being genotype and the other factor being time. Additionally, two-way ANOVA was used to analyze fiber type distribution and CSA, genotype by fiber type. Differences in *in vitro* force production, NMJ innervation, mitochondrial function, mitochondrial content, ROS production, mtDNA damage and autophagy protein expression between genotypes were analyzed by one-way ANOVAs. Overall fiber distribution was analyzed by Chi-squared. All data were required to pass normality (Shapiro-Wilk) and equal variance tests (Brown-Forsythe *F* test) before proceeding with the two-way RM ANOVA. Significant interactions were tested with Tukey's *post hoc* test using JMP statistical software (SAS, Cary, NC) to find differences between groups. Group main effects are reported where significant interactions were not observed. An α level of 0.05 was used for all analyses and all values are means ± SD.

Results

Age-related declines in autophagy-related proteins LC3 (MAP1LC3A) and ATG7 have previously been reported, and these declines are thought to contribute to sarcopenia (Carnio et al., 2014). To gain insight into the Ulk1 protein content changes with age, we analyzed total and activated Ulk1 (pSer555) protein content in LM young adults (4 months) and middle-aged (16 months) mice. Total Ulk1 protein content was 40% greater in middle-aged mice (Supp Fig 4.1A, p=0.0239), yet activated Ulk1 was 36% less (Supp Fig 4.1B, p=0.0168) compared to young adult mice.

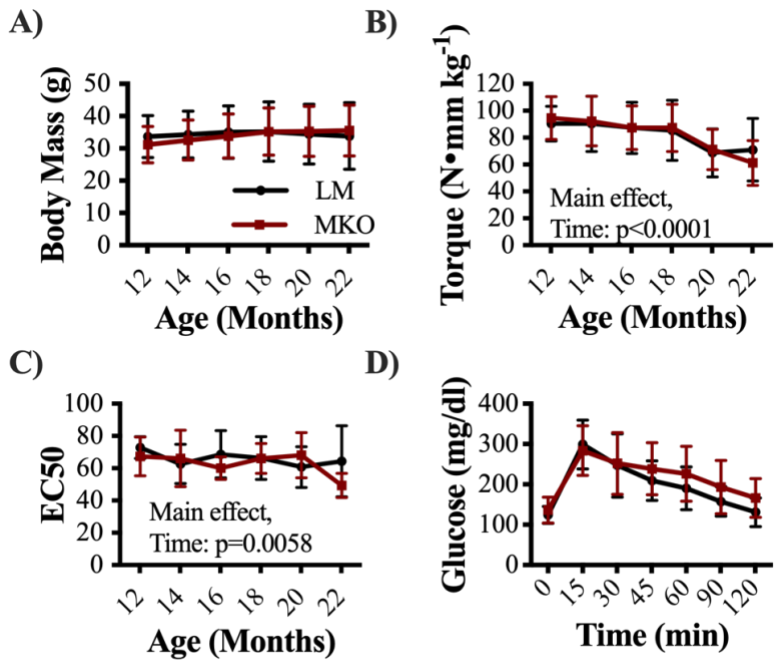

Figure 4.1: Decline in skeletal muscle function with age
A) Average longitudinal body mass measurements of Ulk1 MKO mice and LM controls starting at 12 months of age through 22 months. B) Average longitudinal *in vivo* muscle torque measurements from 12-22 months of age. C) EC50 calculated from longitudinal force frequency measurements. D) Average glucose levels recorded during a glucose tolerance test at 22 months of age in both Ulk1 MKO and LM control mice. All data are presented as mean ± SD n=10 mice. Main effects are listed where observed.

Ulk1 autophagy-deficient mice (MKO) at 22 months of age were used to interrogate how reduced Ulk1 protein content and/or signaling may contribute to age-related skeletal muscle dysfunction. Body mass did not differ between LM age-matched controls and MKO mice or change significantly with time during the longitudinal portion of this study (12-22 months; Fig 4.1A, $p=0.4181$). Over the 12-month longitudinal period there was a 40% loss of peak isometric dorsiflexion torque independent of genotype (Fig 4.1C, $p<0.0001$). Sarcopenia is associated with a preferential loss of fast-twitch fibers such that muscles take on a more slow-twitch phenotype. We therefore analyzed the stimulation frequency at which dorsiflexor muscles reached half of their peak isometric torque in order to gain insight into potential fiber type shifts between LM and MKO

mice. The frequency at which 50% of peak torque was reached (EC50) decreased by age, independent of genotype indicating a more slow-twitch phenotype. (70.1±9.9 vs. 52.4±20.3 Hz, 12- and 22-months, Fig 4.1C, Main effect: Time p=0.0058). Prior to sacrifice, we used a glucose tolerance test to evaluate the impact of Ulk1 on insulin resistance in aged mice. MKO and LM mice showed similar glucose excursions and clearance after an injected glucose bolus (Fig 4.1D, p=0.8538). Since 40% of the body is made up of muscle and consumes a large portion of blood glucose, we investigated muscle masses after sacrifice and did not find any differences between genotypes in TA, EDL or soleus (SOL) muscle masses (Supp Fig. 4.2, p ≥0.07). However, gastrocnemius muscle and heart mass were significantly reduced in MKO mice when normalized to body mass (Supp Fig. 4.2, p≤0.04).

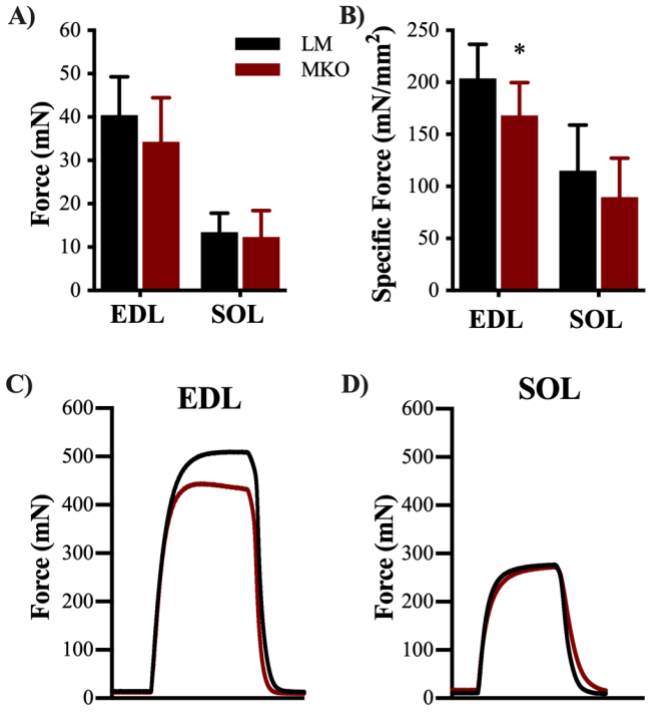

Figure 4.2: Ulk1 deficiency predominately affects type II muscle fibers strength
A) Average *in vitro* maximum contraction force from both EDL and SOL muscles (p>0.05) B) Average specific force from both EDL and SOL muscles (p=0.0277, and p=0.2371, respectfully). Representative torque tracing from C) EDL and D) SOL muscles. All data are presented as mean ± SD n=10 mice. *=Significantly different from LM

In vitro contractility of the EDL and soleus muscles was assessed in isolated muscles to determine if muscle Ulk1 deficiency with age disproportionately affected fast- vs. slow-twitch muscles, respectively. We detected no difference in EDL maximal isometric force (Fig 4.2A, p=0.1750), however when accounting for muscle CSA, EDL specific force production was 17% less in the MKO mice compared to the LM (Fig 4.2B, p=0.0277). No difference was detected between genotypes for either soleus maximal isometric force or specific force (Fig 4.2, p=0.2371) which suggests that fast-twitch muscles may be affected to a greater extent by Ulk1 deficiency throughout life.

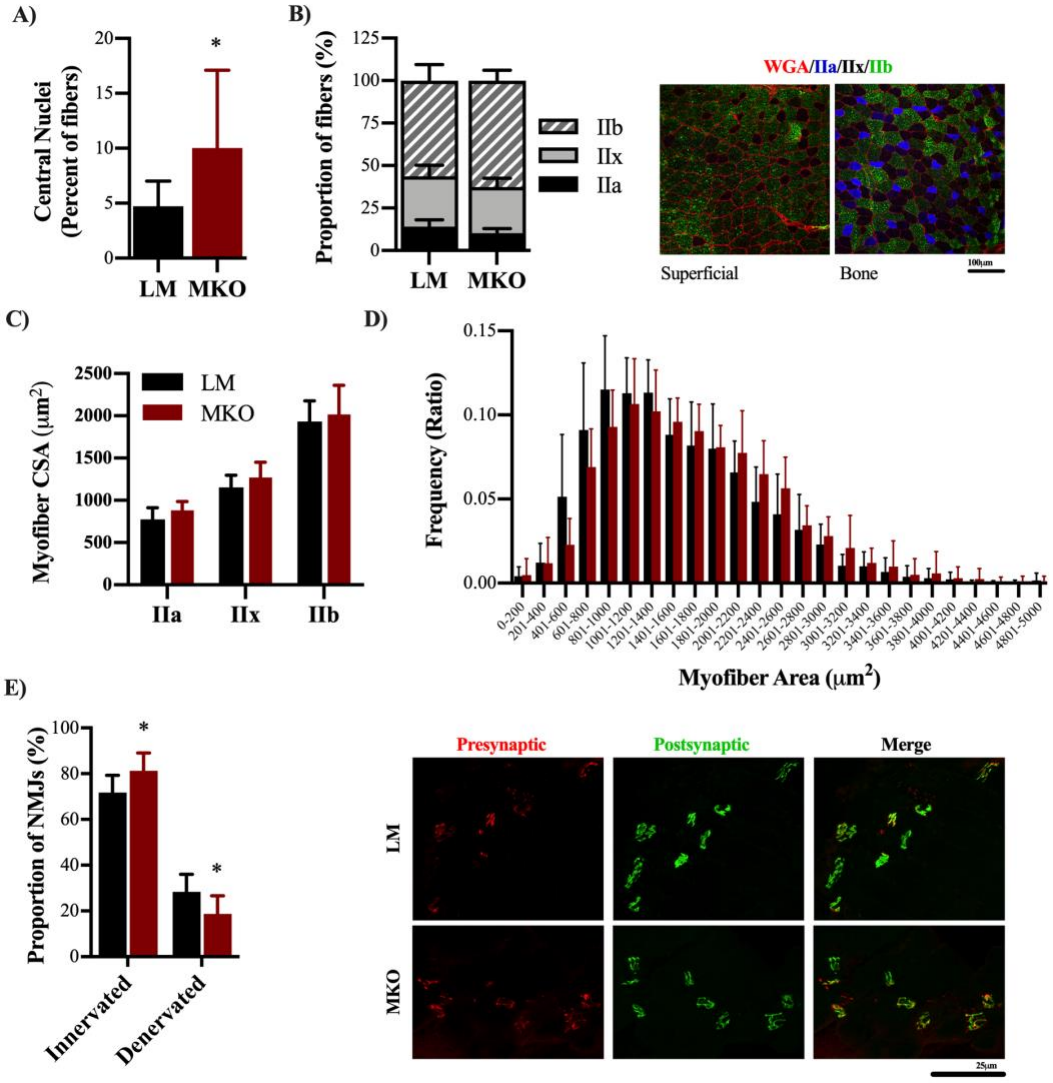

Figure 4.3: Ulk1 deficiency throughout life leads to enlarged but less functional muscle fibers and altered NMJs.
A) Percent of centrally located nuclei (p=0.0487) B) Distribution of fiber types within TA muscle sections analyzed and representative images of fiber type staining. C) CSA of different fiber types D) Frequency distributions of fiber CSAs from TA muscles. E) Average number of innervated and denervated NMJs in the diaphragm of MKO and LM mice with representative image of neuromuscular junction staining (p=0.0227). All data are presented as mean ± SD. *= significantly different from LM

The primary ankle dorsiflexor muscle, the TA muscle, was analyzed for differences in fiber number, fiber type specific distribution, and CSA. There was no difference in total fiber number between genotypes (2342±498 vs. 2036±678, LM and MKO, respectively, p=0.2640). There were expected differences in fiber type distribution of type IIa, IIx, and IIb fibers of the TA muscle, however there was no differences in the proportion of fibers types between genotypes (Fig. 4.3A, p=0.0210, main effect of fiber type). *In vivo* and *in vitro* contractile properties (e.g., twitch half-relaxation time) that can reflect fiber type shifts were also analyzed and there were no significant differences between genotypes (Supp table 4.1, $p \geq 0.068$). Expected differences in fiber type-specific CSA were measured, with IIa being the smallest and IIb the largest (Fig 4.3B, $p<0.0001$), yet no difference between genotypes was observed (p=0.9633). Furthermore, the distribution of overall fiber CSAs independent of fiber type were shifted rightward, indicative of larger muscle fibers overall in MKO compared to LM (Fig. 4.3D, p=0.0035). The mean CSA of all fibers was 10% greater in the TA muscle of MKO compared to LM (1539±215 vs. 1692±248 μm^2, LM and MKO, respectively). The TA muscle contributes greater than 80% to peak-isometric torque of the ankle dorsiflexors, so we retroactively analyzed peak isometric torque normalized by the TA muscle CSA. Specific peak-isometric torque was 15% less in MKO mice compared to LM controls (Supp Fig 4.3, p=0.0078).

Centrally-located nuclei were assessed in TA muscles and NMJ integrity in diaphragm muscles from LM and MKO mice. In agreement with a previous report involving muscle-specific Atg7 knockouts(Carnio et al., 2014), there was a greater percentage of centrally-located nuclei in autophagy deficient MKO muscles compared to LM (Fig. 4.3B, p=0.0487). Previous aging research and autophagy-deficient models have also revealed changes in NMJ integrity, (Carnio et al., 2014; Greising, Stowe, Sieck, & Mantilla, 2015) so in order to determine if Ulk1 influenced NMJs we assessed the innervation of diaphragm muscle NMJs of MKO and LM mice (Fig 4.3G). The diaphragm muscle displays all fiber types and is necessary for life, providing evaluation of a muscle in-between the predominantly slow- and fast-twitch limb muscles. Interestingly, the old MKO mice had a greater proportion of innervated fibers and less denervated fibers compared to age-matched LMs (Fig 4.3E, p=0.0227). The frequency of denervation in the age-matched LM is comparable to that previously reported, and follows a period of rapid denervation between middle and old age. We suspect our evaluation comes at a time in which many fibers have been lost to lack of innervation, i.e., there was survivor bias. Furthermore, we interpret this to indicate Ulk1 deficiency across the lifespan accelerated sarcopenia-related fiber death (i.e., centrally-located nuclei) and supports evaluation of skeletal muscle at an earlier age.

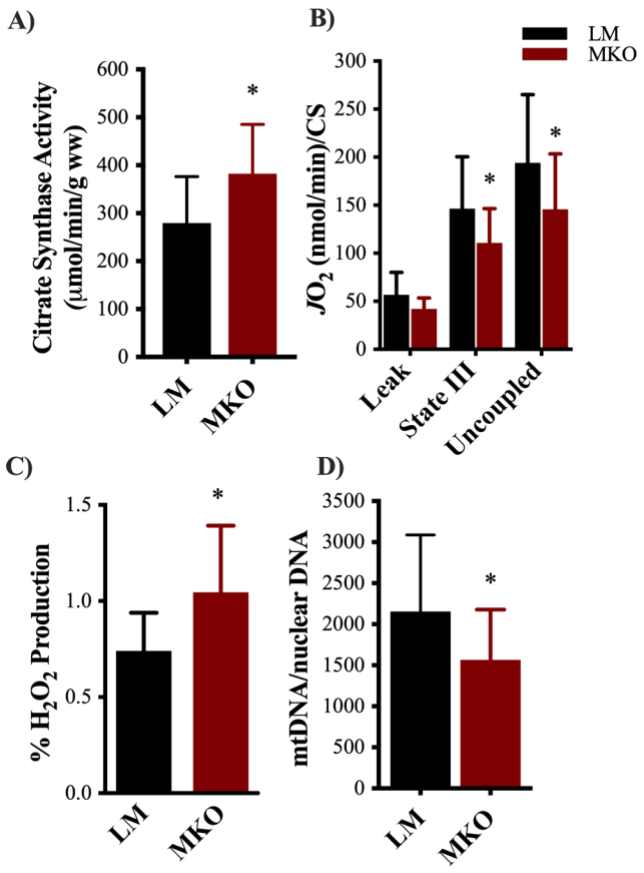

Figure 4.4: Lifelong Ulk1 deficiency results in an accumulation of dysfunctional mitochondria. A) Mitochondrial content assessed through citrate synthase enzyme kinetic rates (p=0.0443). B) Mitochondrial oxygen consumption during Leak, State III, and uncoupled respiration normalized to citrate synthase rate (p=0.0035 and p=0.0118, respectfully). C) Percent ROS production normalized to oxygen consumption during leak respiration to account for differences in oxygen flux (p=0.0428). D) Mitochondrial DNA content normalized to nuclear DNA content (p=0.0309).

Ulk1-mediated autophagy is one of the main degradative pathways for skeletal muscle mitochondria, therefore we decided to investigate mitochondrial content, function, and ROS production after lifelong Ulk1 deficiency. Mitochondrial content (assessed through citrate synthase activity) was 37% greater in the MKO muscle fibers compared to LM (Fig. 4.4A, $p<0.0443$). Despite this, permeabilized muscle fibers from MKO had 24% less State III (max physiological) and 25% less uncoupled (max) respiration compared to LM controls (Fig. 4.4B,

p<0.02), which suggest impaired mitochondrial function. In agreement, MKO also produced more ROS per unit of oxygen flux than the LM permeabilized muscle fibers. (Fig. 4.4C, p=0.0428) To determine the extent to which Ulk1 deficiency and greater ROS production damaged mitochondria, we assessed mitochondrial DNA content and found that it was decreased in Ulk1 MKO muscle compared to LM control muscle (Fig 4.4D, p=0.0309).

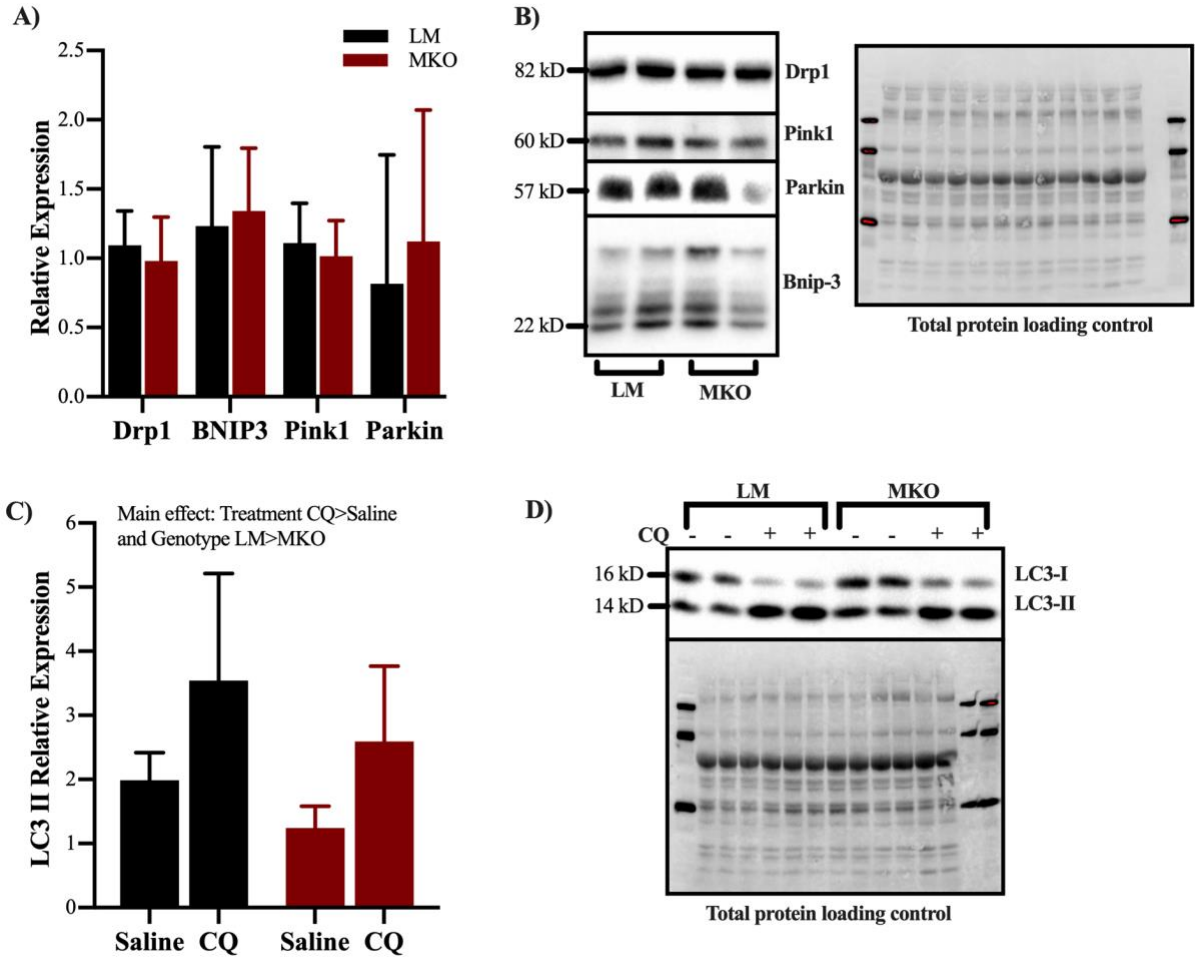

Figure 4.5: Mitophagy and autophagy flux in middle aged Ulk1 MKO mice
A) Relative expression of mitophagy related proteins DRP1, BNIP3, Pink1, and Parkin (p>0.05), B) Representative immunoblot panel C) Relative expression of LC3II in middle aged mice treated with Choloroquine or saline as a control (Main effect of Treatment and Genotype p=0.0007 and p=0.0341, respectfully). D) Representative immunoblots of LC3.

We utilized a second cohort of middle-aged MKO and LM mice to better understand disruptions in autophagy signaling that may elicit the observed aging phenotypes. Middle-aged mice were selected based on the timepoint at which peak isometric torque significantly decreased in our old (22-month) cohort of mice. In a panel of proteins typically indicative of mitophagy signaling (DRP1, BNIP3, Pink1 and Parkin), there were no differences between genotypes in middle-aged mice (Fig. 4.5A, $p>0.05$). Basal autophagy flux was assessed by an acute treatment with the lysosomal inhibitor Chloroquine (CQ). CQ treatment resulted in greater accumulation of LC3II protein content independent of genotype (Fig. 4.5C, $p=0.0007$), and MKO mice had less LC3II protein content independent of treatment (Fig. 4.5C, $p=0.0341$). These data suggest that autophagosome number and/or degradation is impaired in MKO mice but is inconclusive on the extent to which autophagy flux is altered specifically.

Discussion

Herein we provide strong evidence in support of our hypothesis that lifelong Ulk1-defiency exacerbates sarcopenia, as indicated by a worsening of skeletal muscle contractile and metabolic function. Both LM and MKO mice exhibited expected age-related declines in muscle strength, yet muscle weakness was markedly greater in MKO mice when muscle CSA was accounted for in the EDL and TA muscles (Fig 2 and Supp Fig 3). Muscle fibers from MKO mice had poor mitochondrial respiration when normalized by mitochondrial content and produced more mitochondrial-derived ROS compared to muscle from LM mice which supports the notion of greater mitochondrial dysfunction in MKO mice (Fig. 4). An accumulation of dysfunctional mitochondria could, in part, explain the advanced sarcopenia phenotype in MKO mice. Interestingly, we detected no difference in protein content related to mitochondrial removal (DRP1) or mitochondrial targeting for autophagosome encapsulation (BNIP3, Pink1, Parkin)

between LM and MKO mice (Fig. 5). However, Ulk1 deficiency might have influenced autophagosome assembly and/or degradation as our chloroquine experiment showed less LC3II protein content in MKO muscle compared to LM (Fig. 5).

The decline of mitochondrial function throughout life is thought to be a major contributor to many aging phenotypes (Carter et al., 2018; Marzetti et al., 2013; Rajawat et al., 2009; Zhou et al., 2017). We observed herein that with chronic deficient Ulk1, there is an exacerbated accumulation of damaged mitochondria by 22 months of age which produce more ROS and have less mtDNA (a sign of damage) (Fig. 4). Similar findings of accumulated damaged mitochondria have been found in many other aging autophagy knockout models (Bujak et al., 2015; Carnio et al., 2014). Interestingly, our data revealed through weaker EDL muscles that type II fibers were more preferentially affected by this accumulation of damaged mitochondria (Fig. 2). This is supported by two compounding facts: 1) Type II fibers have less endogenous antioxidants, and 2) Type II fibers have less overall mitochondrial maintenance signaling (Crupi et al., 2018; Smith, Soriano-Arroquia, Goljanek-Whysall, Jackson, & McDonagh, 2018). In other words, type II fibers may accumulate damaged mitochondria more quickly, produce more ROS as a consequence, and have less endogenous protection from ROS damage (Crupi et al., 2018; Smith et al., 2018). Finding ways, such as exercise, to stimulate more mitochondrial maintenance signaling, particularly mitophagy, and endogenous antioxidant signaling with age may be a valuable therapeutic to preserve type II fiber function throughout life.

Ulk1 is one of the few autophagy-related kinases and its various roles in autophagy signaling are still being elucidated. Ulk1 appears to play a unique role in mitophagy signaling as it is sensitive to shifts in energy states and is post-translationally modified by energy sensing proteins like AMPK (Egan et al., 2011; Kim, Kundu, Viollet, & Guan, 2011). AMPK

phosphorylates Ulk1 at s555 prompting Ulk1 to co-localize to the mitochondria which is responsible for inducing mitophagy, as is the case in response to exercise (Laker et al., 2017). Specifically, AMPK-induced Ulk1 co-localization recruits autophagy-related machinery and lysosomes to the mitochondria to complete autophagic degradation (Laker et al., 2017). Not surprisingly, aged AMPK-deficient mice have weaker muscles with enlarged and damaged mitochondria (reduced mtDNA and increased ROS) similar to the data presented herein with Ulk1 MKO (Bujak et al., 2015). Overall, this strongly supports the AMPK-Ulk1 signaling cascade for the degradation of damaged mitochondria though mitophagy is important with age. Because autophagy is a dynamic process, degradation and flux through the process must also be taken into account when assessing overall autophagic function. We have previously shown that although autophagy signaling is greatly upregulated in response to muscle injury, autophagic flux does not increase to the same extent which results in an autophagosome clearance bottleneck (Call & Nichenko, 2020). It is unclear whether other scenarios result in a bottleneck, however recent research has expanded the role of Ulk1 beyond autophagosome regulation and associated it with regulating autophagy flux (Wang et al., 2018). Wang et al. reported that in yeast, Atg1 (a Ulk1 homologue) kinase activity regulates the tethering of autophagosomal and lysosomal SNARE proteins which leads to autophagolysosome fusion and subsequent degradation (Wang et al., 2018). Post-translational modifications and kinase activities of Ulk1 were not within the scope of this paper but with that said, the absence of Ulk1 did not alter the expression of mitophagy proteins. This does not necessarily mean that Ulk1 is not critical for mitophagy proteins, it may simply reflect that the alternative autophagy pathways compensate such as the AMPK-independent Drp1 pathway and/or the alternative Ulk1 isoform, Ulk2, pathway (Fuqua et al., 2019; Laker et al., 2017).

Sarcopenia is associated with a reduction in motor units and some of the denervated muscle fibers can be inappropriately reinnervated such that a slow-twitch fiber is innervated by a fast-fatigable motor unit leading to altered recruitment patterns and changes in NMJ structure. Carnio et al. investigated the relationship between autophagy and NMJs specifically using ATG7 knockout mice and found that the muscle fibers from KO mice were expressing more NCAM, an attractant for alpha motoneurons, as a way to recruit new terminal axons to NMJs (Carnio et al., 2014). It is unclear the extent to which our results support the work of Carnio et al., as our aged autophagy deficient mice actually appeared to have greater innervation (Fig. 3) (Carnio et al., 2014). NMJ structure and innervation are a dynamic, ongoing processes and there is potential that we captured ongoing reinnervation in the MKO mice subsequent to loss of innervation. Alternatively, the absence of Ulk1 was associated with an undefined compensatory mechanism to increase alpha motoneuron innervation in order to try and improve muscle contractile function. Nonetheless, data presented here and reported by Carnio et al. are in agreement that deficient autophagy results in altered NMJ structure and innervation ratios (Carnio et al., 2014), and autophagy may be a therapeutic target to mitigate NMJ changes with age.

Throughout life there is ongoing myonuclei turnover in uninjured muscle fibers in order to maintain muscle homeostasis. Specifically, satellite cells are reported to be responsible for this myonuclei turnover and this process results in increased centrally-located nuclei with age, a marker typically reflecting muscle injury and ongoing repair (Gallegly et al., 2004; Li, Lee, & Thompson, 2011; Pawlikowski, Pulliam, Betta, Kardon, & Olwin, 2015). It is unclear why centrally-located nuclei increase with age, but it appears to coincide with age-related changes in NMJ integrity (Li et al., 2011; Valdez et al., 2010). Autophagy deficiency may pre-dispose fibers to NMJ remodeling with age, and this could influence satellite cell dynamics and/or a muscle fibers susceptibility to

contraction-induced injury based on changing motor unit recruitment patterns. The inverse is also possible, as we reported a protracted recovery process after injury in autophagy deficiency muscle and this could influence satellite cell behavior and NMJ integrity. Toward therapeutics, caloric restriction (a potent autophagy stimulus) decreases NMJ denervation and centrally located nuclei in aged mice (Valdez et al., 2010). Collectively there is support for further investigating the role of autophagy in mediating the relationship between NMJ and myonuclei maintenance in aged muscle.

The influence of sex and age on autophagy is an interesting conundrum that requires further investigation. A limitation herein is that we included both male and female mice in this study but we were statistically underpowered to detect specific sex differences. There were three data outcomes that showed significant trends in sex differences, centrally-located nuclei were greater in MKO males, and in our mitophagy panel we detected that males had greater BNIP3 and decreased DRP1 protein expression independent of genotype. To our knowledge, there has been limited research on the sex specific differences but one study linked estrogen receptor signaling to autophagy and mitochondrial function, and testosterone signaling involved in autophagy has been under investigated (Ribas et al., 2016). Deciphering the sex differences in autophagy regulation specifically with age may be an important avenue for further research.

In summary, lifelong Ulk1 deficiency results in an accumulation of dysfunctional, ROS producing mitochondria that coincides with reduced muscle force production, alter NMJs, and increase centrally-located nuclei. This aging phenotype may be due to a reduction in autophagosome formation and degradation as a consequence of absent Ulk1 signaling. Considering that Ulk1 activation naturally declines with age and its dual role in autophagosome

formation and degradation, Ulk1 provides an interesting therapeutic target to maintain muscle quality throughout life.

Supplemental Tables and Figures

Supplemental Table 4.1: *in vivo* and *in vitro* contractile properties

	LM (n=10)	MKO (n=10)	P-value
In Vivo			
+d*P*/d*t* (N/s)	291.64	285.73	0.8886
-d*P*/d*t* (N/s)	277.40	244.27	0.3603
In Vitro			
EDL			
Length (mm)	11.7 (0.5)	11.4 (0.4)	0.117
Mass (mg)	10.6 (1.2)	10.5 (1.8)	0.892
CSA	1.95 (0.27)	1.98 (0.35)	0.796
P_t (nM)	84.6 (14.6)	63.6 (14.8)	0.041
P_t TTP (ms)	20.4 (2.6)	18.5 (2.6)	0.166
P_t HRT (ms)	23.2 (3.1)	19.7 (3.9)	0.068
P_o +d*P*/d*t* (N/s)	14.5 (3.2)	13.2 (3.2)	0.453
P_o -d*P*/d*t* (N/s)	27.0 (5.1)	23.6 (7.5)	0.300
Soleus			
Length (mm)	10.1 (1.0)	10.1 (1.1)	0.995
Mass (mg)	9.0 (1.9)	10.0 (2.5)	0.442
CSA	1.21 (0.31)	1.33 (0.42)	0.511
P_t (nM)	20.8 (3.1)	17.1 (5.6)	0.475
P_t TTP (ms)	41.6 (10.9)	35.3 (9.6)	0.531
P_t HRT (ms)	61.5 (14.2)	47.8 (11.7)	0.277
P_o +d*P*/d*t* (N/s)	6.4 (1.6)	6.4 (2.5)	0.947
P_o -d*P*/d*t* (N/s)	5.3 (2.0)	6.9 (1.5)	0.405

P_t=peak twitch force. TTP=time-to-peak force. HRT=half-relaxation time. P_o=maximal isometric tetanic force. +dP/dt=maximal rate of contraction. −dP/dt=maximal rate of relaxation
Mean (SD)

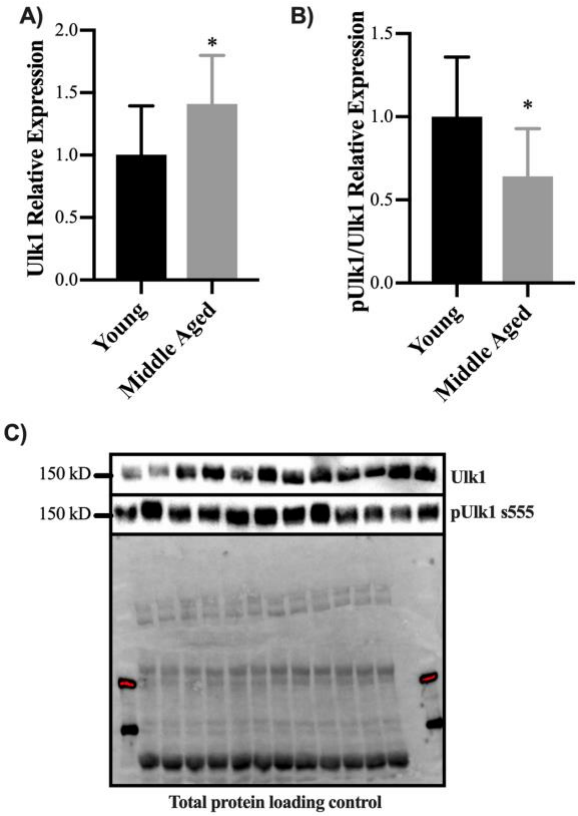

Supplemental Figure 4.1: Ulk1 and pUlk1 expression changes with age
A) Relative expression of Ulk1 in young (4 month old) and middle-aged (16 month old) mice. B) Relative expression of pUlk1 normalized to Ulk1 in young and middle-aged mice. C) Representative immunoblot images of Ulk1 and pUlk1 (s555). All data are presented as mean ± SD n=7 mice. *= significantly different from LM

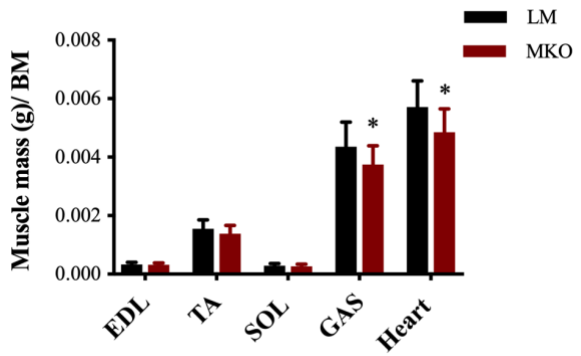

Supplemental Figure 4.2: Muscle masses in old MKO and LM mice
Muscle masses normalized to body mass. All data are presented as mean ± SD n=10 mice. *= significantly different from LM

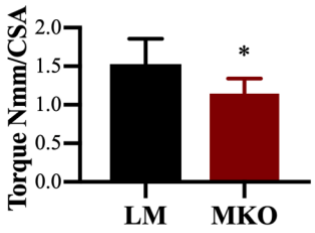

Supplemental Figure 4.3: *in vivo* torque normalized by CSA
in vivo torque normalized to CSA to account for fiber size differences between genotypes. All data are presented as mean ± SD n=10 mice. *= significantly different from LM.

References

Aas, S. N., Hamarsland, H., Cumming, K. T., Rognlien, S. H., Aase, O. J., Nordseth, M., . . . Raastad, T. (2019). The impact of age and frailty on skeletal muscle autophagy markers and specific strength: A cross-sectional comparison. *Exp Gerontol, 125*, 110687. doi:10.1016/j.exger.2019.110687

Arribat, Y., Broskey, N. T., Greggio, C., Boutant, M., Conde Alonso, S., Kulkarni, S. S., . . . Amati, F. (2019). Distinct patterns of skeletal muscle mitochondria fusion, fission and mitophagy upon duration of exercise training. *Acta Physiol (Oxf), 225*(2), e13179. doi:10.1111/apha.13179

Balan, E., Schwalm, C., Naslain, D., Nielens, H., Francaux, M., & Deldicque, L. (2019). Regular Endurance Exercise Promotes Fission, Mitophagy, and Oxidative Phosphorylation in Human Skeletal Muscle Independently of Age. *Front Physiol, 10*, 1088. doi:10.3389/fphys.2019.01088

Baltgalvis, K. A., Call, J. A., Nikas, J. B., & Lowe, D. A. (2009). Effects of prednisolone on skeletal muscle contractility in mdx mice. *Muscle Nerve, 40*(3), 443-454. doi:10.1002/mus.21327

Baumann, C. W., Kwak, D., Liu, H. M., & Thompson, L. V. (2016). Age-induced oxidative stress: how does it influence skeletal muscle quantity and quality? *J Appl Physiol (1985), 121*(5), 1047-1052. doi:10.1152/japplphysiol.00321.2016

Brunk, U. T., & Terman, A. (2002). The mitochondrial-lysosomal axis theory of aging: accumulation of damaged mitochondria as a result of imperfect autophagocytosis. *Eur J Biochem, 269*(8), 1996-2002. doi:10.1046/j.1432-1033.2002.02869.x

Bujak, A. L., Crane, J. D., Lally, J. S., Ford, R. J., Kang, S. J., Rebalka, I. A., . . . Steinberg, G. R. (2015). AMPK activation of muscle autophagy prevents fasting-induced hypoglycemia and myopathy during aging. *Cell Metab, 21*(6), 883-890. doi:10.1016/j.cmet.2015.05.016

Call, J. A., & Lowe, D. A. (2016). Eccentric Contraction-Induced Muscle Injury: Reproducible, Quantitative, Physiological Models to Impair Skeletal Muscle's Capacity to Generate Force. *Methods Mol Biol, 1460*, 3-18. doi:10.1007/978-1-4939-3810-0_1

Call, J. A., & Nichenko, A. S. (2020). Autophagy: an essential but limited cellular process for timely skeletal muscle recovery from injury. *Autophagy*, 1-4. doi:10.1080/15548627.2020.1753000

Calvani, R., Joseph, A. M., Adhihetty, P. J., Miccheli, A., Bossola, M., Leeuwenburgh, C., . . . Marzetti, E. (2013). Mitochondrial pathways in sarcopenia of aging and disuse muscle atrophy. *Biol Chem, 394*(3), 393-414. doi:10.1515/hsz-2012-0247

Carnio, S., LoVerso, F., Baraibar, M. A., Longa, E., Khan, M. M., Maffei, M., . . . Sandri, M. (2014). Autophagy impairment in muscle induces neuromuscular junction degeneration and precocious aging. *Cell Rep, 8*(5), 1509-1521. doi:10.1016/j.celrep.2014.07.061

Carter, H. N., Kim, Y., Erlich, A. T., Zarrin-Khat, D., & Hood, D. A. (2018). Autophagy and mitophagy flux in young and aged skeletal muscle following chronic contractile activity. *J Physiol, 596*(16), 3567-3584. doi:10.1113/jp275998

Collins, M. A., An, J., Peller, D., & Bowser, R. (2015). Total protein is an effective loading control for cerebrospinal fluid western blots. *J Neurosci Methods, 251*, 72-82. doi:10.1016/j.jneumeth.2015.05.011

Crupi, A. N., Nunnelee, J. S., Taylor, D. J., Thomas, A., Vit, J. P., Riera, C. E., . . . Goodridge, H. S. (2018). Oxidative muscles have better mitochondrial homeostasis than glycolytic muscles throughout life and maintain mitochondrial function during aging. *Aging (Albany NY), 10*(11), 3327-3352. doi:10.18632/aging.101643

Egan, D. F., Shackelford, D. B., Mihaylova, M. M., Gelino, S., Kohnz, R. A., Mair, W., . . . Shaw, R. J. (2011). Phosphorylation of ULK1 (hATG1) by AMP-activated protein kinase connects energy sensing to mitophagy. *Science, 331*(6016), 456-461. doi:10.1126/science.1196371

Fuqua, J. D., Mere, C. P., Kronemberger, A., Blomme, J., Bae, D., Turner, K. D., . . . Lira, V. A. (2019). ULK2 is essential for degradation of ubiquitinated protein aggregates and homeostasis in skeletal muscle. *Faseb j, 33*(11), 11735-11745. doi:10.1096/fj.201900766R

Gallegly, J. C., Turesky, N. A., Strotman, B. A., Gurley, C. M., Peterson, C. A., & Dupont-Versteegden, E. E. (2004). Satellite cell regulation of muscle mass is altered at old age. *J Appl Physiol (1985), 97*(3), 1082-1090. doi:10.1152/japplphysiol.00006.2004

Green, D. R., Galluzzi, L., & Kroemer, G. (2011). Mitochondria and the autophagy-inflammation-cell death axis in organismal aging. *Science, 333*(6046), 1109-1112. doi:10.1126/science.1201940

Greising, S. M., Stowe, J. M., Sieck, G. C., & Mantilla, C. B. (2015). Role of TrkB kinase activity in aging diaphragm neuromuscular junctions. *Exp Gerontol, 72*, 184-191. doi:10.1016/j.exger.2015.10.013

Kim, J., Kundu, M., Viollet, B., & Guan, K. L. (2011). AMPK and mTOR regulate autophagy through direct phosphorylation of Ulk1. *Nat Cell Biol, 13*(2), 132-141. doi:10.1038/ncb2152

Klionsky, D. J., Abdelmohsen, K., Abe, A., Abedin, M. J., Abeliovich, H., Acevedo Arozena, A., . . . Zughaier, S. M. (2016). Guidelines for the use and interpretation of assays for monitoring autophagy (3rd edition). *Autophagy, 12*(1), 1-222. doi:10.1080/15548627.2015.1100356

Kundu, M., Lindsten, T., Yang, C. Y., Wu, J., Zhao, F., Zhang, J., . . . Thompson, C. B. (2008). Ulk1 plays a critical role in the autophagic clearance of mitochondria and ribosomes during reticulocyte maturation. *Blood, 112*(4), 1493-1502. doi:10.1182/blood-2008-02-137398

Laker, R. C., Drake, J. C., Wilson, R. J., Lira, V. A., Lewellen, B. M., Ryall, K. A., . . . Yan, Z. (2017). Ampk phosphorylation of Ulk1 is required for targeting of mitochondria to lysosomes in exercise-induced mitophagy. *Nat Commun, 8*(1), 548. doi:10.1038/s41467-017-00520-9

Li, Y., Lee, Y., & Thompson, W. J. (2011). Changes in aging mouse neuromuscular junctions are explained by degeneration and regeneration of muscle fiber segments at the synapse. *J Neurosci, 31*(42), 14910-14919. doi:10.1523/jneurosci.3590-11.2011

Marzetti, E., Calvani, R., Cesari, M., Buford, T. W., Lorenzi, M., Behnke, B. J., & Leeuwenburgh, C. (2013). Mitochondrial dysfunction and sarcopenia of aging: from

signaling pathways to clinical trials. *Int J Biochem Cell Biol, 45*(10), 2288-2301. doi:10.1016/j.biocel.2013.06.024

Masser, D. R., Clark, N. W., Van Remmen, H., & Freeman, W. M. (2016). Loss of the antioxidant enzyme CuZnSOD (Sod1) mimics an age-related increase in absolute mitochondrial DNA copy number in the skeletal muscle. *Age (Dordr), 38*(4), 323-333. doi:10.1007/s11357-016-9930-1

Moran, A. L., Warren, G. L., & Lowe, D. A. (2005). Soleus and EDL muscle contractility across the lifespan of female C57BL/6 mice. *Exp Gerontol, 40*(12), 966-975. doi:10.1016/j.exger.2005.09.005

Moulis, M., & Vindis, C. (2017). Methods for Measuring Autophagy in Mice. *Cells, 6*(2). doi:10.3390/cells6020014

Nichenko, A. S., Southern, W. M., Atuan, M., Luan, J., Peissig, K. B., Foltz, S. J., . . . Call, J. A. (2016). Mitochondrial maintenance via autophagy contributes to functional skeletal muscle regeneration and remodeling. *Am J Physiol Cell Physiol, 311*(2), C190-200. doi:10.1152/ajpcell.00066.2016

Nichenko, A. S., Southern, W. M., Tehrani, K. F., Qualls, A. E., Flemington, A. B., Mercer, G. H., . . . Call, J. A. (2020). Mitochondrial-specific autophagy linked to mitochondrial dysfunction following traumatic freeze injury in mice. *Am J Physiol Cell Physiol, 318*(2), C242-c252. doi:10.1152/ajpcell.00123.2019

Pawlikowski, B., Pulliam, C., Betta, N. D., Kardon, G., & Olwin, B. B. (2015). Pervasive satellite cell contribution to uninjured adult muscle fibers. *Skelet Muscle, 5*, 42. doi:10.1186/s13395-015-0067-1

Rajawat, Y. S., Hilioti, Z., & Bossis, I. (2009). Aging: central role for autophagy and the lysosomal degradative system. *Ageing Res Rev, 8*(3), 199-213. doi:10.1016/j.arr.2009.05.001

Ribas, V., Drew, B. G., Zhou, Z., Phun, J., Kalajian, N. Y., Soleymani, T., . . . Hevener, A. L. (2016). Skeletal muscle action of estrogen receptor alpha is critical for the maintenance of mitochondrial function and metabolic homeostasis in females. *Sci Transl Med, 8*(334), 334ra354. doi:10.1126/scitranslmed.aad3815

Smith, N. T., Soriano-Arroquia, A., Goljanek-Whysall, K., Jackson, M. J., & McDonagh, B. (2018). Redox responses are preserved across muscle fibres with differential susceptibility to aging. *J Proteomics, 177*, 112-123. doi:10.1016/j.jprot.2018.02.015

Turturro, A., Witt, W. W., Lewis, S., Hass, B. S., Lipman, R. D., & Hart, R. W. (1999). Growth curves and survival characteristics of the animals used in the Biomarkers of Aging Program. *J Gerontol A Biol Sci Med Sci, 54*(11), B492-501. doi:10.1093/gerona/54.11.b492

Valdez, G., Tapia, J. C., Kang, H., Clemenson, G. D., Jr., Gage, F. H., Lichtman, J. W., & Sanes, J. R. (2010). Attenuation of age-related changes in mouse neuromuscular synapses by caloric restriction and exercise. *Proc Natl Acad Sci U S A, 107*(33), 14863-14868. doi:10.1073/pnas.1002220107

Vigelso, A., Dybboe, R., Hansen, C. N., Dela, F., Helge, J. W., & Guadalupe Grau, A. (2015). GAPDH and beta-actin protein decreases with aging, making Stain-Free technology a superior loading control in Western blotting of human skeletal muscle. *J Appl Physiol (1985), 118*(3), 386-394. doi:10.1152/japplphysiol.00840.2014

Wang, C., Wang, H., Zhang, D., Luo, W., Liu, R., Xu, D., . . . Liu, Z. (2018). Phosphorylation of ULK1 affects autophagosome fusion and links chaperone-mediated autophagy to macroautophagy. *Nat Commun, 9*(1), 3492. doi:10.1038/s41467-018-05449-1

Wohlgemuth, S. E., Lees, H. A., Marzetti, E., Manini, T. M., Aranda, J. M., Daniels, M. J., . . . Anton, S. D. (2011). An exploratory analysis of the effects of a weight loss plus exercise program on cellular quality control mechanisms in older overweight women. *Rejuvenation Res, 14*(3), 315-324. doi:10.1089/rej.2010.1132

Wohlgemuth, S. E., Seo, A. Y., Marzetti, E., Lees, H. A., & Leeuwenburgh, C. (2010). Skeletal muscle autophagy and apoptosis during aging: effects of calorie restriction and life-long exercise. *Exp Gerontol, 45*(2), 138-148. doi:10.1016/j.exger.2009.11.002

Zeitler, A. F., Gerrer, K. H., Haas, R., & Jimenez-Soto, L. F. (2016). Optimized semi-quantitative blot analysis in infection assays using the Stain-Free technology. *J Microbiol Methods, 126*, 38-41. doi:10.1016/j.mimet.2016.04.016

Zhou, J., Chong, S. Y., Lim, A., Singh, B. K., Sinha, R. A., Salmon, A. B., & Yen, P. M. (2017). Changes in macroautophagy, chaperone-mediated autophagy, and mitochondrial metabolism in murine skeletal and cardiac muscle during aging. *Aging (Albany NY), 9*(2), 583-599. doi:10.18632/aging.101181

Ziegler, D. V., Wiley, C. D., & Velarde, M. C. (2015). Mitochondrial effectors of cellular senescence: beyond the free radical theory of aging. *Aging Cell, 14*(1), 1-7. doi:10.1111/acel.12287

CHAPTER 5

DISCUSSION AND CONCLUSIONS

The primary goal of my dissertation was to better understand the role of autophagy in skeletal muscle, specifically Ulk1-mediated autophagy. With that goal in mind, my first study investigated the extent to which autophagy was activated following muscle injury. My second study determined whether or not Ulk1-mediated autophagy was required for the recovery of contractility and metabolic function after muscle injury. My final study elucidated whether Ulk1-mediated autophagy was required for maintaining muscle function during the aging process. The results from these studies advanced our understanding of many of the questions raised in my introduction. The following is a summary of those important questions and how my research addressed them.

Activators of autophagy

There are other cellular processes that induce an energy state imbalance in skeletal muscle, for example, muscle injury, however, it is unclear the extent to which autophagy is activated in response to these circumstances. To address this question my first study was designed to induce a muscle injury and look at the autophagy response 14 days after injury. Injured muscles had greater LC3II, and p62 protein expression compared to uninjured muscles as well as increased Ulk1 activation and AMPK content (Figure 2.6 and 2.7). Moreover, when mitigating this autophagy response with a pharmacological inhibitor (3MA) there was less recovery of contractile function and mitochondrial enzyme kinetics (Figure 2.2 &2.3). In my

second study, I expanded upon injury as an activator of autophagy by using different severities of injury (eccentric-contraction induced and traumatic muscle injury) and discovered that the autophagy response scales to the severity of the injury (Figure 2.3). This is clear evidence that muscle injury is a powerful activator of autophagy and suggests that autophagy is an important process for metabolic and contractile functional recovery after injury. These studies definitively add muscle injury to the list of activators of autophagy alongside exercise and caloric restriction.

Outcomes of Autophagy

There are fatty acids, amino acids, and nucleotides that are released following autophagosome degradation and these can be used as nutrients to restore energy balance, as building blocks for protein or organelle synthesis, or as signaling cues within the cell or extracellularly. Although I did not directly design a study to investigate each potential outcome, some of my results do advance our understanding of degraded components used for signaling cues. I used a myogenin-Cre driven promotor to knock out Ukl1 in adult muscle fibers only, meaning the satellite cells within the Ulk1 knockout mice still had functioning Ulk1. I then induced a traumatic muscle injury in the Ulk1 adult muscle fiber knockout mice and their LM controls and measured satellite cell function through proliferation and differentiation rates. Despite the satellite cells having functional Ulk1, there was less proliferation in the satellite cells of knockout mice compared to LMs (Figure 3.8). This suggests that something from successful Ulk1-mediated autophagy may signal to satellite cells and regulate their function. This signal could occur directly to the satellite cells through the extracellular matrix or it could occur indirectly through an inflammatory response due to reduced autophagy. This contributes to our understanding of the products from autophagy efflux as not only being important building blocks but also serving as potential signaling molecules for other cellular processes.

Autophagy Flux

The extent to which autophagy degradation is regulated to match autophagosome assembly after autophagy activation is currently unclear. To directly address this question, I assessed autophagy flux following muscle injury by utilizing a GFP-LC3-RFP-LC3ΔG fluorescent plasmid transfected into muscle and imaged with two-photon microscopy. This plasmid is sensitive to autophagy flux because LC3 is cleaved into a GFP and RFP portion upon autophagy activation where the GFP portion is incorporated into the autophagosome membrane and eventually degraded when autophagosome-lysosome fusion occurs, and the RFP portion remains in the cytosol as an internal control. Although injured muscle had an abundance of autophagosomes compared to uninjured muscle (Figure 3.6), the autophagosomes were degraded at a slower rate (Figure 3.7). This indicates that autophagosome degradation does not match autophagosome assembly after muscle injury and suggest the occurrence of an autophagy bottleneck in injured muscle where autophagosomes are waiting around to be degraded. This research identifies a potential target for advancing muscle recovery therapeutics by improving the capacity for autophagosome degradation during muscle recovery.

Mitophagy

It is well known that mitochondria undergo mitochondrial specific autophagy however it is currently unclear which forms of cellular stress activate mitophagy and the extent to which mitophagy is necessary for adaptations to that stress. To directly address this, I injured skeletal muscles and used a differential centrifugation protocol to isolate mitochondrial fractions. After probing these fractions for autophagosome markers, I found that a large portion of the autophagosomes formed after traumatic muscle injury was localized to the mitochondria (Figure 3.4). Furthermore, the mitophagy specific proteins Bnip3, Pink1, and Parkin were all

significantly elevated in injured muscle compared to uninjured muscle (Figure 3.4). This data indicated that muscle injury is a potent activator of mitophagy. Moreover, Ulk1 is known to be required for mitophagy and there was less contractile recovery in injured Ulk1 knockout muscles compared to LMs (Figure 3.5) which reveals that mitophagy may be required for functional recovery after muscle injury.

Ulk1's role in autophagy

Despite the well-established role of Ulk1 in autophagy, very little research has characterized the role of Ulk1-mediated autophagy specifically in skeletal muscle. To combat this, I designed two studies; one that investigated the role of Ulk1-mediated autophagy in response to muscle injury, and one that elucidated the role of Ulk1-mediated autophagy in healthy skeletal muscle aging. As mentioned in the previous paragraph there was a contractile deficit in the Ulk1 knockout mice compared to LMs following muscle injury (Figure 3.5). In aged Ulk1 knockout mice, we observed an accumulation of ROS producing mitochondria which were associated with mitochondrial damage evident by reduced mtDNA (Figure 4.5). This appeared to more preferentially influence contractility of fast-twitch muscle fibers resulting in weaker EDL muscles in the age Ulk1 knockout mice (Figure 4.2). Overall, this indicates that Ulk1-mediated autophagy is required for the healthy aging of muscle in terms of both metabolic and contractile function. Finally, I probed the extent to which Ulk1 may be implicated in regulating autophagy flux throughout life. To investigate this, I used middle-aged mice treated with the lysosomal inhibitor chloroquine and untreated controls to compare autophagosome accumulation. While the data was slightly ambiguous, it does appear that Ulk1 knockout mice have both reduced autophagosome formation and reduced flux (Figure 4.5). Further research and more specific methods may be needed to address Ulk1's role in regulating autophagy flux,

nonetheless, Ulk1-mediated autophagy has a definitive role in maintaining muscle function after injury and with age.

Future Directions

There are several lines of research for future direction produced from these studies. First, although statistically underpowered to report, I did detect sex differences in a few of the data outcomes from the aging Ulk1 study. Specifically, there were differences in autophagy-related protein expression between sexes independent of genotype. This is somewhat supported by one other study that investigated the role of estrogen receptor alpha in skeletal muscle autophagy signaling (Ribas et al., 2016). Additionally, there have been many reports of differential regulation of autophagy by sex hormones in disease progression (like certain cancers and Alzheimer's) (Shang, Wang, Klionsky, Cheng, & Zhou, 2020). Future studies should investigate the impact of sex hormones on autophagosome assembly and degradation specifically in skeletal muscle and with age. Second, I used multiple methods to assess autophagy flux including LC3I/II ratios, treatment with a lysosomal inhibitor (chloroquine), and a fluorescently tagged plasmid transfection. While there is strong evidence to suggest an autophagy bottleneck following a large autophagy activation stimulus, the role Ulk1 plays in regulating autophagy flux is inconclusive and needs to be further elucidated. This is particularly hard to tease apart in an autophagy knockout model like Ulk1 because there are less autophagosomes assembled which means the turnover of autophagosomes may occur at the same rate as the LMs however the capacity of degradation may different. In order to adequately assess Ulk1's role in flux, a transgenic model of Ulk1 that allows for normal autophagosome assembly but impairs Ulk1's ability to regulate flux would need to be utilized. Another area of future investigation includes further deciphering the role of fatty acids, amino acids, and nucleotides that result from complete

autophagosome degradation. These may function as signaling molecules indirectly by influencing the inflammatory response and affecting satellite cell function or they may act directly as metabolites to be used by the satellite cells to help provide energy for the energy demanding processes of activation and proliferation (Tang & Rando, 2014). The specific molecules responsible for signaling as well as the downstream signaling pathway targets need to be further characterized to truly understand the widespread role of autophagy. Lastly, the age-related decline in autophagy is well known and therapeutic interventions like exercise or caloric restriction that delay or impair this phenomenon should be further characterized. Specifically, research should be conducted on the specific autophagy signaling cascades these interventions work through and if this is affected in an aging context.

Conclusion

In closing, the studies contained herein touched on many physiological processes required for maintaining healthy muscle function after injury and throughout life. Maintaining muscle function is of the utmost importance because reductions in function can lead to many comorbidities resulting in an overall decreased quality of life and a substantial public health burden. Clearly, autophagy plays a role in maintaining cellular health and my dissertation work has advanced our understanding of that role in skeletal muscle function. This enhanced understanding of autophagy provides a very powerful therapeutic target to enhance muscle function and benefit the overall quality of life in many different populations.

REFERENCES

Call, J. A., Warren, G. L., Verma, M., & Lowe, D. A. (2013). Acute failure of action potential conduction in mdx muscle reveals new mechanism of contraction-induced force loss. *J Physiol, 591*(15), 3765-3776. doi:10.1113/jphysiol.2013.254656

Egan, D. F., Shackelford, D. B., Mihaylova, M. M., Gelino, S., Kohnz, R. A., Mair, W., . . . Shaw, R. J. (2011). Phosphorylation of ULK1 (hATG1) by AMP-activated protein kinase connects energy sensing to mitophagy. *Science, 331*(6016), 456-461. doi:10.1126/science.1196371

Hanna, R. A., Quinsay, M. N., Orogo, A. M., Giang, K., Rikka, S., & Gustafsson Å, B. (2012). Microtubule-associated protein 1 light chain 3 (LC3) interacts with Bnip3 protein to selectively remove endoplasmic reticulum and mitochondria via autophagy. *J Biol Chem, 287*(23), 19094-19104. doi:10.1074/jbc.M111.322933

Heymsfield, S. B., Thomas, D. M., Bosy-Westphal, A., & Müller, M. J. (2019). The anatomy of resting energy expenditure: body composition mechanisms. *Eur J Clin Nutr, 73*(2), 166-171. doi:10.1038/s41430-018-0319-3

Hood, D. A., Memme, J. M., Oliveira, A. N., & Triolo, M. (2019). Maintenance of Skeletal Muscle Mitochondria in Health, Exercise, and Aging. *Annu Rev Physiol, 81*, 19-41. doi:10.1146/annurev-physiol-020518-114310

Janssen, I., Shepard, D. S., Katzmarzyk, P. T., & Roubenoff, R. (2004). The healthcare costs of sarcopenia in the United States. *J Am Geriatr Soc, 52*(1), 80-85. doi:10.1111/j.1532-5415.2004.52014.x

Laker, R. C., Drake, J. C., Wilson, R. J., Lira, V. A., Lewellen, B. M., Ryall, K. A., . . . Yan, Z. (2017). Ampk phosphorylation of Ulk1 is required for targeting of mitochondria to lysosomes in exercise-induced mitophagy. *Nat Commun, 8*(1), 548. doi:10.1038/s41467-017-00520-9

Marzetti, E., Calvani, R., Tosato, M., Cesari, M., Di Bari, M., Cherubini, A., . . . Landi, F. (2017). Sarcopenia: an overview. *Aging Clin Exp Res, 29*(1), 11-17. doi:10.1007/s40520-016-0704-5

Moulis, M., & Vindis, C. (2017). Methods for Measuring Autophagy in Mice. *Cells, 6*(2). doi:10.3390/cells6020014

Ribas, V., Drew, B. G., Zhou, Z., Phun, J., Kalajian, N. Y., Soleymani, T., . . . Hevener, A. L. (2016). Skeletal muscle action of estrogen receptor alpha is critical for the maintenance of mitochondrial function and metabolic homeostasis in females. *Sci Transl Med, 8*(334), 334ra354. doi:10.1126/scitranslmed.aad3815

Shang, D., Wang, L., Klionsky, D. J., Cheng, H., & Zhou, R. (2020). Sex differences in autophagy-mediated diseases: toward precision medicine. *Autophagy*, 1-12. doi:10.1080/15548627.2020.1752511

Tang, A. H., & Rando, T. A. (2014). Induction of autophagy supports the bioenergetic demands of quiescent muscle stem cell activation. *Embo j, 33*(23), 2782-2797. doi:10.15252/embj.201488278

Vainshtein, A., & Hood, D. A. (2016). The regulation of autophagy during exercise in skeletal muscle. *J Appl Physiol (1985), 120*(6), 664-673. doi:10.1152/japplphysiol.00550.2015

Wang, C., Wang, H., Zhang, D., Luo, W., Liu, R., Xu, D., . . . Liu, Z. (2018). Phosphorylation of ULK1 affects autophagosome fusion and links chaperone-mediated autophagy to macroautophagy. *Nat Commun, 9*(1), 3492. doi:10.1038/s41467-018-05449-1

Warren, G. L., Summan, M., Gao, X., Chapman, R., Hulderman, T., & Simeonova, P. P. (2007). Mechanisms of skeletal muscle injury and repair revealed by gene expression studies in mouse models. *J Physiol, 582*(Pt 2), 825-841. doi:10.1113/jphysiol.2007.132373

Yang, L., Licastro, D., Cava, E., Veronese, N., Spelta, F., Rizza, W., . . . Fontana, L. (2016). Long-Term Calorie Restriction Enhances Cellular Quality-Control Processes in Human Skeletal Muscle. *Cell Rep, 14*(3), 422-428. doi:10.1016/j.celrep.2015.12.042